Studies on recognition mechanism for branched polysaccharides in family 55 and 74 glycoside hydrolases

(ファミリー55および74に属する糖質加水分解酵素における分岐多糖の認識メカニズム)

Takuya Ishida

石田　卓也

Index

1. Introduction

2. Characterization and X-ray crystallography of PcXgh74B

3. X-ray crystallography of PcLam55A

Appendix

Abbreviation

BLAST	basic local alignment search tool
BMCC	bacterial microcrystalline cellulose
CAZy	carbohydrate-active enzymes
CBH	cellobiohydrolase
CBM	carbohydrate binding modules
CE	carbohydrate esterase
CMC	carboxymethylcellulose
DP	degree of polymerization
GH	glycoside hydrolase
GPC	gel permeation chromatography
GT	glycosyl transferase
HCA	hydrophobic cluster analysis
HPLC	high performance liquid chromatography
MS	mass spectrometry
NMR	nuclear magnetic resonance
PAHBAH	*p*-hydroxybenzoic acid hydrazide
PASC	phosphoric acid swollen cellulose
PL	polysaccharides lyase
RMSD	root mean square deviation
TXG	xyloglucan from tamarind seed
XGO4	oligosaccharides derived from TXG with DP of 7-9
XGO8	oligosaccharides derived from TXG with DP of 16-18

Enzymes

AlgE4A	A-module of mannuronan C-5-epimerase from *Azotobacter vinelandii*
BsIFTase	inulin fructotransferase from *Bacillus sp. snu-7*
CtXgh74A	xyloglucan hydrolase from *Clostridium thermocellum*
Geotrichum XEG	xyloglucan specific endoglucanase from *Geotrichum sp. M128*
HjCel74A	endo-β-1,4-glucanase A from *Hypocrea jecorina*
OREX	oligo xyloglucan reducing end specific xyloglucanobiohydrolase from *Asperigillus nidulans*
OXG-RCBH	oligo xyloglucan reducing end specific cellobiohydrolase from *Geotrichum sp. M128*
Paenibacillus XEG74	xyloglucan specific endoglucanase from *Paenibacillus sp. KM21*
PcLam55A	exo-β-1,3-glucanase from *Phanerochaete chrysosporium*
PcXgh74B	xyloglcan hydrolase from *Phanerochaete chrysosporium*
Sf6 TSP	endorhamnsidase from *Shigella fleneri* Phage sf6

Chapter 1

Introduction

1-1 Structures of polysaccharides in nature

Polysaccharides are abundantly found in nature, and play important roles as structural components or storage materials for various organisms. Structure of polysaccharides consists of many monosaccharides linked via glycosidic linkages. There are numerous types of polysaccharides which have different structure, because the types of monosaccharides are quite diverse and each of them have five or six hydroxyl groups that can form glycodsidic bonds with adjacent sugar residues. Some example of polysaccharides and their structure are summarized in Table 1-1. Except small number of linear polysaccharides such as cellulose, many polysaccharides have branched structure, containing main-chain and side-chain. The side-chain structure affects properties of the polysaccharides such as molecular conformation and affinity to other molecules, which differs solubility, crystallinity, and pattern of molecular assembly. The organisms that produce polysaccharides ingeniously utilize the different properties of polysaccharides resulted from different side-chain structures.

Table 1-1 Structure of polysaccharides found in nature.

polysaccharide	main-chian	side-chain[*1]
cellulose	β-1,4-glucan	-
chitin	β-1,4-linked GlcNAc	-
amylose/amylopectin	α-1,4-glucan	α-D-Glc$p$-(1→6)-
dextran	α-1,6-glucan	α-D-Glc$p$-(1→2,3,4)-
β-1,3/1,6-glucan	β-1,3-glucan	β-D-Glc$p$-(1→6)-
xylan	β-1,4-xylan	α-L-Ara$f$-(1→3)-, 4-O-Me-α-D-GlcAp-(1→3)-...
glucomannan	β-1,4- linked Glc$p$ and Man$p$	α-D-Gal$p$-(1→2,3,6)- [*2]
xyloglucan	β-1,4-glucan	α-D-Xyl$p$-(1→6)- etc...[*3]
arabinogalactan	β-1,3-galactan	β-D-Gla$p$-(1→6)- (long chain)[*4]

*1 Glc: glucose; Ara: arabinose; GlcA: glucuronate; Gal: galactose; Xyl: xylose, GlcNAc: *N*-acetyl glucose.
*2 The substitution occur at O-2, O-3, and O-6 position of mannnose residues, and O-2 and O-3 position of glucose residues.
*3 The detailed description is in the section 1-3-1 and introduction of chapter 2.
*4 β-L-Ara$f$ residues were attached at O-3 position of side-chain galactose residues.

1-2 Glycoside Hydrolases

  1-2-1 Classification of glycoside hydrolases by Carbohydrate Active enZymes (CAZy) data base
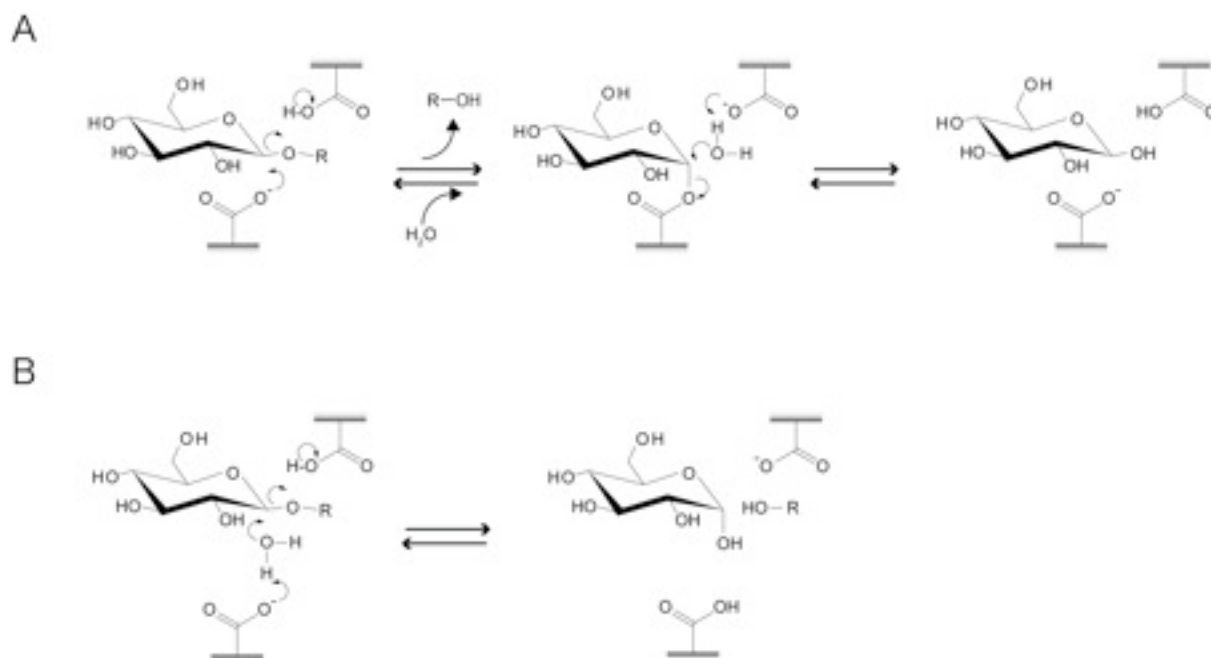
As the tools for degradation of polysaccharides, glycoside hydrolases (GHs) are produced by various organisms, and also diverse as well as their substrates. Generally, International Union of Biochemistry nomenclature of enzymes are used for identification and classification of enzymes. According to the IUB nomenclature, EC numbers are assigned to enzymes based on the substrate specificity of the enzymes and on the type of reaction that the enzymes catalyze (International Union of Biochemistry. Nomenclature Committee, 1984) However, at least for GHs, the classification is sometimes problematic. For example, same EC number can be assigned to evolutionarily distinct GHs active on same substrate, and assignment of EC number is difficult for GH which exhibits broad specificity (Henrissat, 1991).

  Henrissat *et al*. proposed a novel classification method for GHs based on the amino acid sequence similarity and the hydrophobic cluster analysis (HCA) (Henrissat, 1991). HCA is the analysis that predict secondary structure of proteins from its sequence (Gaboriaud *et al*., 1987). The classification of GHs reflected not only evolutionary relationships but also structural feature such as protein folds and localization of catalytic residues. As the number of sequences and known three dimensional (3-D) structures increase, it have been elucidated that protein folds and catalytic mechanism was completely conserved in each GH family (Henrissat & Davies, 1997). The GH family classification is now widely accepted as a convenient framework to understand mechanistic properties and evolutionary relationships of GHs, and it is used also for designation of GHs (Cantarel *et al*., 2008).

  The classification method was also applied to the other Carbohydrate Active enZYmes (CAZymes) and protein modules, Glycosyl Transferases: GT; Polysaccharide Lyases: PLs; Carbohydrate Esterases: CEs; Carbohydrate Binding Modules: CBMs, (Campbell *et al*., 1997, Coutinho & Henrissat, 1999, Coutinho *et al*., 2003, Boraston *et al*., 2004). The results are updated frequently and released at CAZy website URL: http:// www.cazy.org/. At present, 115 GH families are defined in the database (Henrissat & Bairoch, 1993, 1996, Cantarel *et al*., 2008)

1-2-2 Catalytic mechanisms

The reaction mechanism of GHs can be separated into two distinct classes, retaining and inverting mechanism. Retaining GHs hydrolyze glycosidic bond with net retention of anomeric configuration, whereas inverting GHs catalyze the reaction with net inversion (Sinnott, 1990, McCarter & Withers, 1994, Davies & Henrissat, 1995). The proposed reaction scheme in these mechanisms are shown in Fig. 1-1, where the hydrolysis of β-linkages via the two mechanisms are depicted. Generally, both mechanisms are believed to require a pair of carboxylic acids at the active site. In the retaining GHs, the two carboxyl groups at a distance of approximately 5.5 Å catalyze the reaction via covalent intermediate of glycosyl-enzyme complex (double-displacement mechanism). On the other hand, the two catalyst of inverting GHs have larger spacing of approximately 10 Å, because a water molecules activated by general base catalyst directly attack the anomeric carbon (single-displacement mechanism). Thus, the distance between two catalytic residues is highly related to the mechanism by which the GH catalyze the hydrolysis. Since the localization of catalytic residues are highly related to overall-folds of the proteins, all the enzymes in a GH family share both of protein fold and mechanism, with conserved catalytic residues.


Fig. 1-1
Reaction mechanism of GHs, retaining (A) and inverting (B).

1-2-3 Mode of action

For long time, it has been known that many GHs exhibit endo- and/or exo- activity during degradation of polysaccharides. In a endo-type manner, scissile bonds in the polysaccharides are hydrolyzed randomly as shown in Fig. 1-2A. In exo-type manner, the enzyme cleaves glycosidic bonds at reducing or non-reducing ends of the substrate and releases terminal sugar moieties, as shown in Fig. 1-2B. The difference of substrate-binding manner are also used for identification of GHs, and different EC numbers are assigned to the enzymes showing endo- or exo-activity. Since the difference in mode of action influence on changes of degree of polymerization of substrates and products, endo- or exo- mode of action can be determined by measuring increase of reducing power and decrease of viscosity during the hydrolysis reaction. When the enzyme degrade the polysaccharide in a endo-type manner, the rapid decrease of the viscosity followed by gradual increase of reducing sugar are observed, because long chains of substrate which generate viscosity are rapidly degraded to small chain by the hydrolysis on the middle of the substrate molecule. In the case of exo-acting enzymes, reducing sugar is rapidly increased without decrease of the viscosity because the product of mono- or di- saccharides are generated even in a initial phase of the reaction where the original DP of substrate are almost remained. Structural analyzes on many GHs revealed relationship between mode of action and active-site topologies (Davies & Henrissat, 1995). As indicated in Fig. 1-3A (Sakon *et al.*, 1996), endo-acting enzymes show cleft-shaped binding site. This topology appears to be appropriate to bind polysaccharide randomly. In contrast, many exo-acting enzymes exhibit the pocket shaped substrate binding site (Fig. 1-3B, (Nijikken *et al.*, 2007)).

GHs such as GH family 14 β-amylases (Nakatani, 1997), GH family 13 α-amylase (Abdullah *et al.*, 1966), and some of chitinases belonging to GH family 18 have been known to exhibit "multiple attack" or "processive hydrolysis". In the mode of action, enzymes cleave several glycosidic linkages in original substrate chain without dissociation (Fig. 1-4) The acidic residue near the active site of β-amylase stabilize the productive binding with the product of first hydrolysis and thus contribute to multiple attack by the enzyme. The 3-D structure of GH family 6 and 7 cellobiohydrolase (CBH) and chitinase suggest that tunnel like active site topology where the loops cover the substrate binding cleft are related to the processive hydrolysis by the enzymes (Divne *et al.*, 1994).
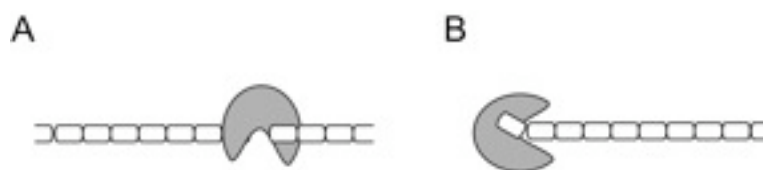
Fig. 1-2
Types of substrate binding by GHs. The localization of cleavage site of the first hydrolysis is different in Endo- (A) and exo- (B) mode of action.
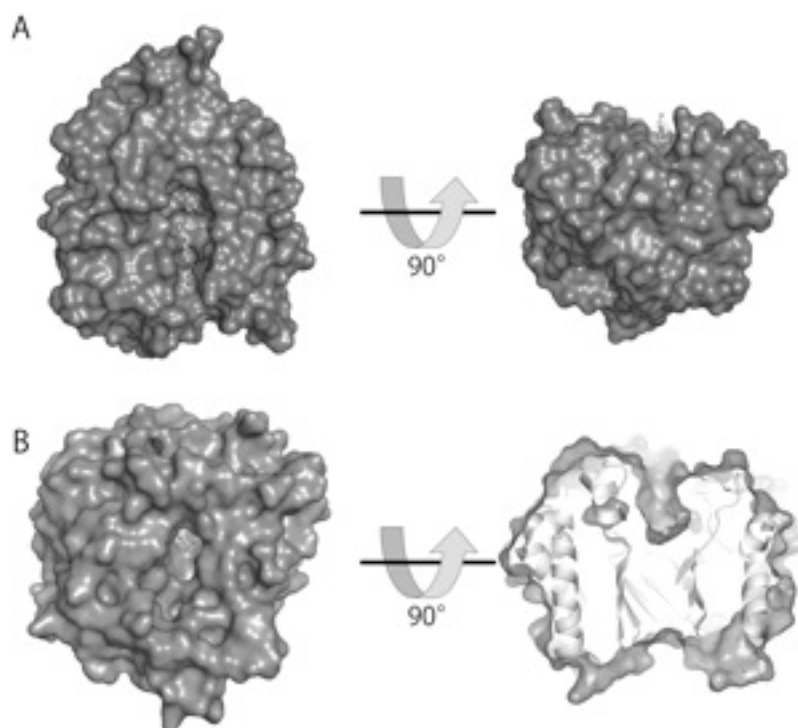
Fig. 1-3
Two types of active site topology found in GHs. The molecular surface of GH family 5 endo-glucanase E1 from *Acidothermus cellulolyticus* : PDB ID=1ECE (A) and family 1 β-glucosidase BGL1A from *Phanerochaete chrysosporium*: PDBID=2E40 (B) exhibit cleft and pocket-shaped active site, respectively. The side view of BGL1A (lower right) is shown by transparent molecular surface at 8 Å slab with ribbon representation of polypeptide.
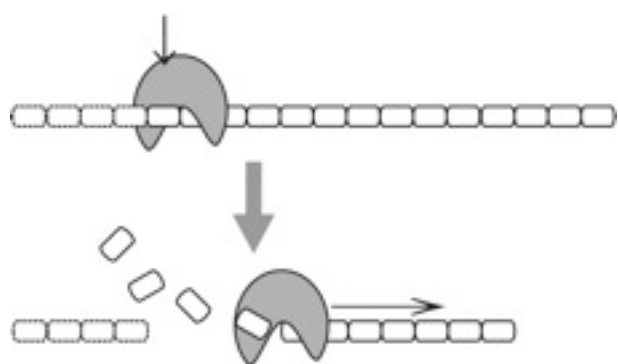
Fig. 1-4
Shematic representation of processive hydolysis or multiple attack. The enzyme hydrolyzes several adjacent cleavage sites without dissociation of substrate-enzyme complex.

1-2-4 Protein folds and clan

There are some GH families that share the fold and catalytic mechanism. For example, $(\beta/\alpha)_8$ barrel fold are shared by many GH families in CAZy, and many of them also share the two glutamate residues on strands 4 and 7 that catalyzes hydrolysis with net retention. Such commonality can be found in many GH families, which is due to better conservation of protein structure than that of sequence. The GH families sharing same protein folds, localization of catalytic residues, and catalytic mechanism are further grouped in "clans" (Henrissat & Davies, 1997). The properties of clans established so far are summarized in Table 1-2. The GH families having $(\beta/\alpha)_8$ barrel fold mentioned above are classified in the largest clan GH-A. Known structures of GH families that is not grouped in clans are summarized in Table 1-3. As shown in Table 1-2 and 1-3, many distinct protein folds are found in CAZy data base. 5 major examples are depicted in Fig. 1-5.

Table 1-2 protein folds and mechanism of GH families belonging to "clans".

Fold	Mechanism	catalytic residues	Clan	Family
$(\beta / \alpha)8$ barrel	Retaining	Glu / Glu	GH-A	1, 2, 5, 10, 17, 26, 30, 35, 39, 42, 50, 51, 53, 59, 72, 79, 86, 113
β-jelly roll	Retaining	Glu / Glu	GH-B	7, 16
β-jelly roll	Retaining	Glu / Glu	GH-C	11, 12
$(\beta / \alpha)8$ barrel	Retaining	Asp / Asp	GH-D	27, 31, 36
6-bladed β-propeller	Retaining	Tyr + Glu / Not known	GH-E	33, 34, 83, 93
5-bladed β-propeller	Inverting	Not known / Not known	GH-F	43, 62
$(\alpha / \alpha)6$ barrel	Inverting	Not known / Not known	GH-G	37, 63
$(\beta / \alpha)8$ barrel	Retaining	Asp / Glu	GH-H	13, 70, 77
α+β (lysozyme-like)	Inverting	Not known / Glu	GH-I	24, 46, 80
5-bladed β-propeller	Retaining	Asp / Glu	GH-J	32, 68
$(\alpha / \beta)8$ barrel	Retaining	carbonyl oxygen of C-2 acetamido group of substrate / Glu	GH-K	18, 20, 85
$(\alpha / \alpha)6$ barrel	Inverting	Glu / Glu	GH-L	15, 65
$(\alpha / \alpha)6$ barrel	Inverting	Asp / Glu	GH-M	8, 48
β-helix	Inverting	Asp / Asp	GH-N	28, 49

Table 1-3 protein folds and mechanism of other GH families.

| Fold	Mechanism	catalytic residues	Family
	Retaining	Asp / Glu	3, 29, 101
	Retaining	Glu / Glu	30, 44, 89
	Retaining	carbonyl oxygen of C-2 acetamido group of substrate / Asp	84
	Inverting	Glu / Glu	14
(β / α)8 barrel	Inverting	Not known / Glu	67
	Inverting	Asp + Glu / Glu	98
	Inverting	Phosphate / Glu	112
	Inverting	Asp / Glu	9
	Both	Glu / Glu (Inverting) Asp / Glu (Retaining)	97
	Retaining	carbonyl oxygen of C-2 acetamido group of substrate / Glu	56
(β / α)7 barrel	Retaining	Glu / Not known	57
	Retaining	Asp / Not known	38
	Inverting	Asp / Asp	6
	Retaining	Asp / Glu	22
	Retaining	carbonyl oxygen of C-2 acetamido group of substrate / Glu	103
α+β (lysozyme-like)	Retaining	Not known / Not known	104
	Inverting	Not known / Not known	19
	Not known	Not known / Not known	23
	Not known	Not known / Glu	73, 108
	Inverting	Not known / Not known	78
(α / α)6 barrel	Inverting	Phosphate / Glu	94
	Inverting	Asn activated by Asp / Glu	95
	Not known	Not known / Not known	88, 105
β-helix	Inverting	Asp / Glu	82
	Inverting	Glu or Asp / Glu	90
double ψ β-barrel	Inverting	Asp / Asp	45
	Retaining	Glu / Glu	102
(α / α)7 barrel	Inverting	Not known / Asp	47
β-jelly roll	Retaining	Not known / Not known	54
6-bladed β-propeller	Inverting	water activated by carboxylate of substrate / Glu	58
immunoglobulin-like β-sandwich	Not known	Not known / Not known	61
β-barrel + mixed (α / β)	Inverting	Not known / Not known	64
two 7-bladed β-propeller in tandem	Inverting	Glu / Glu	74
(β / α)5 (β) 3 TIM-like	Inverting	Asp / Glu	25
NAD(P) binding rossman fold + LDH Cterm domain-like	Retaining	-	4
dinucleotide binding rossman fold + α / β domain	Retaining	-	109
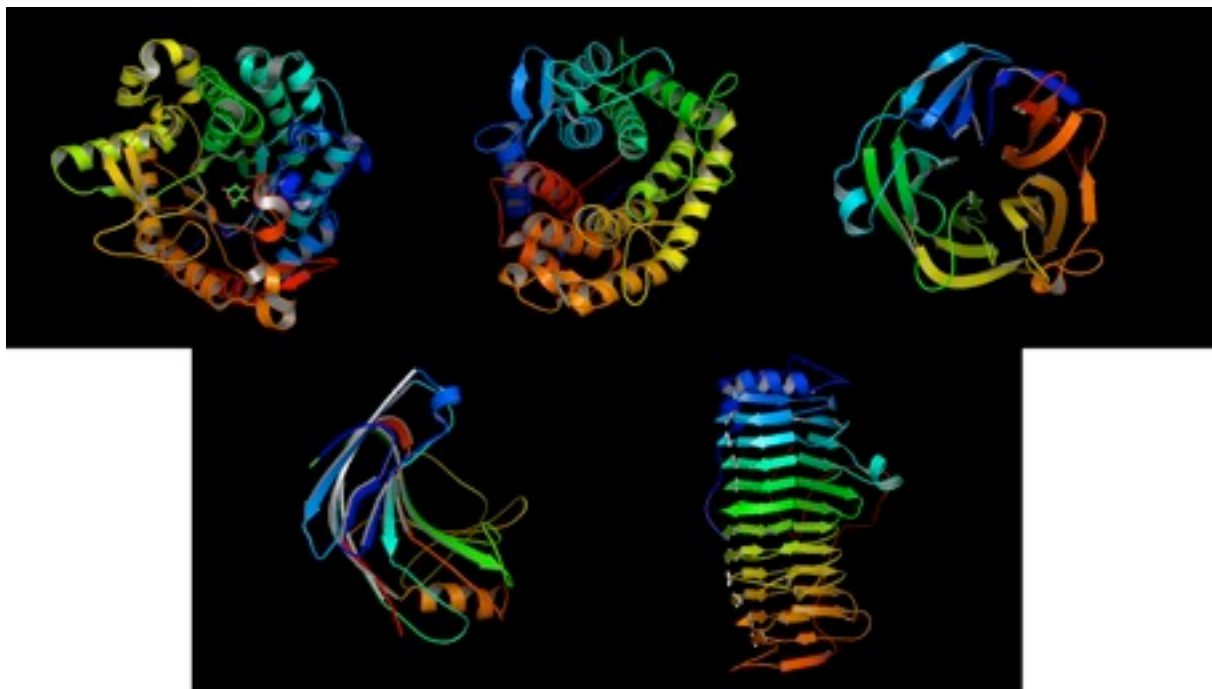
Fig. 1-5
The protein folds often found in GHs. $(\beta/\alpha)_8$ barrel: GH-A, D, and H (upper left); $(\alpha/\alpha)_6$ barrel: GH-G, L, and M (upper center); 5-bladed β-propeller: GH-F and J (upper right); β-jellyroll: GH-B and C (lower left); β-helix: GH-N (lower right).

1-3 Degradation of branched polysaccharides by GHs

Many GHs in nature degrade branched polysaccharides. Degradation of branched polysaccharides can be summarized as shown in Fig. 1-6. Type-A GHs recognize the side-chains and remove it from the polysaccharides, hydrolyzing the linkages of side-chain. Type-B GHs are specific toward main-chain or less branched region of the substrate. To degrade branched polysaccharides, Type-B GHs need to act with type-A GHs since branched structure inhibit the activity of type-B GHs. Such a degradation system where type-A and type-B GHs play distinct roles can be found in degradation system for xylan. In xylan degradation system, α-L-arabinofranosidase (EC 3.2.1.55 : GH family 3, 43, 51, 54 and 62) and α-D-glucuronidase (EC 3.2.1.131 EC 3.2.1.139 : GH family 4, 67 and 115) correspond to type-A GHs. And endo-1,4-β-xylanase (EC 3.2.1.8: GH family 5, 8, l0 and 11) and β-D-xylosidase (EC 3.2.1.37 : GH family 3, 30, 39, 43, 52, and 54) are correspond to type-B enzymes. The glycosidic bonds that these enzymes hydrolyze are indicated in Fig. 1-7 (Collins *et al.*, 2005).

On the other hand, type-C enzymes are not inhibited by side-chains. They cleave main-chain linkages accommodating branched structure including both main-chain and side-chain. Table l-4 summarizes known type-C enzymes. Since identification of type-C enzyme requires characterization using branched oligosaccharides, not so many GHs are known as type-C GH. The detailed characterization of GH family 10 enzymes demonstrated that some of endo-β-xylanase belonging to this family accommodate to arabinose side-chain. Thus, it is likely that many known GHs have activity as type-C GH.
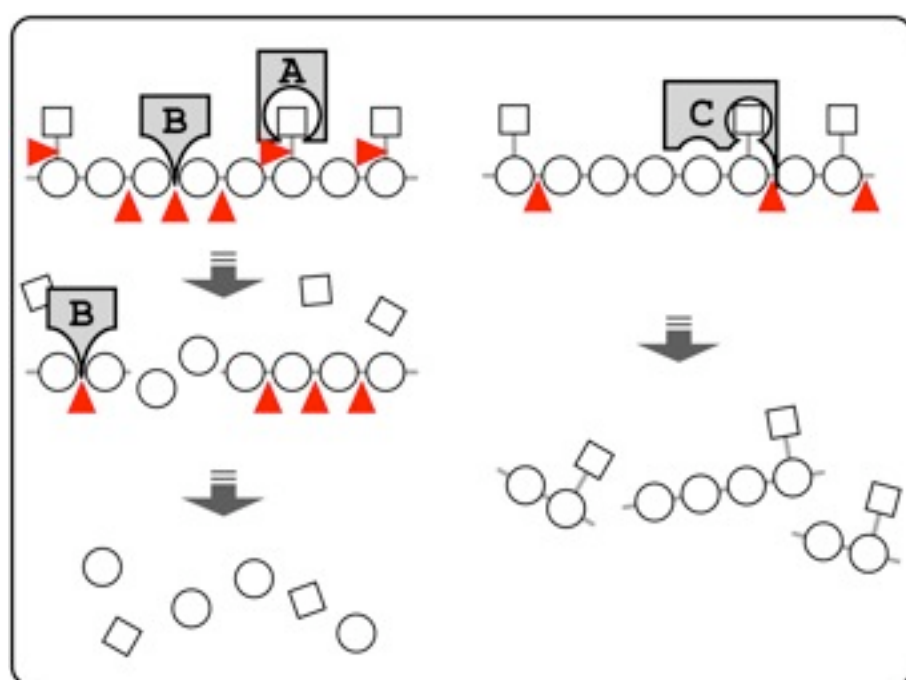
Fig. 1-6
Types of GHs degrating branched poly-saccharides. Type-A GH removes side-chains from branched poly-saccharides, and Type-B hydrolyzes main-chain linkages in debranched region of the saccharides. Type-C GH cleaves main-chain linkages recognizing side-chain residues.
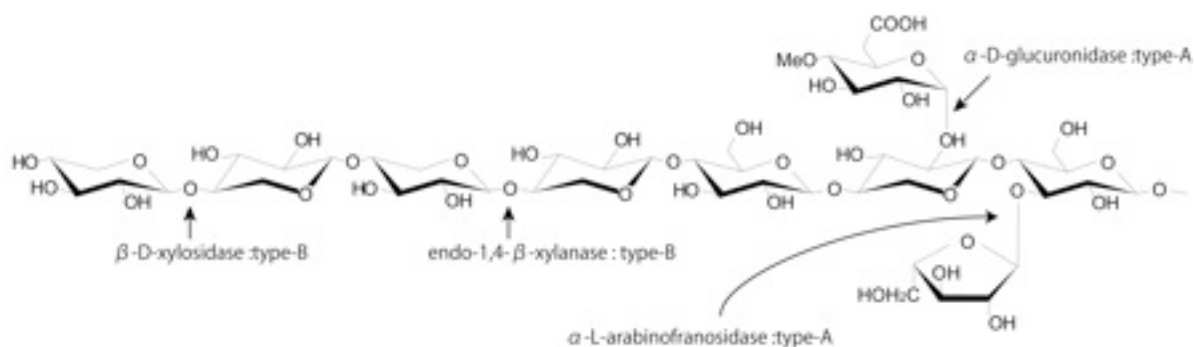
Fig. 1-7
The enzymes in the xylan degrading system. α-glucuronidase and α-L-arabinofranosidase are type-A GHs, whereas β-D-xylosidase and endo-1,4-β-D-xylanase are type-B GHs.

Table 1-4 GH families including type-C GHs.

substrate	GH family	references for type-C GHs	distribution of type A, B, and C-GHs		
			A	B	C
β-1,3/1,6-glucan	16	(Kawai *et al.*, 2006b)	-	+	+
	55	(Kasahara *et al.*, 1992)	-	-	+
xylan	10	(Fujimoto *et al.*, 2004, Pell *et al.*, 2004)	-	+	+
galactoglucomannan	5	(Dias *et al.*, 2004)	-	+	+
xyloglucan	5	(Gloster *et al.*, 2007)	-	+	+
	12		-	+	+
	16*	(Rose *et al.*, 2002)	-	+	+
	44	(Schnorr *et al.*, 2004)	-	+	+
	74	(Hasper *et al.*, 2002)	-	-	+
arabinogalactan	27	(Li *et al.*, 2007)	+	+	+
	43	(Ichinose *et al.*, 2005)	+	+	+

* GH family 16 xyloglucan endo-transglycosylase catalyze transglycosylation including type-C hydrolysis.

1-4 Glycoside hydrolases family 74 and 55

Among GHs classified into type-C GHs in Fig. l-4, GH family 74 and 55 are unique because the enzymes in these families are specific to one type of branched substrate, *i.e.,* all GH family 55 enzymes are specific to β-1,3/1,6-glucans, and all GH famly 74 enzymes are specific to xyloglucan or xyloglucan derived oligosaccharides. In this section, the detailed property of GHs belonging to these families are described.

1-4-1 Glycoside Hydrolase family 74

Xyloglucan is a major hemicellulose in primary cell wall in plant. In the cell wall, xyloglucan associates with cellulose micro-fibrils via hydrogen bonds, forming a cellulose-xyloglucan network (Hayashi & Maclachlan, 1984, Fry, 1989, Hayashi, 1989). During cell expansion and development, partial disassembly of the network is required, and consequently it was proposed that xyloglucan metabolism controls plant cell elongation (Hayashi *et al.*, 1994). In the seeds of some leguminosae, xyloglucan acts as deposited polysaccharide and is available for nutrition when germination occurs (Fry, 1989). Since aqueous solutions of xyloglucan have high viscosity, they are often used as food additives to enhance the viscosity and/or as stabilizers. As mentioned above, xyloglucan has β-1,4-glucan back bone as the main-chain, and α-D-xylose residues attached at the C-6 position of the many of main-chain glucose residues. Galactose, fucose, and arabinose residues are also found in a side-chain. A single-letter nomenclatures are used to simplify the naming of xyloglucan side-chain structures, *e.g.*, G, X, L, F, and S stand for β-D-Glc*p*, α-D-Xyl*p*-(1→6)-β-D-Glc*p*, β-D-Gal*p*-(l→2)-α-D-Xyl*p*-(l→6)-β-D-Glc*p*, α-L-Fuc*p*-(1→2)-β-D-Gal*p*-(l→2)-α-D-Xyl*p*-(l→6)-α-D-Glc*p*, and α-L-Ara*f*-(1→2)-α-D-Xyl*p*-(l→6)-β-D-Glc*p*, respectively (Table l-7) (Fry *et al.*, 1993).

Table 1-3 Single letter nomenclature for xyloglucan structure.

Code letter	Structure represented
G	β-D-Glc*p*
X	α-D-Xyl*p*-(1→6)-β-D-Glc*p*
L	β-D-Gal*p*(1→2)-α-D-Xyl*p*-(1→6)-β-D-Glc*p*
F	α-L-Fuc*p*-(1→2)-β-D-Gal*p*(1→2)-α-D-Xyl*p*-(1→6)-β-D-Glc*p*
A	[α-L-Ara*f*-(1→2)-, α-D-Xyl*p*-(1→6)]-β-D-Glc*p*
B	[β-D-Xyl*p*-(1→2)-, α-D-Xyl*p*-(1→6)]-β-D-Glc*p*
C	[α-L-Ara*f*-(1→3)-β-D-Xyl*p*-(1→2)-, α-D-Xyl*p*-(1→6)]-β-D-Glc*p*
S	α-L-Ara*f*-(1→2)-α-D-Xyl*p*-(1→6)-β-D-Glc*p*

The type of the saccharides in xyloglucan side-chains and distribution of them are diverse depending on the species and growth phase of the plant. Xyloglucans from dicotyledons are occasionally called "fucogalactoxyloglucans" because α-L-Fuc$p$-(1→2)-β-D-Gal$p$-(1→2)-α-D-Xyl$p$-(1→6)-β-D-Glc$p$ moieties, F, and β-D-Gal$p$-(1→2)-α-D-Xyl$p$-(1→6)-β-D-Glc$p$ moieties, L, are often found in their structure (Aspinall $et\ al$., 1969, Bauer $et\ al$., 1973, Ebringerova $et\ al$., 2005). Fucogalactoxyloglucans contains non-substituted glucose residues every four main-chain residues as shown in repeating units of pea xyloglucan demonstrated by Hayashi $et\ al$. (Hayashi & Maclachlan, 1984). On the other hand, xyloglucans from monocotyledons contain no fucose residues and less amount of side-chains compare to fucogalactoxyloglucans. They have significant amount of sequence of non-substituted glucose residues (GG) in main-chain (Kato & Matsuda, 1985, Hayashi, 1989).

All biochemically characterized enzymes in GH family 74, except Cel74 from *Thermotoga maritima,* showed specificity toward xyloglucan or xyloglucan oligosaccharides (Edwards $et\ al$., 1986, Chhabra & Kelly, 2002, Hasper $et\ al$., 2002, Yaoi & Mitsuishi, 2002, Irwin $et\ al$., 2003, Grishutin $et\ al$., 2004, Yaoi & Mitsuishi, 2004, Yaoi $et\ al$., 2005, Zverlov $et\ al$., 2005, Sianidis $et\ al$., 2006). Cel74 from *T. maritima* shows highest activity toward barley β-glucan but still have more than 20% activity on xyloglucan relative to barley β-glucan (Chhabra & Kelly, 2002). All the member of this family are secreted enzymes from bacteria or fungi, and no member from plant or other higher eukaryotic origin has been found. AviIII from *Aspergillus aculeatus* and EglC from *Aspergillus niger* were reported as the initial member of the GH family 74 (Takada $et\ al$., 1998, Hasper $et\ al$., 2002). Since *A. aculeatus* had been investigated as cellulolytic microorganisms and that AviIII showed hydrolytic activity towards β-l,4-glucan substrates, the enzyme have been characterized as one of the cellulases. However, physiological substrate of EglC is xyloglucan which have β-1,4-glucan back bone similar to cellulose in its structure. The hydrolytic activity on xyloglucan by EglC was more than ten times higher than those on carboxymethylcellulose: CMC and barley β-glucan (Hasper $et\ al$., 2002). So far, 13 biochemically characterized enzymes are classified into GH family 74, and many of them were designated as xyloglucan specific endoglucanase: XEG, xyloglucanase, or xyloglucan hydrolase: Xgh.

The series of studies by Yaoi *et al*. elucidated the diversity of the mode of action by GH family 74 enzymes hydrolyzing xyloglucan and xyloglucan oligosaccharides. The exo- type enzymes recognize the reducing end of xyloglucan oligosaccharide (OXG-RCBH: oligoxyloglucan reducing end-specific cellobiohydrolase from *Geotrichum* sp. M128 (Yaoi & Mitsuishi, 2002) and OREX: oligoxyloglucan reducing end-specific xyloglucanobiohydrolase from *Aspergillus nidulans* (Bauer *et al*., 2005)), whereas the endo-type enzymes hydrolyze β-1,4-linkages in the middle of xyloglucan polymer. In addition, XEG74 from *Paenibacillus sp*. KM2l (*Paenibacillus* XEG74) and Cel74A from *Hypocrea jecorina*, formerly known as *Trichoderma reesei*, (HjCel74A) have been reported to have endo-processive or dual-mode endo- and exo- like activities (Grishutin *et al*., 2004, Yaoi *et al*., 2005).

The 3-D structure of OXG-RCBH revealed that the enzyme consists of the tandem structure of seven bladed β-propeller domains (Yaoi *et al*., 2004). The two domains have very similar structure and form a largely opened substrate-binding cleft between them. Interestingly, two catalytic residues are located at topologically same site on each β-propeller domain. The structure also showed that a "exo-loop" blocked the one side of the substrate-binding cleft of OXG-RCBH. In the the sequence alignment of GH family 74 enzymes, exo-loop can be found only in OXG-RCBH and OREX, indicating that exo-mode of action by these exo-type enzymes are driven by exo-loop. The function of exo-loop was confirmed by deletion of the exo-loop disrupting the mode of action of OXG-RCBH (Yaoi *et al*., 2007) and the structure of endo-type enzyme Xgh74A from *Clostridium thermocellum* (CtXgh74A) lacking any structure which blocks the substrate-binding cleft (Martinez-Fleites *et al*., 2006). Although the crystal structure of both exo- and endo- type enzymes demonstrated the contribution of 'exo-loop', the mechanism of the diversity of hydrolytic activities on xyloglucans among Endo-type enzymes still have been unknown.
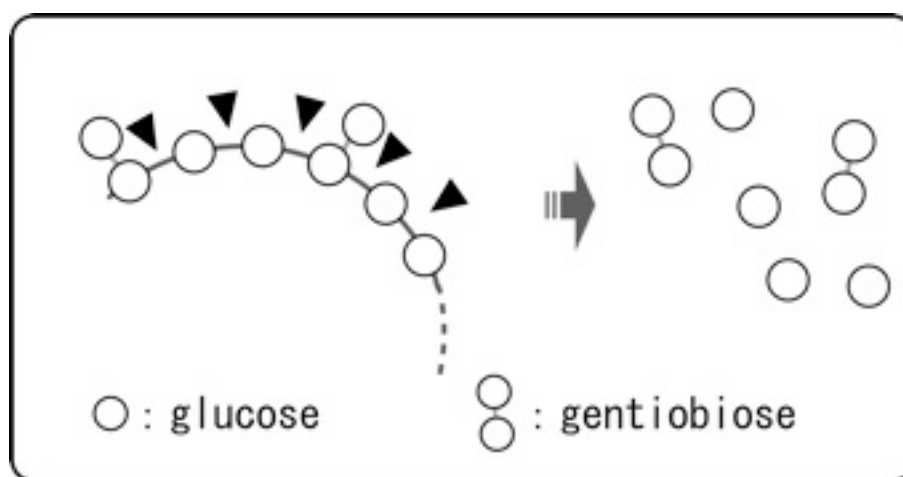
1-4-2 GH family 55

The primary role of fungal β-1,3-glucans is to maintain cell wall rigidity, and thus to protect the cell. The cell wall β-1,3-glucans are also suggested to be degraded for nutritional purpose after exhaustion of external nutrition (Zevenhuizen & Bartnicki-Garcia, 1970). β-1,3-Glucans on the cell surface are thought to be involved in morphogenetic changes, *i.e.*, aggregation and mycelial strand formation (Stone, 1992). Moreover, the hyphal sheath of pathogenic fungi contains extra-cellular β-1,3-glucans, which play an active role in wood cell-wall degradation (Ruel & Joseleau, 1991). Fungal β-1,3-glucans often contain some branches with β-1,6-glycosidic linkages, and these molecules are called β-1,3/1,6-glucans. The pattern of branching in β-1,3/1,6-glucans, *e.g.*, linkage ratio and branch length, varies depending on fungal species, localization in the cell wall, and the growth phase of the cells.

Fungi are the predominant producers of β-1,3-glucanases, possibly due to the wide availability of the substrate in their cell wall (Bielecki & Galas, 1991). Degradation of β-1,3-glucans by fungi often involves the cooperative action of multiple β-1,3-glucanases rather than a single enzyme. Although some fungal β-1,3-glucanases are constitutively produced, their expression levels are often controlled by culture conditions (Pitson *et al.*, 1993). Many β-1,3-glucanases have been characterized, and they exhibit a wide variety of substrate specificities and modes of actions (Martin *et al.*, 2007). These facts suggest the involvement of β-1,3-glucanases in mobilization of cell-wall β-glucans, especially in the case of yeast enzymes (Adams, 2004).

GH family 55 consists of β-1,3-glucanases mainly from filamentous fungi. The cloning of full length cDNA encoding Bgn13.1 from *Trichoderma harzianum* was reported 1995, for the first time in this family. The sequence was considered to be distinct from known β-1,3-glucanases of bacteria, yeast, and plant, since the conserved motifs are lacked only in Bgn13.1 (de la Cruz *et al.*, 1995). Although several genes possibly coding GH family 55 proteins have been found also in recent bacterial genome projects, there is no report about the characterization of bacterial enzyme. The β-1,3-glucanases belonging to this family are occasionally called "Laminarinase" because of the hydrolyzing activities on laminarin from brown algae *Laminaria digitata*. Laminarin is one of the best studied β-1,3/1,6-glucan with an average DP of approximately 25, which consists of β-1,3-glucan main-chain and single glucose side-chain residues attached to main-chain glucose via β-1,6-linkages. However, the physiological substrate for GH family 55 β-1,3-glucanases seems to be β-1,3/1,6-glucans in fungal cell walls, because studies on expression of the enzymes indicated that the enzyme is

involved in the autolysis of the fungi (Pitson *et al.*, 1993).

The majority of the members in GH family 55 are exo-acting enzymes, exo-1,3-β-glucanase (EC, 3.2.1.58). These enzymes cleave the terminal β-1,3-glycosidic linkage at non-reducing end of β-1,3-glucans or β-l,3/1,6-glucans (Fig. 1-8). Many of them produces gentiobiose in addition to glucose during degradation of β-1,3/1,6-glucan (Kasahara *et al.*, 1992, Pitson *et al.*, 1995, Kawai *et al.*, 2006a, Martin *et al.*, 2006). A few members in this family were described as an endo-type enzyme, *i.e.* endo-β-1,3-glucanse (EC. 3.2.1 .39). De la Crus *et al.* demonstrated an endo-mode of action on laminarin by Bgn13.1 from *Hypocrea lixii*, formerly known as *Trichoderma harzianum,* based on DP of limit digestion products confirmed by HPLC analysis and on the absence of inhibition by gluconolactone (de la Cruz *et al.*, 1995). LamAI from *Trichoderma viride* was also mentioned as endo-type enzyme based on the analysis laminariheptaose (L7) and its sequence similarity to Bgn13.1 (Nobe *et al.*, 2003, Nobe *et al.*, 2004).

Fig. 1-8
The schematic representation of hydrolysis of laminarin by exo-1,3-β-glucanases belonging to GH family 55. Glucose and gentiobiose are generated as final products.

The hydrolysis by GH family 55 enzymes proceed with net inversion at anomeric carbon (inverting mechanism), as confirmed by NMR analysis on ExgS from *Aspergillus saitoi* (Kasahara *et al.*, 1992, Oda *et al.*, 2002), polarimetric analysis on the β-glucanases (GNI, II, and III) from *Acremonium persicinum* (Pitson *et al.*, 1995), and HPLC analysis on PcLam55A from *Phanerochaete chrysosporium* (Kawai *et al.*, 2006a). As shown in Table 1-6,

only GH family 55 include fungal exo-1,3-β-glucanases producing gentiobiose from β-1,3/1,6-glucans, indicating that only GH family 55 exo-1,3-β-glucanases hydrolyze all the β-1,3-glycosidic bonds in laminarin without cleaving β-1,6-linkage. The properties of GH family 55 exo-1,3-β-glucanases are consistent with those of several β-1,3-glucanases from fungi that are well investigated in early studies from 1950s, *e.g.* β-1,3-glucanase from *Basidiomycete* QM-806 (Huotari *et al.*, 1968, Nelson *et al.*, 1969, Jeffcoat & Kirkwood, 1987). Although these enzymes have not been cloned yet, they are strongly suggested to be members of GH family 55.

Table 1-6 The properties of β-1,3-glucanases in CAZy data base.

GH family	mechanism	origin	production of gentiobiose	mode of action
GH 5	retaining	fungi and plant	-	both
GH 16	retaining	bacteria, fungi, metazoa, and plants	-	both
GH 17	retaining	fungi and plant	-	endo-acting
GH 55	inverting	mainly filamentous fungi	confirmed for four enzymes	mainly exo-acting
GH 64	inverting	mainly bacteria	-	endo-acting
GH 81	inverting	bacteria and fungi	-	endo-acting

Based on the sequence analysis, Rigden and Franco demonstrated that the sequence of GH family 55 enzymes had tandem repeat of conserved motifs of β-helix fold (Rigden & Franco, 2002). The β-helix fold is often found in polysaccharide active enzymes such as GHs, PLs, and CEs. The findings confirmed the previous description about imperfect copies in sequence of EXGIp from *Cochliobolus carbonum* (Nikolskaya *et al.*, 1998) and a symmetry between first and second halves in sequence of Gluc78 from *T. harzianum* (Donzelli *et al.*, 2001), and also improve understanding of structure of GH family 55 enzymes. However, there is no known structure contains two β-helix folds in single peptide, suggesting the structure of GH family 55 enzyme will exhibit novel whole protein fold or domain structure formed by multiple β-helix folds.

1-4 Basidiomycete *Phanerochaete chrysosporium*

The basidiomycete *Phanerochaete chrysosporium* is a model organism of white rot fungi. This fungus degrades all of cellulose, hemicellulose and lignin in plant cell walls, and causes white rot by which woods become white and soft loosing its color and physical strength. *P. chrysosporium* was isolated from wood chip piles as *Chrysosporium lignorum*. The name *Phanerochaete chrysosporium* has been assigned to it based on the perfect state, after second name *Sporotrichum pulverulentum* assigned for the imperfect stage (Eriksson *et al*., 1990).

For the purpose of investigating the lignin degradation system of the fungus, the total genome of *P. chrysosporium* have been sequenced and released in 2002. The gene models were updated subsequently (Martinez *et al*., 2004). However, completed genome information revealed not only ligninolytic system involving extracellular oxidative enzymes but also impressive diversity among genes possibly encode carbohydrate active enzymes (Vanden Wymelenberg *et al*., 2005). The genome contains the genes encoding more than 240 putative carbohydrate-active enzymes including 166 GHs, 14 CEs, 57 GTs, comprising at least 69 distinct families (Martinez *et al*., 2004). In addition to the basis for comprehensive analysis, the genome sequence provide the useful information for molecular biological study, *e.g*. gene cloning, expression analysis, and enzymatic characterization using recombinant protein (Ichinose *et al*., 2005, Yoshida *et al*., 2005, Kawai *et al*., 2006a, Kawai *et al*., 2006b, Tsukada *et al*., 2006, Vanden Wymelenberg *et al*., 2006, Igarashi *et al*., 2008, Suzuki *et al*., 2008). According to the genome database, *P. chrysosporium* have two genes belonging to GH family 74 and another two genes belonging to GH family 55. PcLam55A is the gene product from one of the GH family 55 genes, which is expressed under various condition. Recently, the biochemical characterization of the enzyme was performed using recombinant protein (Abbas *et al*., 2005, Vanden Wymelenberg *et al*., 2005, Kawai, 2006, Kawai *et al*., 2006a). Though both two genes belonging to GH family 74 are expressed by *P. chrysosporium* under cellulose-containing culture, only one of them have C-terminus cellulose binding domain belonging to CBM family 1 (Vanden Wymelenberg *et al*., 2005).

In the *P. chrysosporium* genome sequence, 5 genes encode GHs belonging to GH family with β-propeller folds and 6 genes that encode β-helical GHs or CEs (Table 1-7). Despite that many PL family have been known to take β-helix fold, no genes coding β-helical PLs are found.

Table 1-7 The genes possibly belonging to CAZyme family which have β-propeller and β-helix fold.

β-propeller		β-helix	
GH-32	0	GH-28	5
GH-33	0	GH-49	0
GH-34	0	GH-55	2
GH-43	3	GH-82	0
GH-58	0	GH-90	0
GH-62	0	PL-1	0
GH-65	0	PL-3	0
GH-74	2	PL-6	0
GH-83	0	PL-9	0
GH-93	0	PL-16	0
		PL-19	0
		CE-8	1

1-6 Aim of thesis

GH family 55 and 74 shared several unique properties.

i) In contrast to other GH families, most of biochemically characterized enzymes belonging to GH family 55 and 74 share high specificity towards β-1,3/1,6-glucans and xyloglucans related saccharides, respectively. These enzymes hydrolyze main-chain of branched substrate, β-1,3/1,6-glucan or xyloglucan, they can be classified in type-C GHs.

ii) Both endo- and exo- acting enzymes have been reported in these families. Although all the member in each family show high specificity towards same substrate, they exhibit various hydrolytic patterns. Both endo- and exo-acting enzyme are reported in GH family 55 and 74, and some of GH family 74 enzyme have been considered to have endo-processive or dual mode of endo and exo-like activity.

Since both of β-1,3/1,6-glucans and xyloglucans have branched structure, it would appear that GH family 55 and 74 are well equipped for recognizing branched structure of the substrates. Considering the conservation of structural properties in GH family, these families seem to share structural properties which have an influence on substrate recognition. The aim of present study is to elucidate the recognition mechanism for branched polysaccharides in the enzymes belonging to GH family 55 and 74, and to demonstrate structure - function relation ships shared by the families. The information from both detailed analyzes on hydrolysis reaction and 3-D structure of the enzymes are necessary.

There are no previously reported 3-D structure of GH family 55 enzymes. In chapter 2, therefore, X-ray crystallography were conducted on PcLam55A from *P. chrysosporium* which are one of the best studied enzyme in this family. And in GH family 74, the diversity of the enzymes in mode of action towards xyloglucan or xyloglucan oligosaccharides have been reported. In chapter 3, detailed biochemical analyzes and crystallography were conducted on PcXgh74B from *P. chrysosporium* which is novel member of the family. In order to obtain the recombinant protein necessary for both analyzes, the genomic information of *P. chrysosporium* was used for cloning of the cDNA sequence which were transformed to yeast for heterologous expression. Mode of action of PcXgh74B and structural element which contribute to the activity will be discussed based on comparison with other GH family 74 enzymes reported previously.

1-7 References

Abbas, A., Koc, H., Liu, F. & Tien, M. Fungal degradation of wood: initial proteomic analysis of extracellular proteins of Phanerochaete chrysosporium grown on oak substrate. *Curr Genet* **47**, 49-56,(2005).

Abdullah, M., French, D. & Robyt, J. F. Multiple attack by alpha-amylases. *Arch Biochem Biophys* **114**, 595-598,(1966).

Adams, D. J. Fungal cell wall chitinases and glucanases. *Microbiology* **150**, 2029-2035, (2004).

Aspinall, G. O., Molloy, J. A. & Craig, J. W. T. Extracellular Polysaccharides from Suspension-Cultured Sycamore Cells. *Can J Biochem* **47**, 1063-&,(1969).

Bauer, S., Vasu, P., Mort, A. J. & Somerville, C. R. Cloning, expression, and characterization of an oligoxyloglucan reducing end-specific xyloglucanobiohydrolase from Aspergillus nidulans. *Carbohydr Res* **340**, 2590-2597,(2005).

Bauer, W. D., Talmadge, K. W., Keegstra, K. & Albershe.P Structure of Plant-Cell Walls . 2. Hemicellulose of Walls of Suspension-Cultured Sycamore Cells. *Plant Physiol* **51**, 174-187,(1973).

Bielecki, S. & Galas, E. Microbial beta-glucanases different from cellulases. *Crit Rev Biotechnol* **10**, 275-304,(1991).

Boraston, A. B., Bolam, D. N., Gilbert, H. J. & Davies, G. J. Carbohydrate-binding modules: fine-tuning polysaccharide recognition. *Biochem J* **382**, 769-781,(2004).

Campbell, J. A., Davies, G. J., Bulone, V. & Henrissat, B. A classification of nucleotide-diphospho-sugar glycosyltransferases based on amino acid sequence similarities. *Biochem J* **326 (Pt 3)**, 929-939,(1997).

Cantarel, B. L., Coutinho, P. M., Rancurel, C., Bernard, T., Lombard, V. & Henrissat, B. The Carbohydrate-Active EnZymes database (CAZy): an expert resource for Glycogenomics. *Nucleic Acids Res* **37**, D233-D238,(2008).

Chhabra, S. R. & Kelly, R. M. Biochemical characterization of Thermotoga maritima endoglucanase Cel74 with and without a carbohydrate binding module (CBM). *FEBS Lett* **531**, 375-380,(2002).

Collins, T., Gerday, C. & Feller, G. Xylanases, xylanase families and extremophilic xylanases. *FEMS Microbiol Rev* **29**, 3-23,(2005).

Coutinho, P. M., Deleury, E., Davies, G. J. & Henrissat, B. An evolving hierarchical family classification for glycosyltransferases. *J Mol Biol* **328**, 307-317,(2003).

Coutinho, P. M. & Henrissat, B. (1999). *Carbohydrate-active enzymes: an integrated database approach.*, edited by H. J. Gilbert, G. J. Davies, B. Henrissat & B. Svensson, 3-12. Cambridge: The Royal Society of Chemistry.

Davies, G. & Henrissat, B. Structures and mechanisms of glycosyl hydrolases. *Structure* **3**, 853-859,(1995).

de la Cruz, J., Pintor-Toro, J. A., Benitez, T., Llobell, A. & Romero, L. C. A novel endo-beta-1,3-glucanase, BGN13.1, involved in the mycoparasitism of Trichoderma harzianum. *J Bacteriol* **177**, 6937-6945,(1995).

Dias, F. M., Vincent, F., Pell, G., Prates, J. A., Centeno, M. S., Tailford, L. E., Ferreira, L. M., Fontes, C. M., Davies, G. J. & Gilbert, H. J. Insights into the molecular determinants of substrate specificity in glycoside hydrolase family 5 revealed by the crystal structure and kinetics of *Cellvibrio mixtus* mannosidase 5A. *J Biol Chem* **279**, 25517-25526,(2004).

Divne, C., Stahlberg, J., Reinikainen, T., Ruohonen, L., Pettersson, G., Knowles, J. K., Teeri, T. T. & Jones, T. A. The three-dimensional crystal structure of the catalytic core of cellobiohydrolase I from Trichoderma reesei. *Science* **265**, 524-528,(1994).

Donzelli, B. G., Lorito, M., Scala, F. & Harman, G. E. Cloning, sequence and structure of a gene encoding an antifungal glucan 1,3-beta-glucosidase from Trichoderma atroviride (T. harzianum). *Gene* **277**, 199-208,(2001).

Ebringerova, A., Hromadkova, Z. & Heinze, T. Hemicellulose. *Adv Polym Sci* **186**, 1-67, (2005).

Edwards, M., Dea, I. C., Bulpin, P. V. & Reid, J. S. Purification and properties of a novel xyloglucan-specific endo-(1->4)-beta-D-glucanase from germinated nasturtium seeds (Tropaeolum majus L.). *J Biol Chem* **261**, 9489-9494,(1986).

Eriksson, K. E. L., Blanchette, R. A. & Ander, P. (1990). *Biodegradation of cellulose*, edited by T. E. Timell, 89-180. Berlin: Springer-Verlag Berlin Heidelberg.

Fry, S. C. The structure and functions of xyloglucan. *J Exp Bot* **40**, 1-11,(1989).

Fry, S. C., York, W. S., Albersheim, P., Darvill, A., Hayashi, T., Joseleau, J. P., Kato, Y., Lorences, E. P., Maclachlan, G. A., Mcneil, M., Mort, A. J., Reid, J. S. G., Seitz, H. U., Selvendran, R. R., Voragen, A. G. J. & White, A. R. An unambiguous nomenclature for xyloglucan-derived oligosaccharides. *Physiologia Plantarum* **89**, 1-3,(1993).

Fujimoto, Z., Kaneko, S., Kuno, A., Kobayashi, H., Kusakabe, I. & Mizuno, H. Crystal structures of decorated xylooligosaccharides bound to a family 10 xylanase from *Streptomyces olivaceoviridis* E-86. *J Biol Chem* **279**, 9606-9614,(2004).

Gaboriaud, C., Bissery, V., Benchetrit, T. & Mornon, J. P. Hydrophobic cluster analysis: an efficient new way to compare and analyse amino acid sequences. *FEBS Lett* **224**, 149-155,(1987).

Gloster, T. M., Ibatullin, F. M., Macauley, K., Eklof, J. M., Roberts, S., Turkenburg, J. P., Bjornvad, M. E., Jorgensen, P. L., Danielsen, S., Johansen, K. S., Borchert, T. V., Wilson, K. S., Brumer, H. & Davies, G. J. Characterization and three-dimensional structures of two distinct bacterial xyloglucanases from families GH5 and GH12. *J Biol Chem* **282**, 19177-19189,(2007).

Grishutin, S. G., Gusakov, A. V., Markov, A. V., Ustinov, B. B., Semenova, M. V. & Sinitsyn, A. P. Specific xyloglucanases as a new class of polysaccharide-degrading enzymes. *Biochim Biophys Acta* **1674**, 268-281,(2004).

Hasper, A. A., Dekkers, E., van Mil, M., van de Vondervoort, P. J. & de Graaff, L. H.
EglC, a new endoglucanase from Aspergillus niger with major activity towards xyloglucan.
Appl Environ Microbiol **68**, 1556-1560,(2002).

Hayashi, T. Xyloglucans in the primary-cell wall. *Annu Rev Plant Phys* **40**, 139-168,(1989).

Hayashi, T. & Maclachlan, G. Pea xyloglucan and cellulose : I. macromolecular organization. *Plant Physiol* **75**, 596-604,(1984).

Hayashi, T., Ogawa, K. & Mitsuishi, Y. Characterization of the adsorption of xyloglucan to cellulose. *Plant Cell Physiol* **35**, 1199-1205,(1994).

Henrissat, B. A classification of glycosyl hydrolases based on amino acid sequence similarities. *Biochem J* **280**, 309-316,(1991).

Henrissat, B. & Bairoch, A. New families in the classification of glycosyl hydrolases based on amino acid sequence similarities. *Biochem J* **293**, 781-788,(1993).

Henrissat, B. & Bairoch, A. Updating the sequence-based classification of glycosyl hydrolases. *Biochem J* **316**, 695-696,(1996).

Henrissat, B. & Davies, G. Structural and sequence-based classification of glycoside hydrolases. *Curr Opin Struct Biol* **7**, 637-644,(1997).

Huotari, F. I., Nelson, T. E., Smith, F. & Kirkwood, S. Purification of an exo-beta-D-(1 bonded to 3)-glucanase from Basidiomycete species QM 806. *J Biol Chem* **243**, 952-956, (1968).

Ichinose, H., Yoshida, M., Kotake, T., Kuno, A., Igarashi, K., Tsumuraya, Y., Samejima, M., Hirabayashi, J., Kobayashi, H. & Kaneko, S. An exo-beta-1,3-galactanase having a novel beta-1,3-galactan-binding module from Phanerochaete chrysosporium. *J Biol Chem* **280**, 25820-25829,(2005).

Igarashi, K., Ishida, T., Hori, C. & Samejima, M. Characterization of an endoglucanase belonging to a new subfamily of glycoside hydrolase family 45 of the basidiomycete Phanerochaete chrysosporium. *Appl Environ Microbiol* **74**, 5628-5634,(2008).

International Union of Biochemistry. Nomenclature Committee, W., Edwin C (1984). *Enzyme Nomenclature 1984: Recommendations of the Nomenclature Committee of the International Union of Biochemistry on the Nomenclature and Classification of Enzyme-Catalysed Reactions*, edited by. London and New York: Academic Press.

Irwin, D. C., Cheng, M., Xiang, B., Rose, J. K. & Wilson, D. B. Cloning, expression and characterization of a family-74 xyloglucanase from Thermobifida fusca. *Eur J Biochem* **270**, 3083-3091,(2003).

Jeffcoat, R. & Kirkwood, S. Implication of histidine at the active site of exo-beta-(1-3)-D-glucanase from Basidiomycete sp. QM 806. *J Biol Chem* **262**, 1088-1091,(1987).

Kasahara, S., Nakajima, T., Miyamoto, C., Wada, K., Furuichi, Y. & Ichishima, E. Characterization and mode of action of exo-1,3-beta-D-glucanase from Aspergillus-saitoi. *J Ferment Bioeng* **74**, 238-240,(1992).

Kato, Y. & Matsuda, K. Xyloglucan in the Cell-Walls of Suspension-Cultured Rice Cells. *Plant Cell Physiol* **26**, 437-445,(1985).

Kawai, R. Functions of extracellular beta-1,3-glucanases from the basidiomycet ePhanerochaete chrysosporium. *Department of Biomaterials sciences* **Ph. D**,(2006).

Kawai, R., Igarashi, K. & Samejima, M. Gene cloning and heterologous expression of glycoside hydrolase family 55 beta-1,3-glucanase from the basidiomycete Phanerochaete chrysosporium. *Biotechnol Lett* **28**, 365-371,(2006a).

Kawai, R., Igarashi, K., Yoshida, M., Kitaoka, M. & Samejima, M. Hydrolysis of beta-1,3/1,6-glucan by glycoside hydrolase family 16 endo-1,3(4)-beta-glucanase from the basidiomycete Phanerochaete chrysosporium. *Appl Microbiol Biotechnol* **71**, 898-906, (2006b).

Li, S., Kim, W. D., Kaneko, S., Prema, P. A., Nakajima, M. & Kobayashi, H. Expression of rice (*Oryza sativa* L. var. Nipponbare) alpha-galactosidase genes in *Escherichia coli* and characterization. *Biosci Biotechnol Biochem* **71**, 520-526,(2007).

Martin, K., McDougall, B. M., McIlroy, S., Chen, J. & Seviour, R. J. Biochemistry and molecular biology of exocellular fungal beta-(1,3)- and beta-(1,6)-glucanases. *FEMS Microbiol Rev* **31**, 168-192,(2007).

Martin, K. L., McDougall, B. M., Unkles, S. E. & Seviour, R. J. The three beta-1,3-glucanases from Acremonium blochii strain C59 appear to be encoded by separate genes. *Mycol Res* **110**, 66-74,(2006).

Martinez, D., Larrondo, L. F., Putnam, N., Gelpke, M. D., Huang, K., Chapman, J., Helfenbein, K. G., Ramaiya, P., Detter, J. C., Larimer, F., Coutinho, P. M., Henrissat, B., Berka, R., Cullen, D. & Rokhsar, D. Genome sequence of the lignocellulose degrading fungus Phanerochaete chrysosporium strain RP78. *Nat Biotechnol* **22**, 695-700, (2004).

Martinez-Fleites, C., Guerreiro, C. I., Baumann, M. J., Taylor, E. J., Prates, J. A., Ferreira, L. M., Fontes, C. M., Brumer, H. & Davies, G. J. Crystal structures of Clostridium thermocellum xyloglucanase, XGH74A, reveal the structural basis for xyloglucan recognition and degradation. *J Biol Chem* **281**, 24922-24933,(2006).

McCarter, J. D. & Withers, S. G. Mechanisms of enzymatic glycoside hydrolysis. *Curr Opin Struct Biol* **4**, 885-892,(1994).

Nakatani, H. Monte Carlo simulation of multiple attack mechanism of beta-amylase-catalyzed reaction. *Biopolymers* **42**, 831-836,(1997).

Nelson, T. E., Johnson, J., Jr., Jantzen, E. & Kirkwood, S. Action pattern and specificity of an exo-beta-(1--3)-D-glucanase from basidiomycetes species QM 806. *J Biol Chem* **244**, 5972-5980,(1969).

Nijikken, Y., Tsukada, T., Igarashi, K., Samejima, M., Wakagi, T., Shoun, H. & Fushinobu, S. Crystal structure of intracellular family 1 beta-glucosidase BGL1A from the basidiomycete Phanerochaete chrysosporium. *FEBS Lett* **581**, 1514-1520,(2007).

Nikolskaya, A. N., Pitkin, J. W., Schaeffer, H. J., Ahn, J. H. & Walton, J. D. EXG1p, a novel exo-beta1,3-glucanase from the fungus Cochliobolus carbonum, contains a repeated motif present in other proteins that interact with polysaccharides. *Biochim Biophys Acta* **1425**, 632-636,(1998).

Nobe, R., Sakakibara, Y., Fukuda, N., Yoshida, N., Ogawa, K. & Suiko, M. Purification and characterization of laminaran hydrolases from Trichoderma viride. *Biosci Biotechnol Biochem* **67**, 1349-1357,(2003).

Nobe, R., Sakakibara, Y., Ogawa, K. & Suiko, M. Cloning and expression of a novel Trichoderma viride Laminarinase AI gene (lamAI). *Biosci Biotechnol Biochem* **68**, 2111-2119,(2004).

Oda, K., Kasahara, S., Yamagata, Y., Abe, K. & Nakajima, T. Cloning and expression of the exo-beta-D-1,3-glucanase gene (exgS) from Aspergillus saitoi. *Biosci Biotechnol Biochem* **66**, 1587-1590,(2002).

Pell, G., Szabo, L., Charnock, S. J., Xie, H., Gloster, T. M., Davies, G. J. & Gilbert, H. J. Structural and biochemical analysis of *Cellvibrio japonicus* xylanase 10C: how variation in substrate-binding cleft influences the catalytic profile of family GH-10 xylanases. *J Biol Chem* **279**, 11777-11788,(2004).

Pitson, S. M., Seviour, R. J. & McDougall, B. M. Noncellulolytic fungal beta-glucanases: their physiology and regulation. *Enzyme Microb Technol* **15**, 178-192,(1993).

Pitson, S. M., Seviour, R. J., McDougall, B. M., Woodward, J. R. & Stone, B. A. Purification and characterization of three extracellular (1-->3)-beta-D-glucan glucohydrolases from the filamentous fungus Acremonium persicinum. *Biochem J* **308**, 733-741,(1995).

Rigden, D. J. & Franco, O. L. Beta-helical catalytic domains in glycoside hydrolase families 49, 55 and 87: domain architecture, modelling and assignment of catalytic residues. *FEBS Lett* **530**, 225-232,(2002).

Rose, J. K., Braam, J., Fry, S. C. & Nishitani, K. The XTH family of enzymes involved in xyloglucan endotransglucosylation and endohydrolysis: current perspectives and a new unifying nomenclature. *Plant Cell Physiol* **43**, 1421-1435,(2002).

Ruel, K. & Joseleau, J. P. Involvement of an Extracellular Glucan Sheath during Degradation of Populus Wood by Phanerochaete chrysosporium. *Appl Environ Microbiol* **57**, 374-384,(1991).

Sakon, J., Adney, W. S., Himmel, M. E., Thomas, S. R. & Karplus, P. A. Crystal structure of thermostable family 5 endocellulase E1 from Acidothermus cellulolyticus in complex with cellotetraose. *Biochemistry* **35**, 10648-10660,(1996).

Schnorr, K., Jorgensen, P. L. & Schulein, M. (2004). Novozymes A/S US 6815192.

Sianidis, G., Pozidis, C., Becker, F., Vrancken, K., Sjoeholm, C., Karamanou, S., Takamiya-Wik, M., van Mellaert, L., Schaefer, T., Anne, J. & Economou, A. Functional large-scale production of a novel Jonesia sp xyloglucanase by heterologous secretion from Streptomyces lividans. *J Biotechnol* **121**, 498-507,(2006).

Sinnott, M. L. Catalytic mechanisms of enzymatic glycosyl transfer. *Chem Rev* **90**, 1171-1202,(1990).

Stone, B. A., and Clarke, A. E. (1992). *Chemistry and biology of 1,3-beta-glucans.*, edited by. Bundoora, Australia: La Trobe University Press.

Suzuki, H., Igarashi, K. & Samejima, M. Real-time quantitative analysis of carbon catabolite derepression of cellulolytic genes expressed in the basidiomycete Phanerochaete chrysosporium. *Appl Microbiol Biotechnol* **80**, 99-106,(2008).

Takada, G., Kawaguchi, T., Yoneda, M., Kawasaki, J., Sumitani, I. & Arai, M. (1998). *Molecular cloning and expression of the cellulolytic system of Aspergillus aculeatus*, edited by K. Ohmiya, K. Hayashi, K. Sakka, Y. Kobayashi, S. Karita & T. Kimura. Tokyo: Uni publishers Co., Ltd.,.

Tsukada, T., Igarashi, K., Yoshida, M. & Samejima, M. Molecular cloning and characterization of two intracellular beta-glucosidases belonging to glycoside hydrolase family 1 from the basidiomycete Phanerochaete chrysosporium. *Appl Microbiol Biotechnol* **73**, 807-814,(2006).

Vanden Wymelenberg, A., Minges, P., Sabat, G., Martinez, D., Aerts, A., Salamov, A., Grigoriev, I., Shapiro, H., Putnam, N., Belinky, P., Dosoretz, C., Gaskell, J., Kersten, P. & Cullen, D. Computational analysis of the Phanerochaete chrysosporium v2.0 genome database and mass spectrometry identification of peptides in ligninolytic cultures reveal complex mixtures of secreted proteins. *Fungal Genet Biol* **43**, 343-356,(2006).

Vanden Wymelenberg, A., Sabat, G., Martinez, D., Rajangam, A. S., Teeri, T. T., Gaskell, J., Kersten, P. J. & Cullen, D. The Phanerochaete chrysosporium secretome: database predictions and initial mass spectrometry peptide identifications in cellulose-grown medium. *J Biotechnol* **118**, 17-34,(2005).

Yaoi, K., Kondo, H., Hiyoshi, A., Noro, N., Sugimoto, H., Tsuda, S., Mitsuishi, Y. & Miyazaki, K. The structural basis for the exo-mode of action in GH74 oligoxyloglucan reducing end-specific cellobiohydrolase. *J Mol Biol* **370**,(2007).

Yaoi, K., Kondo, H., Noro, N., Suzuki, M., Tsuda, S. & Mitsuishi, Y. Tandem repeat of a seven-bladed beta-propeller domain in oligoxyloglucan reducing-end-specific cellobiohydrolase. *Structure* **12**, 1209-1217,(2004).

Yaoi, K. & Mitsuishi, Y. Purification, characterization, cloning, and expression of a novel xyloglucan-specific glycosidase, oligoxyloglucan reducing end-specific cellobiohydrolase. *J Biol Chem* **277**, 48276-48281,(2002).

Yaoi, K. & Mitsuishi, Y. Purification, characterization, cDNA cloning, and expression of a xyloglucan endoglucanase from Geotrichum sp. M128. *FEBS Lett* **560**, 45-50,(2004).

Yaoi, K., Nakai, T., Kameda, Y., Hiyoshi, A. & Mitsuishi, Y. Cloning and characterization of two xyloglucanases from Paenibacillus sp. strain KM21. *Appl Environ Microbiol* **71**, 7670-7678,(2005).

Yoshida, M., Igarashi, K., Wada, M., Kaneko, S., Suzuki, N., Matsumura, H., Nakamura, N., Ohno, H. & Samejima, M. Characterization of carbohydrate-binding

cytochrome b562 from the white-rot fungus Phanerochaete chrysosporium. *Appl Environ Microbiol* **71**, 4548-4555,(2005).

Zevenhuizen, L. P. & Bartnicki-Garcia, S. Structure and role of a soluble cytoplasmic glucan from Phytophthora cinnamomi. *J Gen Microbiol* **61**, 183-188,(1970).

Zverlov, V. V., Schantz, N., Schmitt-Kopplin, P. & Schwarz, W. H. Two new major subunits in the cellulosome of Clostridium thermocellum: xyloglucanase Xgh74A and endoxylanase Xyn10D. *Microbiology* **151**, 3395-3401,(2005).

Characterization and X-ray crystallography of PcXgh74B

2-1 Introduction

In contrust to the complicated structure of xyloglucans in cell walls, xyloglucans from seeds have relatively simple structure. Xyloglucan from tamarind seed (TXG) is one of the best-studied xyloglucans, and is commonly used as a substrate of xyloglucan related enzymes. TXG have side-chains of α-D-xylopyranosyl residues or β-D-galactopyranosyl α-D-xylopyranosyl moiety. Compositional analysis of oligosaccharide units in the polymers has shown that TXG has a repeating tetrasaccharide backbone of XXXG, XLXG, XXLG, or XLLG (Fig. 2-1) (York *et al.*, 1990).

Fig. 2-1
Tetrameric repeating subunits in TXG (York *et al.*, 1990). X, L, and G represent individual monomeric segments in the single-letter nomenclature. Glc, Xyl, and Gal indicate D-glucopyranose, D-xylopyranose, and D-galactopyranose, respectively.
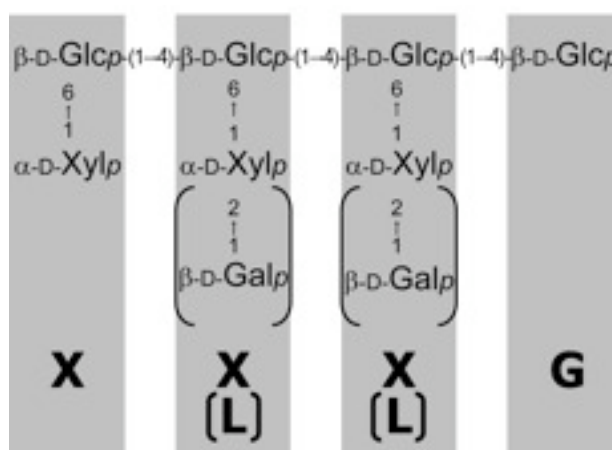
Although, many cellulases (EC 3.2.1.4) have been reported to hydrolyze xyloglucan as a substrate analogue (Vincken *et al.*, 1997), some endo-β-1,4-glucanases have high activity toward xyloglucan with little or no activity towards cellulose or cellulose derivatives (Edwards *et al.*, 1986, Pauly *et al.*, 1999). They have been assigned a new EC number (EC3.2.1.151) and belongs to GH families 5, 12, 44, and 74. Among these enzyme families, xyloglucanases classified into GH family 74 are known to have high specific activity toward xyloglucan, with inversion of anomeric configuration, and both endo- and exo-type hydrolases have been found from several microorganisms (Chhabra & Kelly, 2002, Hasper *et al.*, 2002, Yaoi & Mitsuishi, 2002, Irwin *et al.*, 2003, Grishutin *et al.*, 2004, Yaoi & Mitsuishi, 2004, Bauer *et al.*, 2005, Yaoi *et al.*, 2005).

In order to investigate structural basis for molecular recognition for branched structure of xyloglucan by GH family 74 enzymes, detailed characterization and crystallographic analysis of PcXgh74B, a novel member of GH family 74 are performed.

2-2 Experimental procedures

2-2-1 Materials

The substrate, TXG, was obtained from Dainippon Sumitomo Pharmaceutical Co., Ltd. (Osaka, Japan). PASC (phosphoric acid swollen cellulose) and BMCC (bacterial microcrystalline cellulose) used for binding assay were prepared as described before (Wood, 1988, Samejima *et al.*, 1998). The oligosaccharide, XXXGXXXG used for HPLC and MALDI-TOF MS analysis was prepared as described previously (Hayashi *et al.*, 1994). The oligo saccharides used as the ligands for crystallographic analysis were prepared by incubation of 5%(w/v) TXG with 0.7 μM of PcXgh74Bcat.

2-2-2 Cloning of cDNA encoding PcXgh74B from P. chrysosporium

P. chrysosporium K-3 (Johnsrud & Eriksson, 1985) was cultured at 26.5°C on the Kremer and Wood medium (Kremer & Wood, 1992) containing 2% cellulose (CF11; Whatman, Clifton, NJ, USA) as a sole carbon source, based on a previous report (Habu *et al.*, 1997). After 4 days of cultivation, mycelia were collected by filtration and crushed in liquid nitrogen. Purification of mRNA and first-strand cDNA synthesis were performed as described previously (Kawai *et al.*, 2006). Based on *P. chrysosporium* genome information and the prediction of secretion signal sequence by singnalP 3.0 server (http://www.cbs.dtu.dk/services/SignalP/:(Bendtsen *et al.*, 2004)), the following oligonucleotide primers: xgh74B-F 5'-GCAAGCCCACAAGC-ATACACATGGAAG-3' and xgh74B-R 5'-TCATAGACACAAATTGCCGGTACTCAC-3' were designed in order to amplify the cDNA encoding mature PcXgh74B. The amplified fragment was ligated into the pCR®4Blunt-TOPO vector (Invitrogen, Carlsbad, CA, USA) according to the manufacturer's instructions, and transformed into *Escherichia coli* strain JM109 (Takara Bio, Shiga, Japan). A database search for the deduced amino acid sequence was performed using blastp (http://www.ncbi.nlm.nih.gov/BLAST/) (Altschul *et al.*, 1990, Altschul *et al.*, 1997).

2-2-3 Expression and purification of recombinant PcXgh74B and PcXgh74Bcat

The oligonuceotide primers XGH74B-F 5'-TTT<u>GAATTC</u>GCAAGCCCACAAGCA-TACACATGGAAG-3', XGH74B-R1 5'-TTT<u>GCGGCCGC</u>TCATAGACACAAATTGCC-GGTACTCAC-3', and XGH74B-R2 5'-TTT<u>GCGGCCGC</u>TCAGTCGCCGTAAAAGA-TGCCGCGA-3', introducing *Eco*RI (underlined sequence) and *Not*I (double-underlined sequence) cleavage sites, were used to prepare the fragments for expression. The primer pairs

XGH74B-F and XGH74B-R1, or XGH74B-F and XGH74B-R2 were used to amplify the sequences encoding mature PcXgh74B or PcXgh74Bcat, respectively. These fragments were ligated into the pCR®4Blunt-TOPO vector and transformed into *E. coli* strain JM109 again. The fragments were digested with restriction enzymes, *Eco*RI and *Not*I, and ligated into the *P. pastoris* expression vector, pPICZα-A (invitrogen), at the same restriction sites. The vectors were transformed into *P. pastoris* KM-71H as described previously (Igarashi *et al*., 2005).

The transformants were cultivated in a growth medium, and then in induction medium as described previously (Igarashi *et al*., 2005). After induction for 3 days, the culture was centrifuged (15 min, 1,500 x g), and the supernatant was then mixed with 5% (w/v) of bentonite (Sigma Chemicals, USA) and incubated for 30 minutes at 4℃. The bentonite was removed by centrifugation (30 min, 1,500 x g), and the supernatant was concentrated by ammonium sulfate precipitation (70% saturation). The precipitate was dissolved in 20 mM potassium phosphate buffer (pH 7.0) and applied to a Toyopearl HW-40C gel permeation column (22 x 200 mm; Tosoh Co., Tokyo, Japan) for desalting. The protein fractions were concentrated and applied to a DEAE-Toyopearl 650S column (16 x 120 mm; Tosoh) equilibrated with 20 mM potassium phosphate buffer (pH 7.0). The protein was eluted with a linear gradient of 0 mM to 500 mM NaCl at 1 mL/min. The fractions were assayed for xyloglucanase activity using tamarind gum (Tokyo Chemical industry Co., Ltd., Tokyo, Japan) and *p*-hydroxybenzoic acid hydrazide (PAHBAH, Pfaltz & Bauer, Waterbury, CT, USA) as described in the following section. Then, the fraction containing xyloglucanase activity was equilibrated against 20 mM sodium acetate buffer (pH 5.0) containing 500 mM ammonium sulfate, and applied to a Phenyl Toyopearl 650S column (16 x 180 mm, Tosoh) equilibrated with the same buffer. The proteins were eluted with a linear gradient of 500 mM to 0 mM ammonium sulfate. The fractions containing the recombinant proteins were collected and equilibrated against 20 mM sodium acetate buffer, pH 5.5.

Deglycosylation was performed using endo-β-*N*-acetylglucosaminidase H (endo-H, New England Biolabs, Beverly, MA) as described previously (Yoshida *et al*., 2001). Purity and decrease in molecular weight were confirmed by SDS-PAGE.

2-2-4 *Determination of reducing sugar concentration*

The hydrolysing activity of the enzymes was measured by determination of reducing power of reaction mixture. For purification, adsorption experiments and examining hydrolysis toward various β-1,4-glycan, PAHBAH was used as described previously (Lever, 1972). For

determination of optimum pH, optimum temperature, pH stability, and thermal stability, the enzyme activity was assayed according to the Nelson and Somogyi method (Nelson, 1944, Somogyi, 1945, 1952). 2,2'-Bicinchoninate (Bicinchoninic Acid Disodium Salt, Nacalai Tesque Inc., Kyoto, Japan) was used for determination of kinetic constants as described previously (Waffenschmidt & Jaenicke, 1987, Doner & Irwin, 1992, Yaoi *et al.*, 2005).

2-2-5 Adsorption of PcXgh74B and PcXgh74Bcat on insoluble cellulose

Adsorption experiments were performed as described previously (Yoshida *et al.*, 2005). Intact PcXgh74B and PcXgh74Bcat were incubated with 0.5% PASC, 0.5% Avicel (Funacel SF; Funakoshi Co., Ltd., Tokyo, Japan), or 0.1% BMCC in 20 mM potassium phosphate buffer, pH 6.0. The mixtures of the protein and carbohydrates were incubated for 1 h at 30°C and then separated by centrifugation (10 min, 16,100 x g). The supernatants were centrifuged again to remove the precipitates completely, and remaining activity of the enzyme in each supernatant was determined using tamarind gum and PAHBAH as described above. The amount of protein that had been adsorbed on the cellulose and removed by centrifugation was then calculated.

2-2-6 Substrate specificity and kinetic parameters

The hydrolytic activities towards various β-1,4-glycans, CMC (CMC 7LFD, Hercules Inc., Wilmington, DE, USA), PASC, Avicel, BMCC, glucomannan (Glucomannan, from Konjac Tuber, Wako Pure Chemical Industries, Ltd., Osaka, Japan), galactomannan (Gum, Locust Bean, Sigma-Aldrich, St. Louis, MO. USA), and xylan (Xylan From Birchwood and Xylan From Beechwood, Sigma-Aldrich) were examined. Carbohydrates (0.25% w/v) were incubated with PcXgh74B at 30°C for 6 h in 100 mM sodium acetate buffer (pH 5.0) solutions, and reducing sugar concentration was measured using PAHBAH.

The temperature and pH effects on recombinant PcXgh74B and PcXgh74Bcat were analyzed. Xyloglucan-hydrolysing activity was assayed by measurement of the reducing power using the Nelson-Somogyi method. The optimum temperature for enzyme activity was determined by incubation with TXG (5 mg/mL) in 20 mM sodium phosphate buffer (pH 6.0) for 20 min at various temperatures. Thermostability was analysed by incubating the enzyme without substrate in the same buffer for 20 min at various temperatures, and the remaining activity was then assayed by incubation with TXG (5 mg/mL) at 45°C for 20 min. The optimum pH was determined by incubating the enzyme with TXG (5 mg/mL) at 40°C for 20

min in McIlvaine buffer solutions (0.2 M disodium hydrogen phosphate and 0.1 M citric acid) that varied in pH (from 2.0 to 9.0). The pH stability was assayed by incubating the enzyme in the absence of substrate at 30°C for 20 min in the same buffer solutions. The buffer solutions were then adjusted to pH 6.0, and the remaining enzyme activity was assayed by incubation with TXG (5 mg/mL) at 30°C for 20 min.

Kinetic constants were determined at TXG concentrations ranging from 0.2 to 5 mg/mL using 2.5 µg enzyme/mL in 20 mM sodium phosphate buffer (pH 6.0). The bicinchoninate assay was used to quantify reducing sugars. The Michaelis constant (K_m), specific activity and catalytic rate (k_{cat}) were calculated from a plot of initial reaction rates versus substrate concentration using KaleidaGraph 3.6.4 (Synergy, Reading, PA, USA).

2-2-7 HPLC and MALDI-TOF MS analysis

The reaction products of TXG and XXXGXXXG generated by PcXgh74B treatment were analysed by normal-phase HPLC and MALDI-TOF MS. HPLC was carried out with an Amide-80 normal-phase column (4.6 x 250 mm; Tosoh, Tokyo, Japan) using 65% acetonitrile (isocratic) at a flow rate of 0.8 mL/min. MALDI-TOF MS was performed with a Voyager mass spectrometer (Perseptive Biosystems) at an accelerating energy of 20 kV, in linear mode, and with positive-ion detection. The matrix was 2,5-dihydroxybenzoic acid in 50% acetonitrile at a concentration of 10 mg/mL. XXXG (Tokyo Chemical Industry Co., Ltd., Tokyo, Japan) was used as an external calibration standard.

2-2-8 Viscosimetric assay and gel permeation chromatography

Viscosimetric assays and gel permeation chromatography were carried out as described previously (Yaoi *et al*., 2005). For viscosimetric assays, TXG was incubated with PcXgh74B in 20 mM sodium phosphate buffer (pH 6.0), with *Geotrichum* XEG in 50 mM sodium acetate buffer (pH 5.5), or with *Paenibacillus* XEG74 sodium phosphate buffer (pH 6.0) (Yaoi *et al*., 2005) for different times. For gel permeation chromatography, TXG was incubated with PcXgh74B in 20 mM buffer (sodium acetate buffer: pH 5.0, sodium phosphate buffer: pH 6,0 or 7.0, Tris-HCl buffer: pH 8.0), with Geotrichum XEG in 50 mM sodium acetate buffer (pH 5.5), or with Paenibacillus XEG74 in 20 mM sodium phosphate buffer (pH 6.0) (Yaoi *et al*., 2005).

2-2-9 X-ray crystallographic analysis of PcXgh74Bcat

The initial screen for crystallization of PcXgh74Bcat was performed using Nextal JCSG+ suite (QIAGEN) towards the 10 mg/ml solution of purified PcXgh74Bcat. The condition No. 29 was refined by varying the pH of the buffer and the concentration of the precipitant. Crystals for data collection were prepared by sitting drop vapor diffusion method using the reservoir containing 1 M sodium potassium phosphate, 100 mM sodium citrate pH 7.0, and 5%(v/v) glycerol. The drops made by mixing 0.6 μl of the protein solution and same amount of the reservoir, and the crystals were grown to 0.5 mm during five days equilibration at 298 K (Fig. 2-9). Diffraction data sets were collected at beam line BL6A and BL5A of the Photon Factory, KEK. Prior to data collection, the crystals were transferred to reservoir containing 15%(v/v) glycerol and flash-cooled in a stream of nitrogen gas at 100 K. In order to solve the XGO4 liganded structure, a crystal was soaked into cryoprotectant solution containing approximately 5 mM XGO4 for 30 minutes before data collection. Data were processed and scaled using the HKL2000 program suite (Otwinowski, 1997). Molecular replacement was performed using program Molrep (Vagin & Teplyakov, 1997). The search model used for molecular replacement was made by swiss-model server (Arnold *et al*., 2006) using the structure of CtXgh74A (PDB ID 2CN3) as the template. Manual model rebuilding and refinement were achieved using Coot (Emsley & Cowtan, 2004) and Refmac5 (Murshudov *et al*., 1997). Figures were created using PYMOL ((DeLano, 2002); DeLano Scientific LLC, Palo Alto, CA; http://www.pymol.org) indonesia (Madsen, D., http://xray.bmc.uu.se/dennis/ manual/).

2-3 Results

### 2-3-1 Function of CBM1 in recombinant Phanerochaete chrysosporium PcXgh74B

The cDNA encoding PcXgh74B was heterologously expressed in the yeast *Pichia pastoris*, and the recombinant enzymes with and without CBM1 (PcXgh74B and PcXgh74Bcat, respectively) were purified by column chromatography. As shown in Fig. 2-2, the molecular masses of purified PcXgh74B and PcXgh74Bcat were 130 and 80 kDa, respectively, being apparently higher than the masses calculated from the amino acid sequences (88.4 and 75.5 kDa, respectively). Since there are three N-glycosylation sites in the sequence of the catalytic domain according to the NetNGlyc 1.0 server (http://www.cbs.dtu.dk/services/NetNGlyc/), the N-glycan was eliminated by Endo-H treatment. After the treatment, the molecular mass of PcXgh74Bcat becomes close to the calculated value, whereas that of PcXgh74B was still approximately 20 kDa larger than the calculated value. There are numerous O-glycosylation sites between the catalytic domain and CBM, as predicted by NetOGlyc 3.1 server (http://www.cbs.dtu.dk/services/NetOGlyc/), so the larger-than-calculated molecular weight of intact PcXgh74B presumably reflects both N- and O-glycosylations (Julenius *et al.*, 2005).
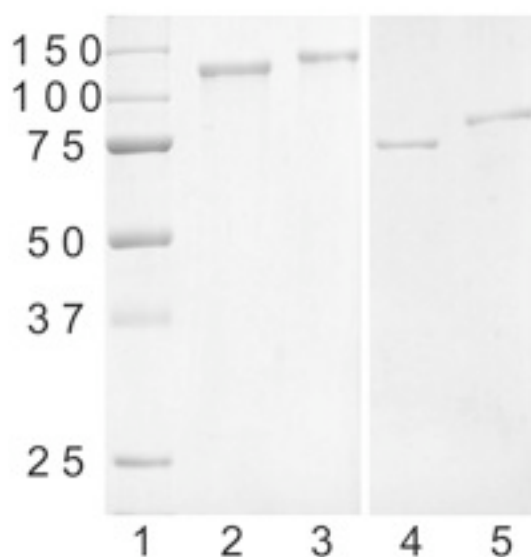
Fig. 2-2
Effect of deglycosylation on purified PcXgh74B. Lane 1, molecular weight standards (kDa); lane 2, PcXgh74B incubated with endo-H; lane 3, PcXgh74B; lane 4, PcXgh74Bcat incubated with endo-H; lane 5, PcXgh74Bcat.

The binding properties of PcXgh74B and PcXgh74Bcat were investigated using solid cellulosic substrates, phosphoric acid swollen cellulose (PASC), Avicel, and bacterial microcrystalline cellulose (BMCC), as shown in Fig. 2-3. PcXgh74B was adsorbed well on all three cellulose samples, whereas the amount of bound PcXgh74Bcat, without CBM1, was lower than that of the intact enzyme. The CBM1 in PcXgh74B may contribute to the binding on a crystalline, rather than amorphous, surface, because increase of crystallinity (PASC < Avicel < BMCC) led to significant differences of adsorption between intact PcXgh74B and PcXgh74Bcat. The kinetic features of the intact enzyme and catalytic domain were compared as shown in Table 2-1. The kinetic constants for TXG of the intact enzyme and catalytic domain were all similar, and no significant difference was observed between the two proteins, suggesting that CBM1 in PcXgh74B may contribute to the localization of this enzyme, but not to its function for hydrolysis of the soluble substrate.
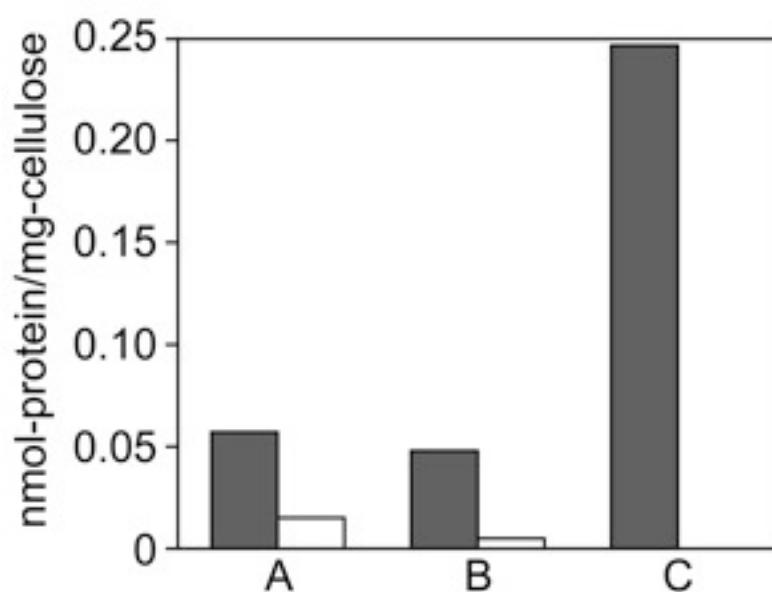
Fig. 2-3
Adsorption of PcXgh74B (grey) and PcXgh74Bcat (white) on cellulose quantified by measuring the activity remaining in the supernatant of a mixture of the enzyme and insoluble cellulose (A, PASC; B, Avicel; C, BMCC).

Table 2-1 Kinetic constants for the hydrolysis of TXG by PcXgh74B and PcXgh74Bcat.

Enzymes	K_m (mg·mL^{-1})	k_{cat} (s^{-1})	k_{cat}/K_m (mL·mg^{-1}·s^{-1})
PcXgh74B	0.25 ± 0.04	28.1 ± 1.4	112
PcXgh74Bcat	0.28 ± 0.04	31.9 ± 1.7	114

2-3-2 Substrate specificity of PcXgh74B

When TXG was used as a substrate, PcXgh74B showed optimum hydrolysis at pH 6.0 and 55℃, and was stable between pH 5.0 and 8.0 at 30℃. The K_m of TXG hydrolysis by PcXgh74B was estimated to be 0.25 mg/mL, and the k_{cat} was 28.1 s^{-1} when the activity was measured for the reducing sugar. However, PcXgh74B showed very low activity (less than 5% relative activity with respect to TXG) toward other β-1,4-glycans, carboxymethyl cellulose (CMC), PASC, Avicel, BMCC, glucomannan, galactomannan, and xylan, indicating that PcXgh74B has typical characteristics of a GH family 74 xyloglucanase.

The hydrolytic products formed from TXG by PcXgh74B were analyzed by normal-phase HPLC and matrix-assisted laser desorption ionization-time-of-flight mass spectrometry (MALDI-TOF MS), as shown in Fig. 2-4. The results of HPLC suggested that the reaction mixture contained oligosaccharides with three different DP (Fig. 2-4B), which showed the same retention times as oligosaccharides with DPs of 7-9, XXXG, XLXG, XXLG, and XLLG. The molecular weights of these fragments estimated by MALDI-TOF MS (Fig. 2-4D) coincided with those of authentic xyloglucan oligosaccharides. We also analyzed the hydrolytic products of xyloglucan oligosaccharide, XXXGXXXG, and obtain a single peak at the retention time of XXXG (Fig. 2-4C), suggesting that PcXgh74B hydrolyzes the unbranched glucose residues in TXG.
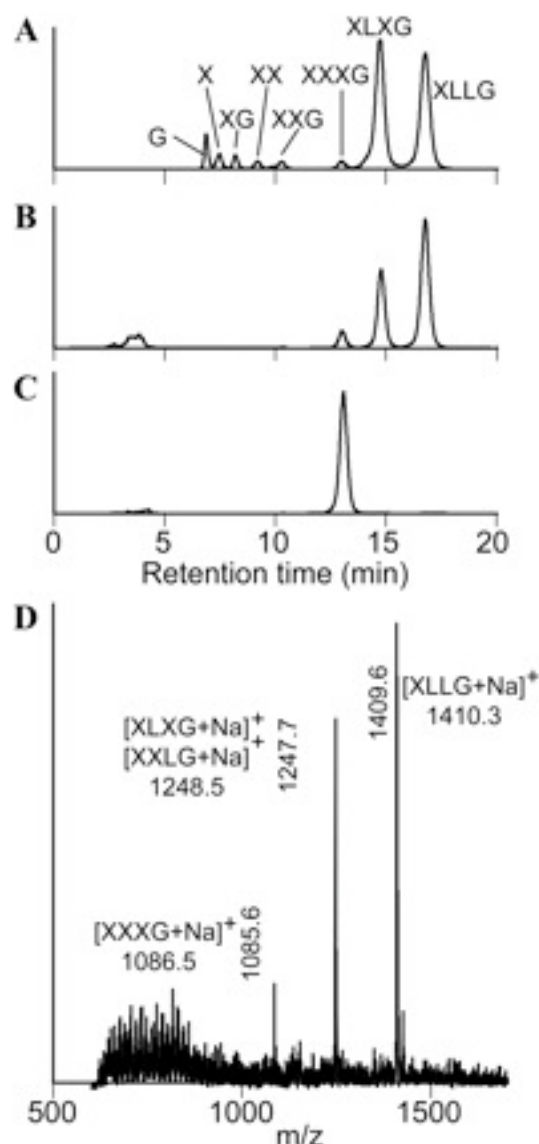
Fig. 2-4

Analysis of the final products resulting from complete digestion of TXG and xyloglucan oligosaccharide, XXXGXXXG, by PcXgh74B. A, standards for HPLC analysis (DP values of G, X, XG, XX, XXG, XXXG, XLXG and XLLG are 1, 2, 3, 4, 5, 7, 8 and 9 respectively); B, HPLC analysis of digestion products of TXG; C, HPLC analysis of digestion products of XXXGXXXG; D, MALDI-TOF MS analysis of digestion products of TXG.

2-3-3 Viscometric assay and gel permeation chromatography of TXG hydrolysis

The viscosity of TXG was monitored during the hydrolysis with PcXgh74B and XEG from *Geotrichum* sp. M128 (*Geotrichum* XEG), and the viscosity is plotted versus amount of reducing sugar in Fig. 2-5. A similar plot for XEG74 from *Paenibacillus* sp. strain KM21 (*Paenibacillus* XEG74) is also shown for reference (Yaoi *et al*., 2005). As described above, PcXgh74B effectively hydrolyzed TXG, and a decrease of viscosity was observed, with the production of reducing sugar, indicating that PcXgh74B is endo-type enzyme, which cleaves polymeric substrates in the middle of the molecule. However, there were differences among the plots for the three enzymes; of the degree of hydrolysis-specific viscosity plot for PcXgh74B is intermediate between those of *Geotrichum* XEG and *Paenibacillus* XEG74. Therefore, the change of the molecular weight distribution of TXG during the hydrolysis was analysed by gel permeation chromatography (GPC) with a refractive index (RI) detector, as shown in Fig. 2-6. In the case of *Geotrichum* XEG, the molecular mass decreased rapidly even at the initial stage of the reaction, suggesting that the degradation process involved random hydrolysis of β-1,4-linkages in the xyloglucan polymer chain. On the other hand, the degradation pattern of PcXgh74B was rather similar to that of *Paenibacillus* XEG74, since the oligosaccharides with DP=7-9 (XXXG, XLXG, XXLG, and XLLG: XGO4) were observed from the initial stage of the reaction (peak B in Fig. 2-6A and Fig. 2-7B). However, in the case of PcXgh74B, there is an additional peak at an earlier retention time (12 min, peak A). Peak A was fractionated and analyzed by MALDI-TOF MS analysis, and was found to consist of oligosaccharides of DP 16-18, as shown in Fig. 2-7A.
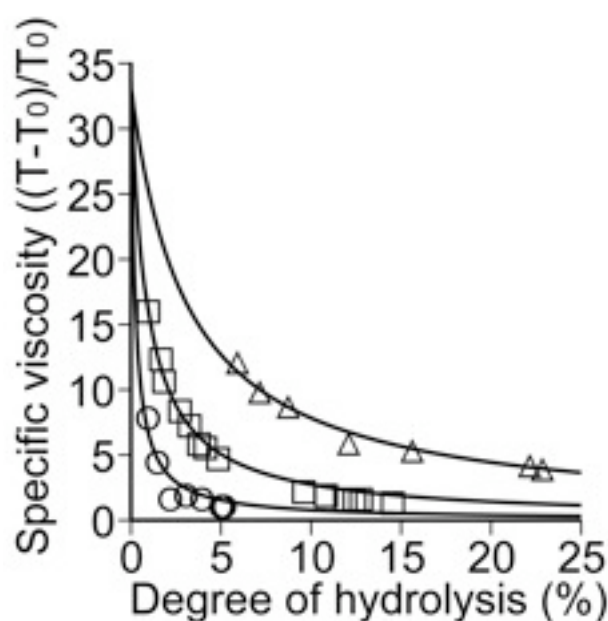
Fig. 2-5
Viscosimetric analysis of TXG incubated with the xyloglucanases. After various incubation times, the specific viscosity was calculated and the hydrolysis ratio was determined by measuring the reducing power. The reducing power obtained by complete digestion with excess enzyme was normalized to 100%. Square, PcXgh74B; circle, *Geotrichum* XEG; triangle, *Paenibacillus* XEG74.
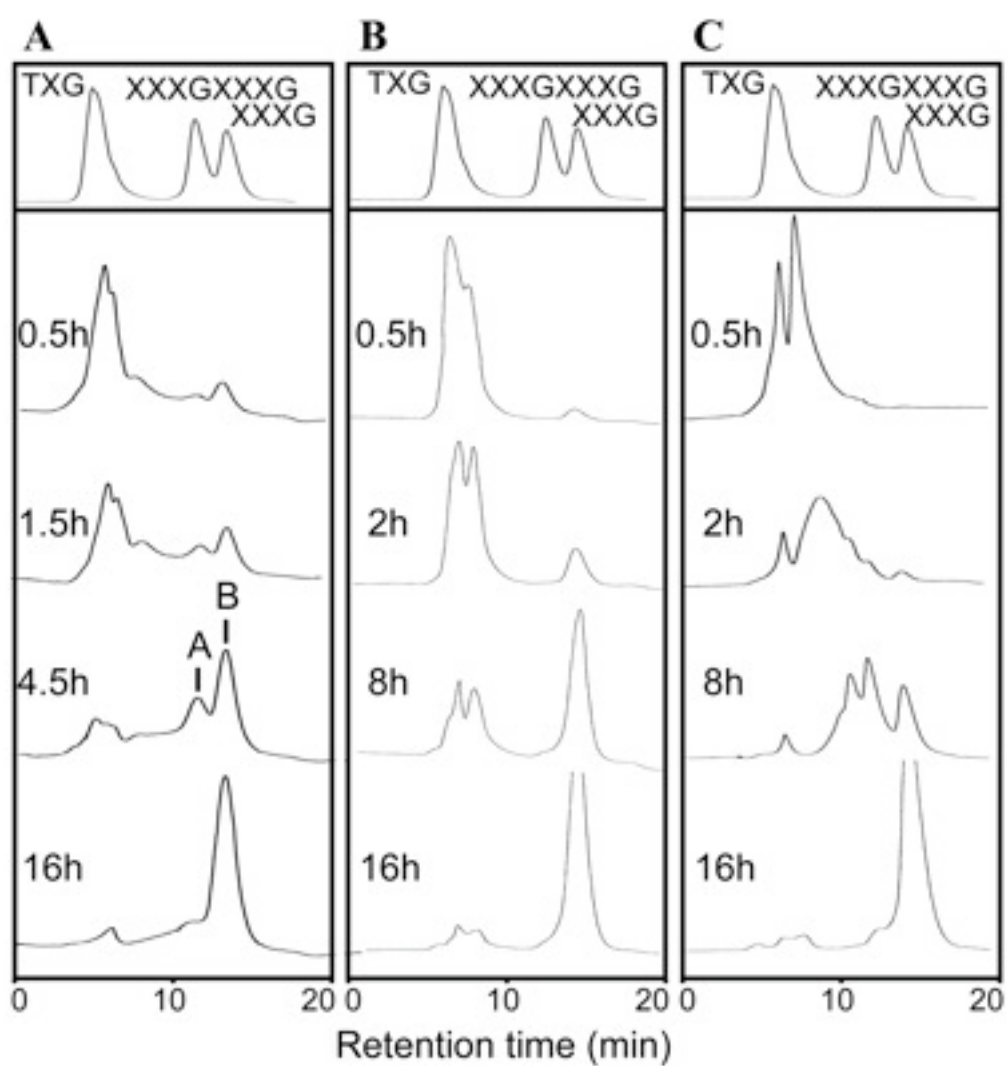
Fig. 2-6
Analysis of xyloglucan hydrolysis products by means of GPC. TXG was incubated with the xyloglucanases for various times, and the reaction products were applied to a gel permeation column. (A) PcXgh74B; (B) *Paenibacillus*XEG74; (C) *Geotrichum*XEG.
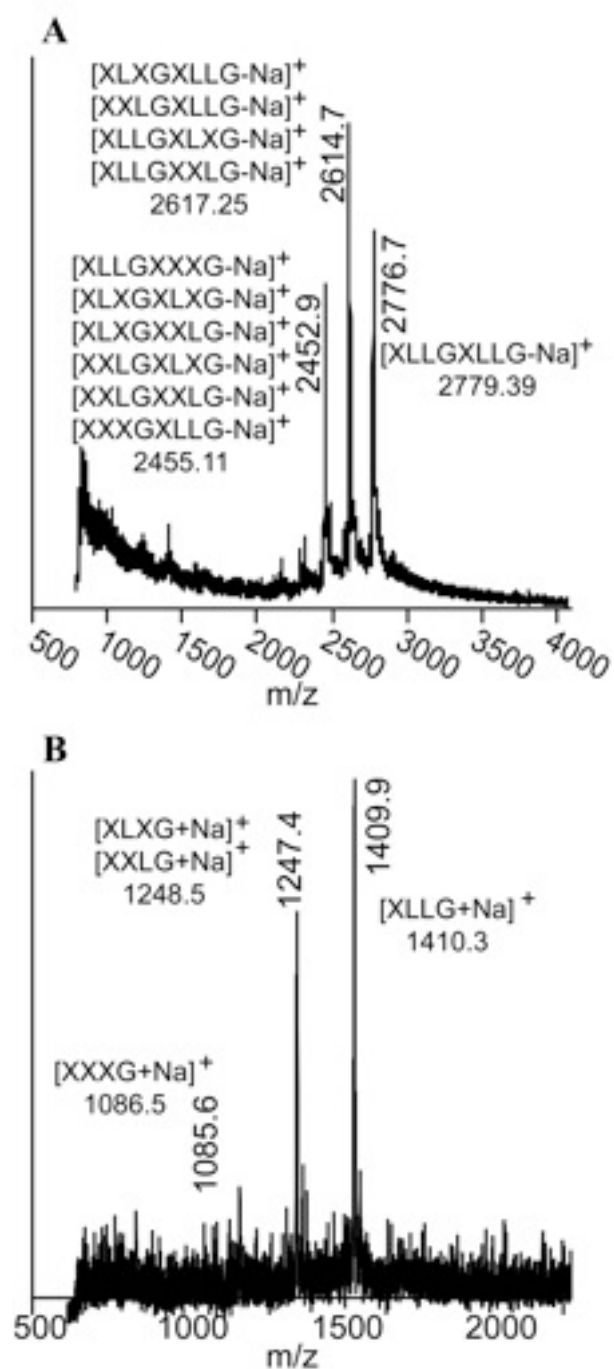
Fig. 2-7
MALDI-TOF-MS analysis of peaks A (A) and B (B) in Fig. 6. The peaks were fractionated and analysed by MALDI-TOF-MS. Peak A included oligosaccharides of DP=16-18, and peak B included oligosaccharides of DP=7-9.

2-3-4 Crystal structure of PcXgh74Bcat

The PcXgh74Bcat crystals (Fig. 2-9) belong to the space group $P6_522$ with unit cell parameters of $a = b = 103.3$ Å, $c = 334.637$ Å. The X-ray diffraction data for both unliganded and products-complexed forms were collected at 2.5 Å resolution. Molecular replacement method using the homology model was successfully employed for structure determination. An asymmetric unit contains one protein molecule of PcXgh74Bcat. The structures of unliganded and XGO-complexed forms were refined to R-values (R-free) of 20.4% (27.1%) and 22.8% (30.4%), respectively. The data collection statistics and refinement statistics are shown in Table 2-2 and 2-3. Since two structures are very similar with the r.m.s.d. for Cα atoms 0.24 Å, products liganded form will be described unless otherwise noted.
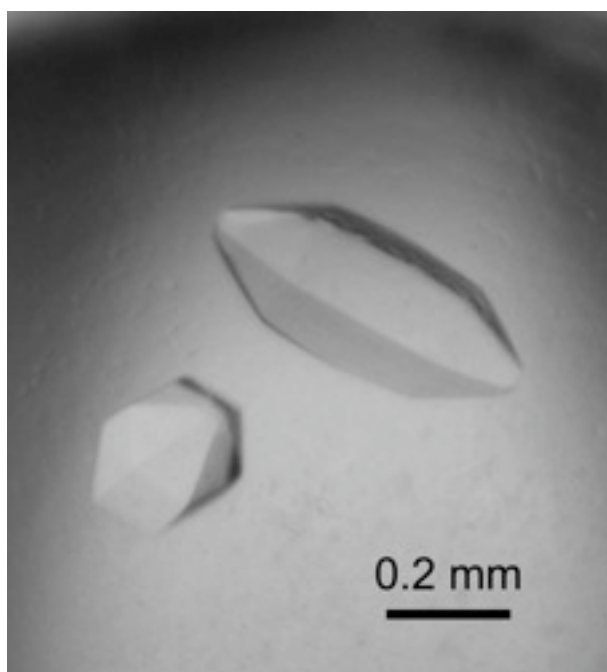
Fig. 2-9
Crystals of PcXgh74Bcat obtained in the optimised sitting-drop condition.

Table 2-2 Data collection statistics.

Data set	Unliganded	product complex
Beamline	BL6A	BL5A
Wavelength (Å)	1.00	1.00
Space group	$P6_522$	$P6_522$
Cell dimensions (Å)	a = b = 103.3, c = 334.6	a = b = 103.4, c = 334.4
Resolution (Å)*	50-2.5 (2.54-2.50)	50-2.5 (2.59-2.50)
Total reflections	2,060,731	4,040,000
Unique reflections	37,816	37,859
Completeness (%)*	100.0 (100.0)	100.0 (100.0)
Multiplicity*	21.1 (21.9)	20.2 (20.2)
Average $I/\sigma(I)$*	46.5 (7.8)	44.1 (4.6)
R_{sym} (%)*	9.7 (50.1)	11.3 (50.5)

*Values in parentheses are for the highest resolution shell.

Table 2-3 Refinement statistics.

Data set	Unliganded	product complex
Resolution (Å)	43.2-2.5	47.3-2.5
R-factor/R-free (%)	20.4/27.1	22.8/30.4
No. of reflections	35788	35764
No. of atoms	5969	5934
r.m.s.d. from ideal values		
Bond length (Å)	0.015	0.016
Bond angles (degree)	1.17	1.24
Average B-factor (Å^2)		
Protein	32.3	47.9
Sugar chain	51.4	63.9
Water	42.5	51.6
Ligands	-	68.8
Ramachandran plot (%)		
Favored	89.3	90.5
Allowed	9.5	7.9
Disallowed	1.3	1.5

The structure includes all 721 amino acid residues of PcXgh74Bcat excluding possible N-terminal residues from expression vector (Glu-Ala-Glu-Ala-Glu-Phe) that were highly disordered. All three *N*-glycosylation sites predicted by NetNGlyc 1.0 server showed the sugar chains. Asn-238 and Asn-413 exhibited two GlcNAc and one mannose residues, and Asn-629 exhibited two GlcNAc residues. As expected from sequence similarity to other three GH family 74 enzymes whose structures have been published, PcXgh74Bcat consists of two seven bladed β-propeller domains, forming large open cleft (Fig. 2-10). Either side of the substrate binding cleft are open, *i.e.* there are no loops or other structure blocking side of the binding cleft.
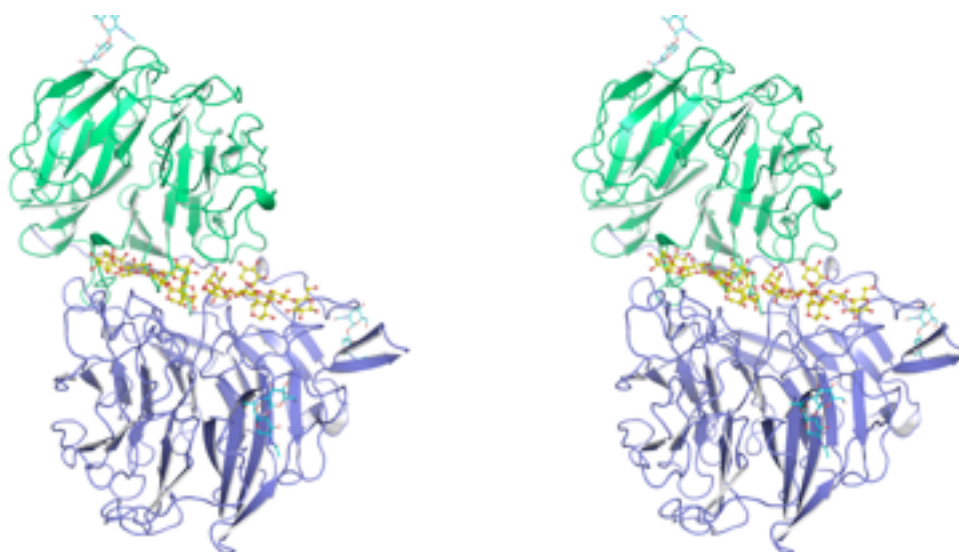
Fig. 2-10
Stereoview of overall structure of PcXgh74B. N- and C- domains are colored blue and green, respectively. Xyloglucan oligosaccharides bound to binding cleft were shown in ball and stick model. *N*-linked sugar residues are shown in stick models colored cyan.

Fig. 2-11 shows electron density map corresponding to two oligosaccharides molecules bound in the open cleft. GXLG (DP = 7) is bound to the subsite -4 to -1, and XXXG (DP = 7) is bound to subsite +1 to +4. Following the designation of sugar residues bound to CtXgh74A structure (Martinez-Fleites *et al.*, 2006), a glucose residue sitting in subsite n are designated as Glc^n, and xylose residues attached to O-6 position of Glc^n are designated as $Xyl^{n'}$. One of expected xylose residues $Xyl^{-4'}$, and galactose residues possibly attached at O-2 position of $Xyl^{-3'}$, $Xyl^{+2'}$, and $Xyl^{+3'}$ were invisible. As shown in Fig. 2-12, the shape of the electron density corresponding to Glc^{-1} apparently displays α-anomeric configuration, confirming the inverting hydrolysis catalyzed by PcXgh74Bcat. The carboxyl group of catalytic residues (Asp-38 and Asp-446) are located on both sides of plane of the Glc^{-1} sugar ring at distances of approximately 3.6 Å from O-1 hydroxyl group and C-1 carbon, respectively. Asp-38 and Asp-446 also form hydrogen bonds with Glc^{-1} O-2 hydroxyl group and ring oxygen (O-5), respectively. The side chain of Leu-445 next to Asp-446 protrude to the cleft, and is contiguously located (approximately 3.3 Å) to O-1 of Glc^{-1}.

Fig. 2-11
The ligand molecules depicted with the F_{obs} - F_{calc} omit electron density map contoured at 1.8 σ. GXLG bound at subsite -4 to -1 (A), XXXG bound at subsite +1 to +4 (B), and side chain residues attached to Glc^{-2} (C) are shown as ball-and-stick models with carbon atoms colored yellow. The subsite numbers are indicated in the center of each sugar ring.
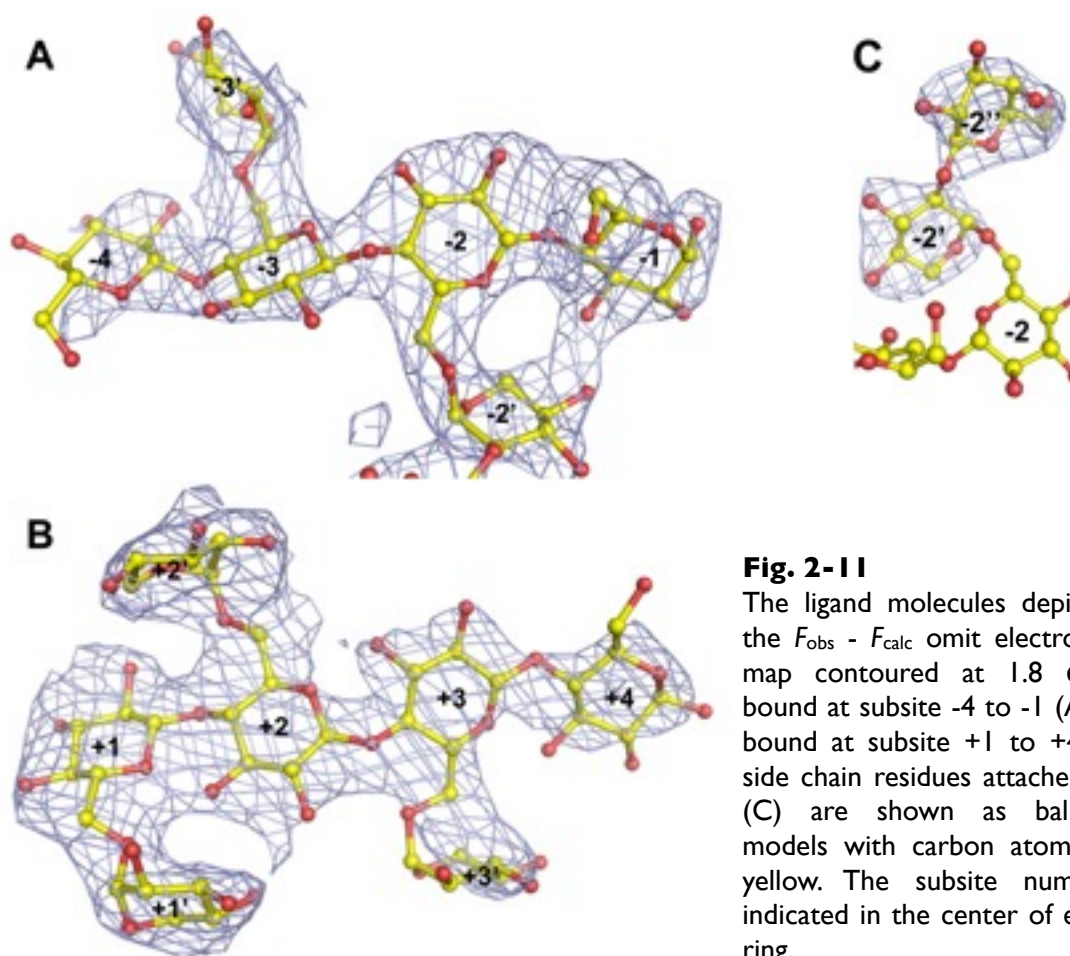
Fig. 2-12

Stereo view of Glc^{-1} with the F_{obs} - F_{calc} omit electron density map contoured at 1.8 σ. The catalytic residues, Asp-38 and Asp-446, and Leu-445 near O6 hydroxy group of Glc^{-1} are drawn as stick models. The residues colored blue and green are those from N- and C- domain, respectively. The distances (Å) from C1 carbon to carboxyl group of Asp446 and from O1 hydroxyl group to Asp38 carboxyl group are indicated.
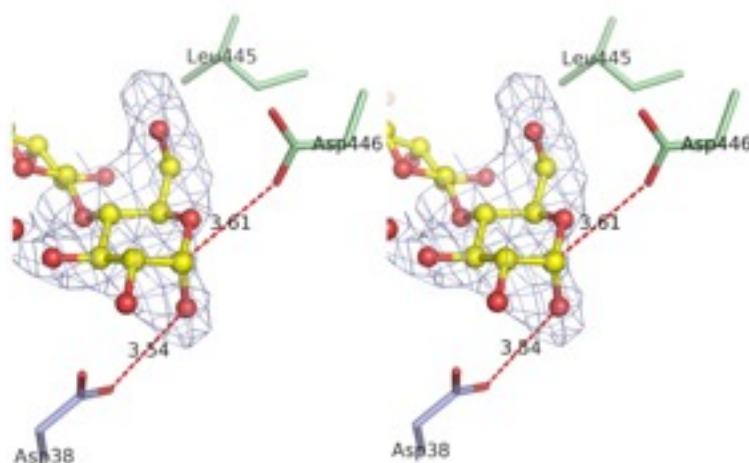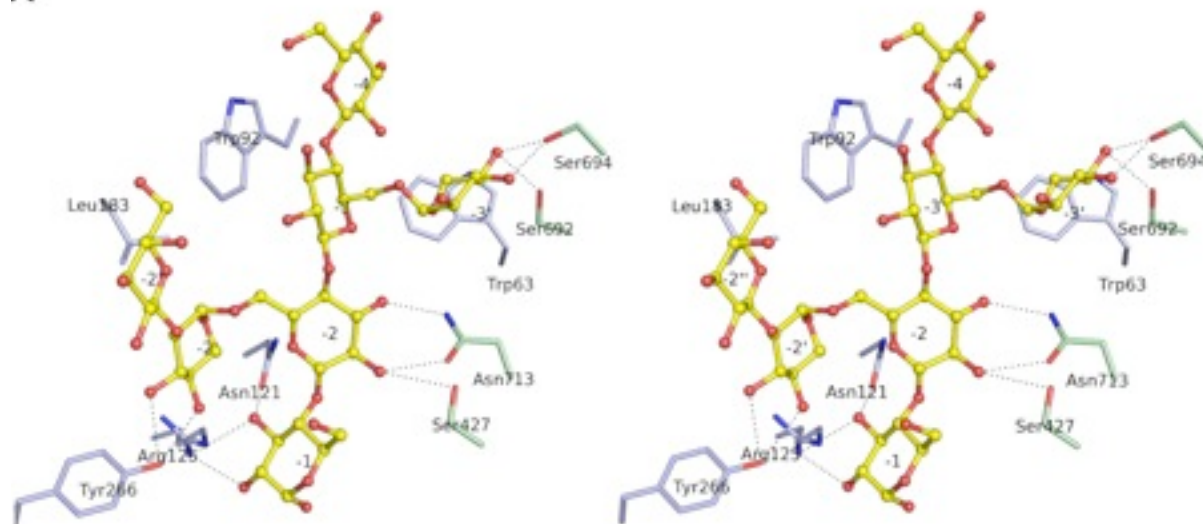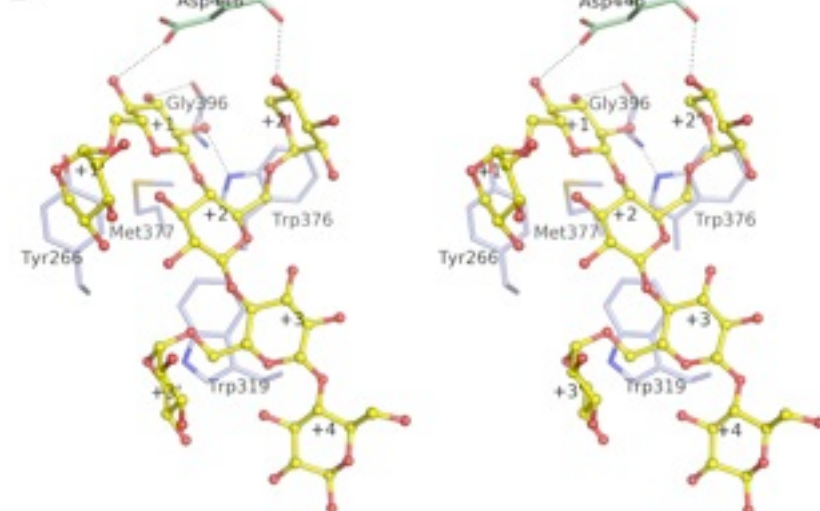
Fig. 2-13

Stereo view of binding of GXLG and XXXG at subsite -4 to -1 (A) and +1 to +4 (B), respectively. Amino acid residues are colored in the same way as Fig. 2-10. Dashed lines indicate hydrogen bonds.

Fig. 2-13 represents direct interactions between PcXgh74B and two xyloglucan oligosaccharides. Glc^{-4} which is the non-reducing end of GXLG are located at the entrance of the cleft and well exposed to solvent. At the other side of the end, four aromatic residues, Tyr-295, Trp-320, Trp-341, and Tyr-344, form hydrophobic surface which extends from Glc^{-4} to the end of the cleft, as shown in Fig. 2-14.

The amino acid residues interact with both main-chain and side-chain residues of the ligands. In the sequence alignment shown in Fig. 2-15, the residues involved in the ligand binding are well conserved among GH family 74 enzyme. However, the Leu-183 which is near the Xyl$^{-3'}$ is substituted to tyrosine residues in the *Paenicacilus*XEG74 and HjCel74A sequence, suggesting that *Paenicacilus*XEG74 and HjCel74A bind Xyl$^{-3'}$ residue more tightly than PcXgh74B.
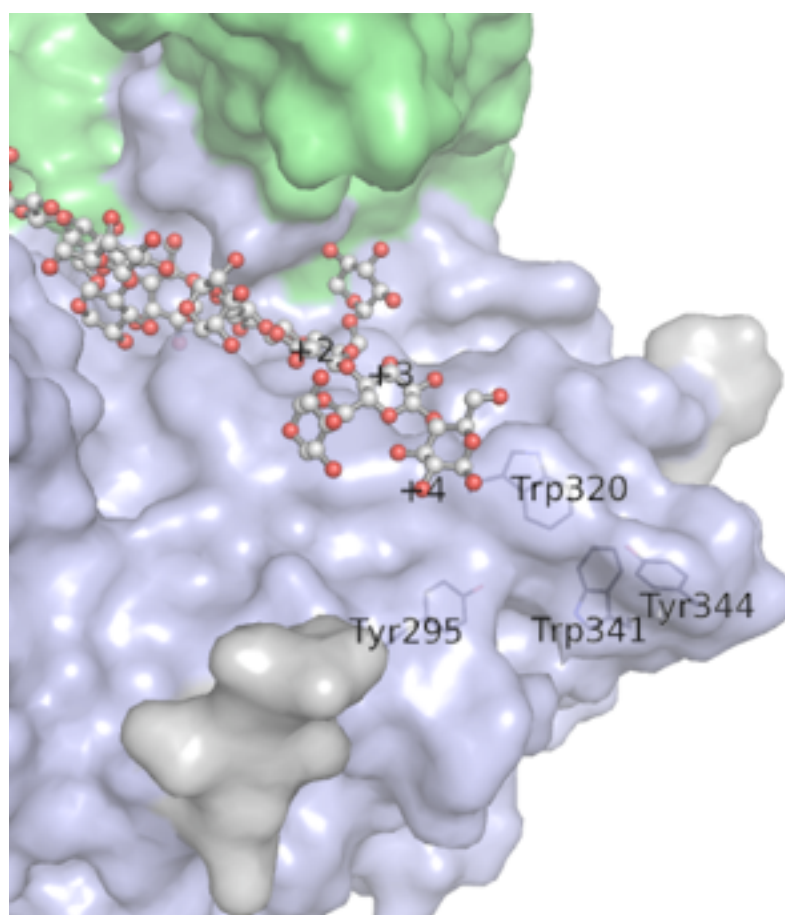
Fig. 2-14 Molecular surface of PcXgh74B. The aromatic residues at reducing end of the cleft are indicated.
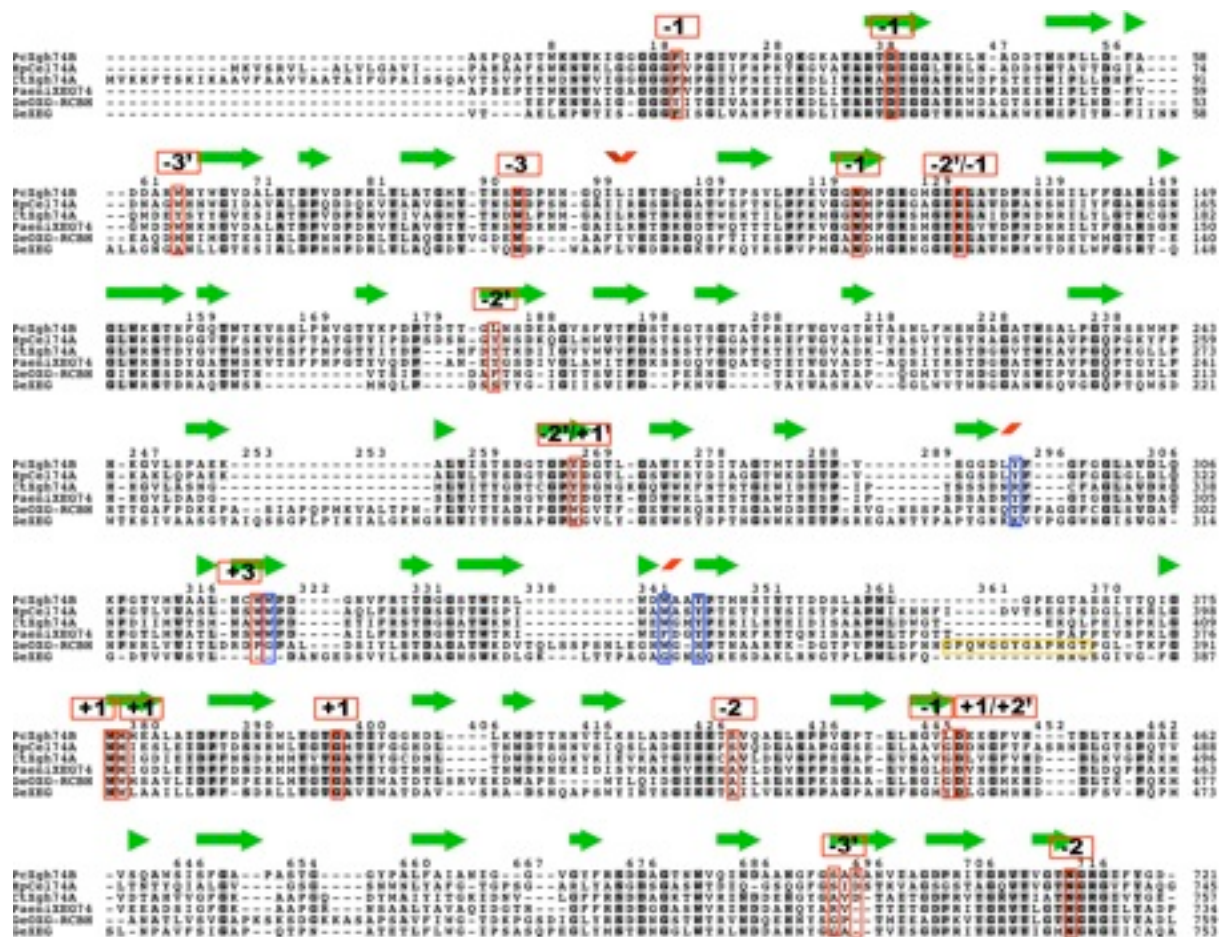
Fig. 2-15

Sequence alignment of the enzymes belonging to GH family 74. The amino acid residues interacting with ligand sugar residues are indicated in the red boxes. The yellow box and the blue boxes indicates 'exo-loop' of OXG-RCBH and aromatic residues found near the reducing end of ligand, respectively.

47

2-4 Discussion

Filamentous fungi produce several extracellular xyloglucanases when they grow on plant cell wall as a carbon source. Before their characterization, fungal GH family 74 xyloglucanases had been thought to be cellulases, since they have apparent activity against amorphous cellulose and soluble cellulose derivatives. Moreover, some fungi produce GH family 74 xyloglucanases with the family 1 CBM, and this also results in enzymes that had been characterized as cellulases. According to the total genome sequence of *P. chrysosporium*, there are two enzymes belonging to GH family 74 (Xgh74A and PcXgh74B), and PcXgh74B is known to have the family 1 CBM at the C-terminal region (Martinez *et al.*, 2004). Therefore, heterologous expression of recombinant PcXgh74B in yeast was performed and the function of CBM1 in PcXgh74B was characterized from adsorption and kinetic points of view. Apparent adsorption of intact PcXgh74B was observed when solid cellulosic substrates were used, but a comparison of the kinetic parameters of intact PcXgh74B and PcXgh74Bcat clearly indicates that the CBM in PcXgh74B does not contribute to the hydrolytic reaction of soluble xyloglucan substrates. The results suggest that the CBM might determine the localization of this enzyme or help in the hydrolysis of insoluble substrates.

Recently, some diversity of substrate specificity and mode of action has been reported for GH family 74 enzymes; for example, OXG-RCBH from *Geotrichum* sp. M128 and OREX from *A. nidulans* have oligoxyloglucan reducing end-specific exo-activity and cannot hydrolyze xyloglucan polymer (Yaoi & Mitsuishi, 2002, Bauer *et al.*, 2005), whereas most enzymes belonging to GH family 74 are β-1,4-glucanases with the highest activity toward xyloglucan (Hasper *et al.*, 2002, Irwin *et al.*, 2003, Grishutin *et al.*, 2004, Yaoi & Mitsuishi, 2004, Yaoi *et al.*, 2005). Among the latter endo-type enzymes, *Geotrichum* XEG randomly hydrolyze xyloglucan molecule, decreasing average DP of TXG gradually. On the other hands, *Paenibacillus*XEG74 and HjCel74A have exo-like activity, producing XGO4 even at the initial stage of the reaction (Grishutin *et al.*, 2004, Yaoi *et al.*, 2005). Crystal structures of three GH family 74 enzymes have been published in past several years, demonstrating structural basis of exo-type OXG-RCBH and endo-type *Geotrichum* XEG. However, 3D structures of *Paenibacillus*XEG74 and HjCel74A that show exo-like mode of action are not available yet. Although crystal structure of CtXgh74A have been reported together with its endo-type activity, it is not clear whether the enzyme produces XGO4 from initial stage of hydrolysis of TXG (Zverlov *et al.*, 2005, Martinez-Fleites *et al.*, 2006).

In this study, PcXgh74B rapidly decreases viscosity of TXG solution, indicating that the enzyme have typical endo-type activity. The result is consistent with the fact that PcXgh74B lacks exo-loop in its sequence (Fig. 2-15). HPLC and MALDI-TOF MS analyses revealed that PcXgh74B produces only XXXG from XXXGXXXG (DP=14), indicating that the enzyme hydrolyzes only glycosidic linkages of unsubstituted glucose residues. The crystal structure of PcXgh74B demonstrates that the recognition mechanism is similar to that of *Geotrichum*XEG, *i.e.* Leu-445 plays the same role as Tyr-457 of *Geotrichum* XEG, blocking the subsite for Xyl$^{-1'}$ (Yaoi *et al.*, 2009). On GPC, however, the final degradation products (XGO4: XXXG, XLXG, XXLG, and XLLG) were observed to be formed at the initial stage of the reaction (Fig. 2-6A). This feature is very similar to those of HjCel74A (Grishutin *et al.*, 2004) and *Paenibacillus*XEG74 (Fig. 3-6B) (Yaoi *et al.*, 2005) rather than *Geotrichum* XEG (Fig. 2-6C). PcXgh74Bcat have no structural element blocking a side of the substrate-binding cleft, suggesting the exo-like pattern of GPC by PcXgh74B are driven by completely distinct mechanism from "exo-loop" found in OXG-RCBH. When comparing the crystal structure of PcXgh74Bcat presented here to that of *Geotrichum* XEG, PcXgh74B lacks hydrophobic stacking with Glc^{+1} and hydrogen bonds with Xyl$^{+1'}$ and Xyl$^{+2'}$, and PcXgh74B forms many interactions with Xyl$^{-3'}$, Glc^{-2}, and Glc^{+3} that are not found in structure of *Geotrichum* XEG (Table 2-4). In addition, Tyr-295, Trp-320, Trp-341, and Tyr-344 form hydrophobic molecular surface around the region corresponding to possible subsite +5 and +6 (Fig. 2-14). These differences strongly suggest the balance of subsite affinity of PcXgh74B is quite different from that of *Geotrichum*XEG. Moreover, multiple alignment of GH family 74 enzymes (Fig. 2-14, Table 2-4, 2-5) indicates that the amino acid residues that corresponds to Tyr-295, Trp-320, Trp-341, and Tyr-344 on PcXgh74B are conserved in *Paenibacillus*XEG74 and HjCel74A, suggesting possible subsites +5 and +6 are related to exo-like activity by these three enzyme.

When we carefully compare GPC patterns of PcXgh74B and *Paenibacillus* XEG74, there is an apparent difference; in the case of PcXgh74B, accumulation of oligosaccharides of DP=16-18 (XGO8) was observed at the initial stage of hydrolysis, and these oligosaccharides subsequently disappeared during the course of hydrolysis. The hydrolysis of TXG by PcXgh74B was depicted in Fig. 2-16. PcXgh74B is the first enzyme which specifically accumulate XGO8 during TXG hydrolysis. Although the mechanism of exo-like activity by *Paenibacillus*XEG74, HjCel74A, and PcXgh74B are still unknown, the possible subsite +5 and +6 might be deeply involved in XGO8 production. When these enzymes bind to substrate

at reducing/non-reducing end of xyloglucan molecule, they prefer to bind XGO8 moiety at positive site using the additional subsites. In addition, the crystal structure and sequence alignment suggests that PcXgh74B lacks aromatic stack with $Xyl^{-2'}$ which is conserved in both *Paenibacillus*XEG74 and HjCel74A (Fig. 2-13A, 2-15). It suggests that affinity at subsite -2' of PcXgh74B is relatively lower than those of *Paenibacillus* XEG74 and HjCel74A. The weak interaction for $Xyl^{-2'}$ by PcXgh74B can cause non-productive binding of XGO8 as indicated in Fig. 2-17.
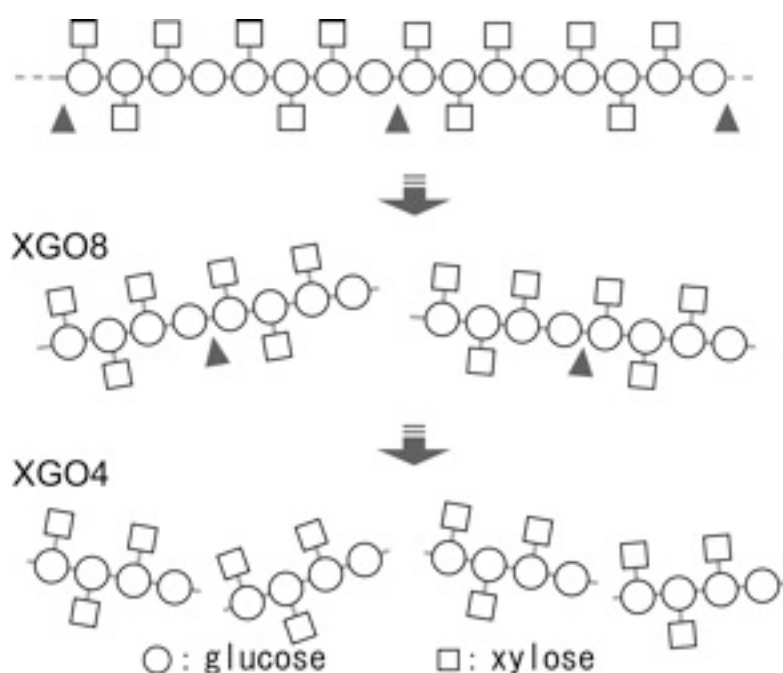
Fig. 2-16 Schematic representation of degradation of TXG by PcXgh74B. Glucose and xylose residues are shown as open circles and open triangles, respectively. The glycosidic bonds hydrolyzed in each steps are indicated by grey triangles.

**Table 2-4 Comparison of interactions with ligand in PcXgh74B, *Geotrichum* OXG-RCBH, and *Geotrichum* XEG.**

PcXgh74B											
subsite	-3	-3'	-2	-2'	-1	-1'	+1	+1'	+2	+2'	+3
H-bond		Ser692 Ser694	Ser427 Asn713	Arg125 Tyr266	Phe19_N Asp38 Asn121 Arg125		Trp376 Gly396_CO Asp446	-		Asp446_CO	Trp319
hydrophobic	Trp92	Trp63		(Leu183)			(Met377)	Tyr266			
blocking						Leu445					
Geotrichum XEG (ligand superposed)*1											
subsite	-3	-3'	-2	-2'	-1	-1'	+1	+1'	+2	+2'	+3
H-bond		- -	(Ala438) Asn744	Arg125 Trp263	Phe15_N Asp34 Asn121 Arg125		Trp388 Gly407_CO Asp458	Arg500		Phe376 Gln377 Asp458_CO His503	(Asn326)
hydrophobic	Trp93	-		-			Trp389	Trp263			
blocking						Tyr457					
Geotrichum OXG-RCBH											
subsite	-3	-3'	-2	-2'	-1	-1'	+1	+1'	+2	+2'	+3
H-bond		- -	(Ala446) Asn753	Arg120 Trp255	Phe16_N Asp35 Asn116 Arg120	Asp465 Asn488	Trp395 Gly415_CO Asp465	Gly380_CO	Asp318 Gly382_N Ala383_N Trp395	-	-
hydrophobic	-	Met61		-			Trp396	Trp263		-	-
blocking					(Gly464)					exo-loop Gly375-His385	

Residues in parentheses indicate lacked interaction and blocking by substitutions of the amino acids.
_CO and _N indicate interaction via main-chain carbonyl and amide group, respectively.
*1 The interactions by *Geotrichum* XEG are predicted from superposition of the ligands bound by OXG-RCBH (Yaoi *et al*., 2007) and PcXgh74B.

Table 2-5 Conserved amino acid residues of *Paenibaccilus* XEG74 and HjCel74A that is predicted to interact with substrate.

Paenibacillus XEG74											
subsite	-3	-3'	-2	-2'	-1	-1'	+1	+1'	+2	+2'	+3
H-bond		? ?	(Ala428) Asn725	Arg126 Tyr263	Phe19 Asp38 Asn122 Arg126		Trp377 Gly397_CO Asp447	-		Asp447_CO	Trp318
hydrophobic	Trp93	Trp64		Tyr182			(Met378)	Tyr263			
blocking						(Gly446)					
HjCel74A											
subsite	-3	-3'	-2	-2'	-1	-1'	+1	+1'	+2	+2'	+3
H-bond		? ?	Ser431 Asn717	Arg122 Tyr263	Phe15 Asp34 Asn118 Arg122		Trp380 Gly400_CO Asp450	Arg500		Asp450_CO	Trp316
hydrophobic	Trp89	Trp60		Tyr180			(Met381)	Trp263			
blocking						(Gly449)					
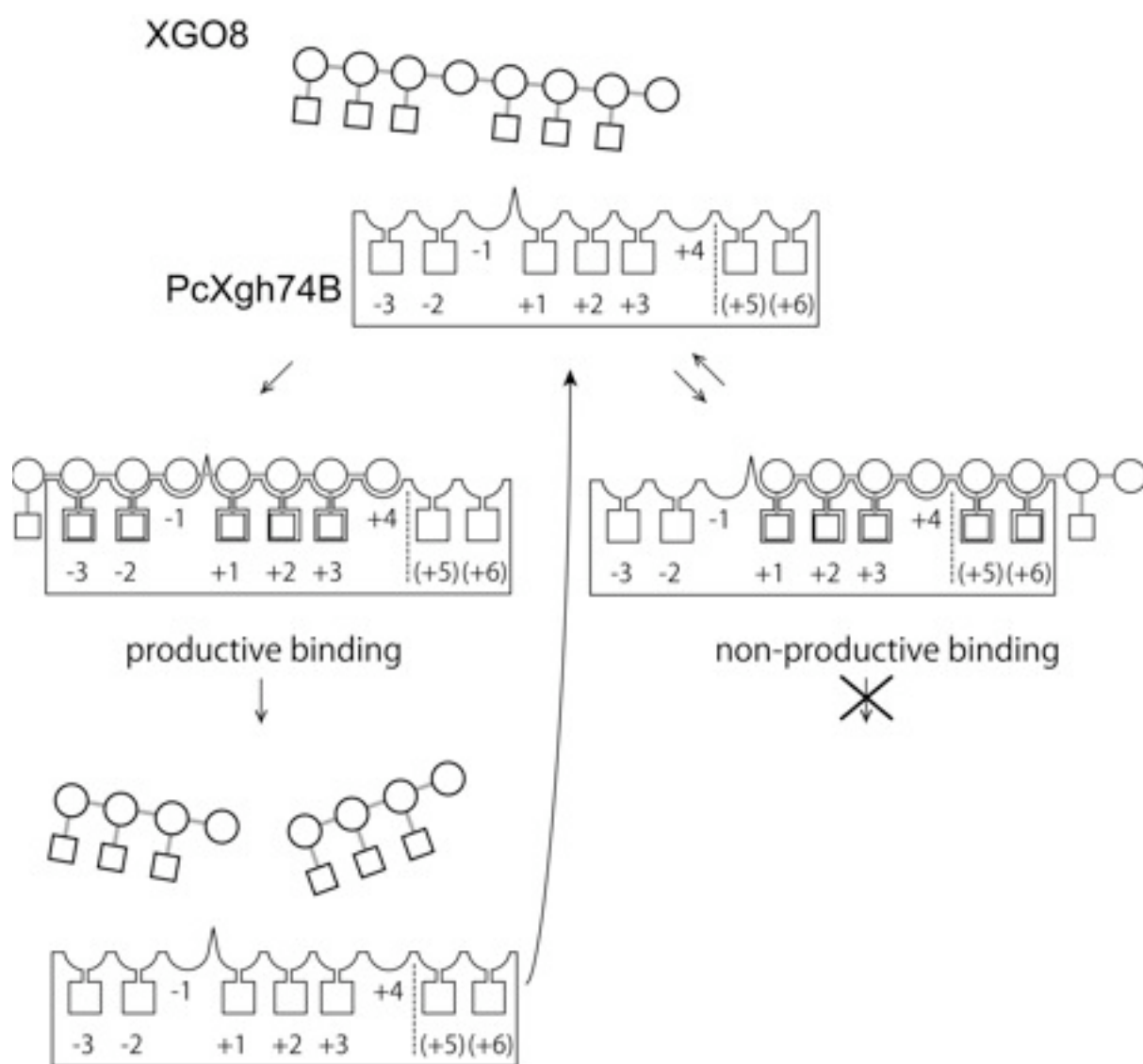
Fig. 2-17 Schematic representation of possible mechanism for XGO8 accumulation during TXG hydrolysis by PcXgh74B. Glucose and xylose residues are shown as open circles and open triangles, respectively.

2-5 Summary

The recombinant PcXgh74B and its catalytic domain PcXgh74Bcat expressed in the yeast *P. pastoris*, had high hydrolytic activity toward xyloglucan from TXG, whereas other β-1,4-glucans examined were poor substrates for the enzyme. The existence of the carbohydrate-binding module significantly affects adsorption of the enzyme on crystalline cellulose, but has no effect on the hydrolysis of xyloglucan, indicating that the domain may contribute to the localization of the enzyme.

HPLC and MALDI-TOF MS analyses of the hydrolytic products of TXG clearly indicated that PcXgh74B hydrolyzes the glycosidic bonds of unbranched glucose residues, like other GH family 74 xyloglucanases. However, viscometric analysis suggested that Xgh74B hydrolyzes TXG in a different manner from other known GH family 74 xyloglucanases. Gel permeation chromatography showed that Xgh74B initially produced oligosaccharides of XGO8 (DP = 16-18) and these oligosaccharides were then slowly hydrolyzed to final products of XGO4 (DP = 7-9).

The crystal structure of PcXgh74Bcat revealed the tandem repeat of 7-bladed β-propeller folds of the enzymes in accordance with the known structures of other GH family 74 enzymes. The complex structure with xyloglucan oligosaccharides elucidate that Leu-445 of PcXgh74B blocks the binding of Xyl^{-1}, suggesting that the steric clashes by Leu-445 result in strict recognition for unbranched glucose residues at subsite -1 by PcXgh74B. The role of Leu-445 is identical to Tyr-457 of *Geotrichum*XEG. The largely opened substrate binding cleft of PcXgh74B is not blocked by any structural elements, indicating the exo-like activity by PcXgh74B is derived by destinct mechanism from exo-loop found in OXG-RCBH.

The structure of PcXgh74B also provided information for the mechanism of unique hydrolysis by PcXgh74B, *i.e.*, additional subsites possibly correspond to subsite +5 and +6 and the weak affinity to Xyl$^{-2'}$ might be involved in the production and the accumulation of XGO8, respectively.

2-6 References

Altschul, S. F., Gish, W., Miller, W., Myers, E. W. & Lipman, D. J. Basic local alignment search tool. *J Mol Biol* **215**, 403-410,(1990).

Altschul, S. F., Madden, T. L., Schaffer, A. A., Zhang, J., Zhang, Z., Miller, W. & Lipman, D. J. Gapped BLAST and PSI-BLAST: a new generation of protein database search programs. *Nucleic Acids Res* **25**, 3389-3402,(1997).

Arnold, K., Bordoli, L., Kopp, J. & Schwede, T. The SWISS-MODEL workspace: a web-based environment for protein structure homology modelling. *Bioinformatics* **22**, 195-201, (2006).

Bauer, S., Vasu, P., Mort, A. J. & Somerville, C. R. Cloning, expression, and characterization of an oligoxyloglucan reducing end-specific xyloglucanobiohydrolase from *Aspergillus nidulans. Carbohydr Res* **340**, 2590-2597,(2005).

Bendtsen, J. D., Nielsen, H., von Heijne, G. & Brunak, S. Improved prediction of signal peptides: SignalP 3.0. *J Mol Biol* **340**, 783-795,(2004).

Chhabra, S. R. & Kelly, R. M. Biochemical characterization of *Thermotoga maritima* endoglucanase Cel74 with and without a carbohydrate binding module (CBM). *FEBS Lett* **531**, 375-380,(2002).

DeLano, W. L. Unraveling hot spots in binding interfaces: progress and challenges. *Curr Opin Struct Biol* **12**, 14-20,(2002).

Doner, L. W. & Irwin, P. L. Assay of reducing end-groups in oligosaccharide homologues with 2,2'-bicinchoninate. *Anal Biochem* **202**, 50-53,(1992).

Edwards, M., Dea, I. C., Bulpin, P. V. & Reid, J. S. Purification and properties of a novel xyloglucan-specific endo-(1->4)-beta-D-glucanase from germinated nasturtium seeds (*Tropaeolum majus* L.). *J Biol Chem* **261**, 9489-9494,(1986).

Emsley, P. & Cowtan, K. Coot: model-building tools for molecular graphics. *Acta Crystallogr D Biol Crystallogr* **60**, 2126-2132,(2004).

Grishutin, S. G., Gusakov, A. V., Markov, A. V., Ustinov, B. B., Semenova, M. V. & Sinitsyn, A. P. Specific xyloglucanases as a new class of polysaccharide-degrading enzymes. *Biochim Biophys Acta* **1674**, 268-281,(2004).

Habu, N., Igarashi, K., Samejima, M., Pettersson, B. & Eriksson, K. E. Enhanced production of cellobiose dehydrogenase in cultures of *Phanerochaete chrysosporium* supplemented with bovine calf serum. *Biotechnol Appl Biochem* **26**, 97-102,(1997).

Hasper, A. A., Dekkers, E., van Mil, M., van de Vondervoort, P. J. & de Graaff, L. H. EglC, a new endoglucanase from *Aspergillus niger* with major activity towards xyloglucan. *Appl Environ Microbiol* **68**, 1556-1560,(2002).

Hayashi, T., Takeda, T., Ogawa, K. & Mitsuishi, Y. Effects of the degree of polymerization on the binding of xyloglucans to cellulose. *Plant Cell Physiol* **35**, 893-899,(1994).

Igarashi, K., Yoshida, M., Matsumura, H., Nakamura, N., Ohno, H., Samejima, M. & Nishino, T. Electron transfer chain reaction of the extracellular flavocytochrome cellobiose dehydrogenase from the basidiomycete *Phanerochaete chrysosporium*. *Febs J* **272**, 2869-2877,(2005).

Irwin, D. C., Cheng, M., Xiang, B., Rose, J. K. & Wilson, D. B. Cloning, expression and characterization of a family-74 xyloglucanase from *Thermobifida fusca*. *Eur J Biochem* **270**, 3083-3091,(2003).

Johnsrud, S. C. & Eriksson, K. E. Cross-breeding of selected and mutated homokaryotic strains of *Phanerochaete-chrysosporium* K-3 - new cellulase deficient strains with increased ability to degrade lignin. *Appl Environ Microbiol* **21**, 320-327,(1985).

Julenius, K., Molgaard, A., Gupta, R. & Brunak, S. Prediction, conservation analysis, and structural characterization of mammalian mucin-type O-glycosylation sites. *Glycobiology* **15**, 153-164,(2005).

Kawai, R., Igarashi, K., Yoshida, M., Kitaoka, M. & Samejima, M. Hydrolysis of beta-1,3/1,6-glucan by glycoside hydrolase family 16 endo-1,3(4)-beta-glucanase from the basidiomycete *Phanerochaete chrysosporium*. *Appl Microbiol Biotechnol* **71**, 898-906, (2006).

Kremer, S. M. & Wood, P. M. Evidence that cellobiose oxidase from *Phanerochaete chrysosporium* is primarily an Fe(III) reductase. Kinetic comparison with neutrophil NADPH oxidase and yeast flavocytochrome b_2. *Eur J Biochem* **205**, 133-138,(1992).

Lever, M. A new reaction for colorimetric determination of carbohydrates. *Anal Biochem* **47**, 273-279,(1972).

Martinez, D., Larrondo, L. F., Putnam, N., Gelpke, M. D., Huang, K., Chapman, J., Helfenbein, K. G., Ramaiya, P., Detter, J. C., Larimer, F., Coutinho, P. M., Henrissat, B., Berka, R., Cullen, D. & Rokhsar, D. Genome sequence of the lignocellulose degrading fungus *Phanerochaete chrysosporium* strain RP78. *Nat Biotechnol* **22**, 695-700, (2004).

Martinez-Fleites, C., Guerreiro, C. I., Baumann, M. J., Taylor, E. J., Prates, J. A., Ferreira, L. M., Fontes, C. M., Brumer, H. & Davies, G. J. Crystal structures of Clostridium thermocellum xyloglucanase, XGH74A, reveal the structural basis for xyloglucan recognition and degradation. *J Biol Chem* **281**, 24922-24933,(2006).

Murshudov, G. N., Vagin, A. A. & Dodson, E. J. Refinement of macromolecular structures by the maximum-likelihood method. *Acta Crystallogr D Biol Crystallogr* **53**, 240-255, (1997).

Nelson, N. A photometric adaptation of the Somogyi method for the determination of glucose. *J Biol Chem* **153**, 375-380,(1944).

Otwinowski, Z., Minor, W. Processing of X-ray diffraction data collected in oscillation mode. *Methods Enzymol* **276**, 307-326,(1997).

Pauly, M., Andersen, L. N., Kauppinen, S., Kofod, L. V., York, W. S., Albersheim, P. & Darvill, A. A xyloglucan-specific endo-beta-1,4-glucanase from *Aspergillus aculeatus*:

expression cloning in yeast, purification and characterization of the recombinant enzyme. *Glycobiology* **9**, 93-100,(1999).

Samejima, M., Sugiyama, J., Igarashi, K. & Eriksson, K. E. L. Enzymatic hydrolysis of bacterial cellulose. *Carbohydr Res* **305**, 281-288,(1998).

Somogyi, M. A new reagent for the determination of sugars. *J Biol Chem* **160**, 61-68,(1945).

Somogyi, M. Notes on sugar determination. *J Biol Chem* **195**, 19-23,(1952).

Vagin, A. & Teplyakov, A. MOLREP: an automated program for molecular replacement. *J Appl Crystallogr* **30**, 1022-1025,(1997).

Vincken, J. P., Beldman, G. & Voragen, A. G. Substrate specificity of endoglucanases: what determines xyloglucanase activity? *Carbohydr Res* **298**, 299-310,(1997).

Waffenschmidt, S. & Jaenicke, L. Assay of reducing sugars in the nanomole range with 2,2'-bicinchoninate. *Anal Biochem* **165**, 337-340,(1987).

Wood, T. M. Preparation of crystalline, amorphous, and dyed cellulase substrates. *Methods Enzymol* **160**, 19-25,(1988).

Yaoi, K., Kondo, H., Hiyoshi, A., Noro, N., Sugimoto, H., Tsuda, S., Mitsuishi, Y. & Miyazaki, K. The structural basis for the exo-mode of action in GH74 oligoxyloglucan reducing end-specific cellobiohydrolase. *J Mol Biol* **370**,(2007).

Yaoi, K., Kondo, H., Hiyoshi, A., Noro, N., Sugimoto, H., Tsuda, S. & Miyazaki, K. The crystal structure of a xyloglucan-specific endo-beta-1,4-glucanase from *Geotrichum sp.* M128 xyloglucanase reveals a key amino acid residue for substrate specificity. *FEBS J* **276**, 5094-5100,(2009).

Yaoi, K. & Mitsuishi, Y. Purification, characterization, cloning, and expression of a novel xyloglucan-specific glycosidase, oligoxyloglucan reducing end-specific cellobiohydrolase. *J Biol Chem* **277**, 48276-48281,(2002).

Yaoi, K. & Mitsuishi, Y. Purification, characterization, cDNA cloning, and expression of a xyloglucan endoglucanase from *Geotrichum* sp. M128. *FEBS Lett* **560**, 45-50,(2004).

Yaoi, K., Nakai, T., Kameda, Y., Hiyoshi, A. & Mitsuishi, Y. Cloning and characterization of two xyloglucanases from *Paenibacillus* sp. strain KM21. *Appl Environ Microbiol* **71**, 7670-7678,(2005).

York, W. S., van Halbeek, H., Darvill, A. G. & Albersheim, P. Structural analysis of xyloglucan oligosaccharides by 1H-n.m.r. spectroscopy and fast-atom-bombardment mass spectrometry. *Carbohydr Res* **200**, 9-31,(1990).

Yoshida, M., Igarashi, K., Wada, M., Kaneko, S., Suzuki, N., Matsumura, H., Nakamura, N., Ohno, H. & Samejima, M. Characterization of carbohydrate-binding cytochrome b_{562} from the white-rot fungus *Phanerochaete chrysosporium*. *Appl Environ Microbiol* **71**, 4548-4555,(2005).

Yoshida, M., Ohira, T., Igarashi, K., Nagasawa, H., Aida, K., Hallberg, B. M., Divne, C., Nishino, T. & Samejima, M. Production and characterization of recombinant

Phanerochaete chrysosporium cellobiose dehydrogenase in the methylotrophic yeast *Pichia pastoris*. *Biosci Biotechnol Biochem* **65**, 2050-2057,(2001).

Zverlov, V. V., Schantz, N., Schmitt-Kopplin, P. & Schwarz, W. H. Two new major subunits in the cellulosome of Clostridium thermocellum: xyloglucanase Xgh74A and endoxylanase Xyn10D. *Microbiology* **151**, 3395-3401,(2005).

Chapter 3

X-ray crystallography of PcLam55A

3-1 Introduction

As described in Chapter 1, β-1,3-glucanases are found in the GH families 5, 16, 17, 55, 64, and 81. However, gentiobiose producing exo-β-1,3-glucanases are found only in GH family 55. In addition, many all the biochemically characterized enzymes in GH family 55 exhibit exo- or endo-1,3-β-glucanase activities (Kasahara *et al.*, 1992, Schaeffer *et al.*, 1994, de la Cruz *et al.*, 1995, Cohen-Kupiec *et al.*, 1999, Donzelli *et al.*, 2001, Giczey *et al.*, 2001, Nobe *et al.*, 2003, Nobe *et al.*, 2004). The situation is similar to GH family 74 in which all the enzymes are highly specific to the xyloglucan or xyloglucan derived oligosaccharides. In addition, tandem repeat of β-helix motif in sequence of GH family 55 enzymes implies resemblance to domain structure of GH family 74. The aim of this chapter is to reveal the structural basis of GH family 55 β-1,3-glucanase and to demonstrate possible relationship between hydrolytic activity towards branched substrate and structural features by means of crystallography.

PcLam55A is the exo-1,3-β-glucanase (or laminarinase A) from the basidiomycete *P. chrysosporium*, which belongs to GH family 55. Recently, detailed characterization for biochemical properties of PcLam55A are performed by Kawai *et al.* using the recombinant protein of PcLam55A expressed in *P. pastoris*. The enzyme has no hydrolytic activity toward β-1,6- or β-1,3/1,4-glucan, but exhibits high activity toward laminarin from *Laminaria digitata*. As summarized in Table 3-1, the catalytic efficiency (k_{cat}/K_m) for laminarioligosaccharides increase depending on DP of the substrate, suggesting PcLam55A have at least five subsites. The HPLC analysis using 6-*O*-glucosyl-laminaritriose elucidate that the enzyme releases gentiobiose unit from non-reducing end of the substrate (Fig. 3-1). However, significant increase of hydrolytic activity on 6-*O*-glucosyl-laminaritriose was not detected compared to laminaritriose. A quantitative analysis on limit digestion products during hydrolysis of laminariheptaose by PcLam55A suggested that PcLam55A exhibit multiple attack hydrolysis on linear substrate (Kawai, 2006b).

Table 3-1 Kinetic parameters of PcLam55A for laminarioligosaccharides with various DP.

	K_m (μM)	k_{cat} (s^{-1})	k_{cat} / K_m (x10^5 s^{-1} M^{-1})
laminaribiose	1960 ± 309	3.18 ± 0.20	0.0162
laminaritriose	284 ± 32	30.4 ± 0.5	1.07
laminaritetraose	30.4 ± 3.4	53.4 ± 2.2	17.6
laminaripentaose	8.01 ± 0.23	59.1 ± 0.2	73.8
laminarihexaose	4.07 ± 0.19	73.4 ± 0.6	180
laminariheptaose	3.28 ± 0.14	83.3 ± 0.6	254

(Kawai, 2006b)
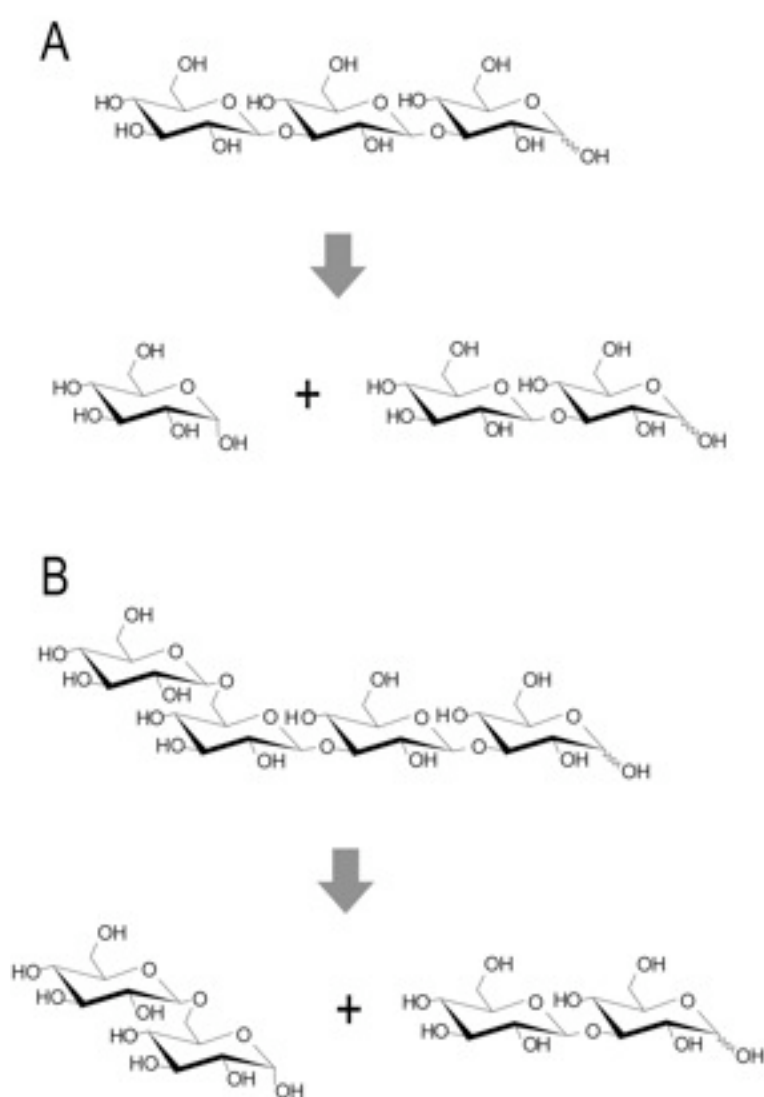
Fig. 3-1

Schematic representation of hydrolysis of *A*. laminaritriose and *B*. 6-*O*-glucosyl laminaritriose by PcLam55A. PcLam55A hydrolyzes the glycosidic bond of the glucose residue at the non-reducing end, independently of substitution at the O-6 position.

3-2 Experimental procedures

3-2-1 *Protein Preparation*

Native PcLam55A protein was heterologously expressed in *P. pastoris* and purified as described previously (Kawai *et al*., 2006). Selenomethionine-labeled PcLam55A PcLam55A was expressed in Buffered Minimal Methanol media (100 mM potassium phosphate pH 6.0, 1.34% yeast nitrogen base without amino acids (Wako Pure Chemical Industries Ltd., Osaka, Japan), 4 x 10^{-5}% biotin, 1% methanol), containing 0.1 mg·ml^{-1} L-selenomethionine, 0.09 mg·ml^{-1} L-isoleucine, L-lysine, and 0.6 mg·ml^{-1} L-threonine (Xu *et al*., 2002, Larsson *et al*., 2003), using the same transformant of *P. pastoris* as that for native PcLam55A. The purification procedures for selenomethionine-labeled PcLam55A were the same as those for non-labeled PcLam55A. For the crystallization experiments, the enzymes were treated with Endo-H (New England Biolabs, Beverly, MA, USA) as described previously (Yoshida *et al*., 2001), and further purified by gel permeation chromatography.

3-2-2 *Crystallography*

Crystals of native and selenomethionine-labeled PcLam55A were obtained by means of the hanging-drop vapor-diffusion method with microseeding. The drops were formed by mixing 2 μl of protein solution (10 mg·ml^{-1}) and 2 μl of the reservoir solution composed of 100 mM zinc acetate, 15% (w/v) PEG3350, 50 mM MES pH 6.4, 10% (w/v) glycerol, and 2% (v/v) ethanol. The drops were microseeded after equilibration for 48 h at 25°C. The microseeds were prepared by crushing native PcLam55A crystals. The crystals were transferred to reservoir solutions containing 25% glycerol, and then flash-cooled in a stream of nitrogen gas at 100 K. To obtain crystals of the complex with gluconolactone, the reservoir solution containing 50 mM gluconolactone was used for co-crystallization, and then 30% gluconolactone instead of glycerol was used as a cryoprotectant for the flash-cooling step. The X-ray adsorption spectrum was determined by measuring the fluorescence signal perpendicular to the beam at NW12A of the Photon Factory, High Energy Accelerator Research Organization (KEK), Tsukuba, Japan. X-Ray diffraction data sets were collected using synchrotron radiation at beam lines BL5A and NW12A of the Photon Factory, and data were processed and scaled using the HKL2000 program suite (Otwinowski, 1997). The programs SHARP (Vonrhein *et al*., 2007) and RESOLVE (Terwilliger, 2000) were used for initial phase calculation and density modification, respectively. Automated model building was performed using the program ARP/wARP (Perrakis *et al*., 1999). Manual model

rebuilding and refinement were achieved using Coot (Emsley & Cowtan, 2004) and Refmac5 (Murshudov *et al*., 1997). The gluconolactone complex structure was solved starting from the refined native structure. Data collection and refinement statistics are shown in Table 3-2 and Table 3-3, respectively. Figures were prepared using PyMol (DeLano, 2002) and ESPript (Gouet *et al*., 1999).

3-3 Result

### 3-3-1 *Structure determination*

For the initial phase determination by the multiwavelength anomalous dispersion method, crystals of selenomethionine-substituted PcLam55A produced by *P. pastoris* cells cultured in selenomethionine-containing medium (Xu *et al.*, 2002, Larsson *et al.*, 2003). The crystals (Fig. 3-2) were prepared by microseeding method as described above. The peak of 12.67 keV in the X-ray adsorption spectrum (Fig. 3-3) corresponds to the Se *K* edge, indicating the presence of the selenium in the crystals. The PcLam55A structures were determined in unliganded and gluconolactone-complexed forms at 1.7 Å and 2.3 Å resolutions, and they were refined to R-values (R-free) of 14.9% (18.4%) and 14.2% (20.0%), respectively. The data collection statistics and refinement statistics are summarized in Table 3-2 and 3-3, respectively. Both crystal structures contained two molecules (A and B) of mature PcLam55A in the asymmetric unit. The structures of the four chains determined here, two molecules from two crystals, are very similar, the root mean square deviations (RMSD) for Cα atoms being less than 0.22 Å in all combinations of the four. Chain A of each crystal structure were described, unless otherwise noted.

The N-terminal residues from the expression vector (Glu-Ala-Glu-Ala-Glu-Phe) were highly disordered, and were removed from the models. Six Zn^{2+} ions, four sodium ions, four acetate molecules, and eleven glycerol molecules were found in the ligand-free structure, whereas only two Zn^{2+} ions were found in the gluconolactone complex structure. At one of the four potential *N*-glycosylation sites in the PcLam55A sequence, Asn-231 exhibited extra electron density arising from its side-chain amide nitrogen atom. The electron density of two *N*-acetyl-β-D-glucosamine (GlcNAc) residues and one β-D-mannose residue were clearly visible, indicating that this glycosylation site was not susceptible to deglycosylation by endoH. Further substitution by mannose residues, possibly attached at the O-3 or O-6 position of the terminal mannose residue, was only partially observed, with unclear electron density.
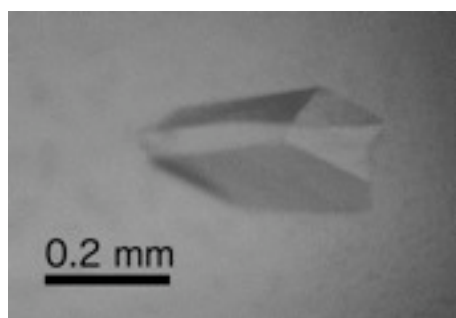
Fig. 3-2
Crystal of selenomethionine-labeled PcLam55A obtained in the hanging-drop. The drops were microseeded after equilibration for 48 h at 25°C, and the crystals belong to space group *P*1.
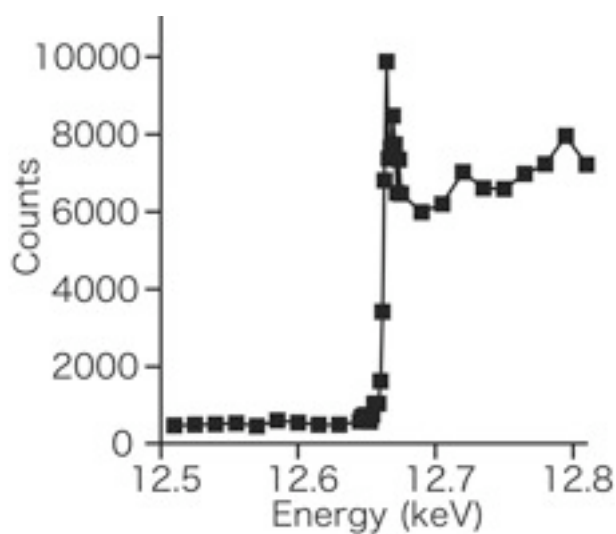
Fig. 3-3
Se *K*-edge fluorescence scan of the crystal performed on beam line NW12A at PF. The peak of 12.66 keV indicate the presence of selenium in the crystal.

Table 3-2 Data collection statistics

Data set	Unliganded	Gluconolactone complex	Selenomethionine		
			Peak	**Edge**	**Remote**
Beamline	PF BL5A	PF BL5A	PF-AR NW12A	PF-AR NW12A	PF-AR NW12A
Wavelength (Å)	1.000	1.000	0.97898	0.97917	0.96395
Space group	*P1*	*P1*		*P1*	
Cell dimensions					
a (Å)	66.3	66.5		66.1	
b (Å)	67.1	67.1		67.2	
c (Å)	105.2	109.8		105.0	
α (degree)	81.0	93.9		81.1	
β (degree)	76.3	106.8		76.5	
γ (degree)	61.4	97.1		61.4	
Resolution (Å)[a]	50.00 - 1.70 (1.76 - 1.70)	50.00 - 2.25 (2.3 - 2.25)		50.00 - 2.18 (2.26 -2.18)	
Total reflections	502,749	262,450	604,805	589,541	564,876
Unique reflections	149,947	77,511	78,414	77,974	76,496
Completeness (%)[a]	88.8 (64.5)	91.9 (74.5)	97.8 (91.7)	96.8 (85.0)	94.7 (73.9)
Average $I/\sigma(I)$[a]	19.1 (3.0)	10.9 (2.7)	21.0 (4.92)	20.6 (4.1)	17.9 (3.2)
R_{sym} (%)[a]	6.5 (24.7)	9.7 (25.7)	9.0 (27.0)	9.5 (30.3)	9.7 (33.6)

[a] Values in parentheses are for the highest resolution shell.

Table 3-3 Refinement statistics

PDB accession code	3EQN ligand-free	3EQO gluconolactone complex
Resolution (Å)	27.2 - 1.70	31.5 - 2.3
R-factor / R_{free} (%)	14.9/18.4	14.2/20.0
No. of Reflections	142,399	73,632
No. of atoms	13,016	12,519
r.m.s.d. from ideal values		
Bond lengths (Å)	0.01	0.02
Bond angles (degree)	1.375	1.797
Average B-factor (Å^2)		
Protein (chain A/B)	14.5/14.3	18.9/21.1
Sugar chain (chain A/B)	32.9/25.4	44.0/44.8
Glycerol	22.3	-
Acetate ion	25.4	-
Zinc ion	20.7	39.1
Sodium ion	25.0	-
Gluconolactone (chain A/B)	-	24.6/26.3
Water	29.7	28.8
Ramachandran plot (%)		
Favored (chain A/B)	87.4/87.9	84.5/84.4
Allowed (chain A/B)	12.4/11.9	15.3/15.3
Disallowed (chain A/B)	0.2/0.2	0.2/0.3

3-3-2 *Overall structure*

PcLam55A consists of two domains with a right-handed parallel β-helix fold (N-domain, residues 1–361; C-domain, residues 391–752), connected by a linker region (28 residues, 362–390). The two β-helix domains are positioned side-by-side, forming an overall shape like a rib cage (Fig. 3-4). As shown in Fig. 3-5C, the torsion angle between the helical axes of the two β-helix domains is approximately 25°. The two domains are bound tightly via many interactions that include the disulfide bond between Cys-5 and Cys-424. The other disulfide bonds, Cys-73–Cys-77, Cys-539–Cys-549, and Cys-692–Cys-698 exist in long loops between β-strands (Fig. 3-5A and B). A helical repeating unit of the β-helix fold, which is formed by three β-strands (designated as PB1, PB2, and PB3) linked by three turns (T1, T2, and T3), is termed a "coil" (Jenkins & Pickersgill, 2001). The PBm β-strand and Tm turn included in the n-th coil will be designate as PBm-n and Tm-n, respectively. Both the N- and C-domains of PcLam55A consist of twelve coils, but flanking (first, second, 11th and 12th) coils are incomplete or irregular (Fig. 3-6A). Both domains lack PB1-1, PB1-2, and PB3-11, and the C-domain lacks PB2-12 (Fig. 3-6A, B). Two C-terminal β-strands in the N-domain (PB2-11 and PB2-12) protrude to the adjacent C-terminal domain, and exhibit antiparallel interactions (Fig. 3-4, 3-5A). In addition, there are several antiparallel interactions in the 11th and 12th coils in both domains (indicated as "AP" in Fig. 3-6B). "Aromatic stack" and "asparagine ladder" are commonly found features in β-helical proteins, in which a number of aromatic (tyrosine and phenylalanine) or asparagine residues are located at equivalent positions in coils (Yoder *et al.*, 1993). Both of these features are found in the N-domain of PcLam55A, but not in the C-domain. The "aromatic stack" and "asparagine ladder" in the N-terminal domain are formed by three phenylalanine residues (Phe-185, Phe-213, and Phe-234), and four asparagine residues (Asn-236, Asn-258, Asn-290, and Asn-318), respectively (Fig. 3-6C). As shown in Fig. 2A and B, the topologies of secondary structures in the two β-helix domains are very similar, whereas the pattern of loop insertion into the turn segments is significantly different.
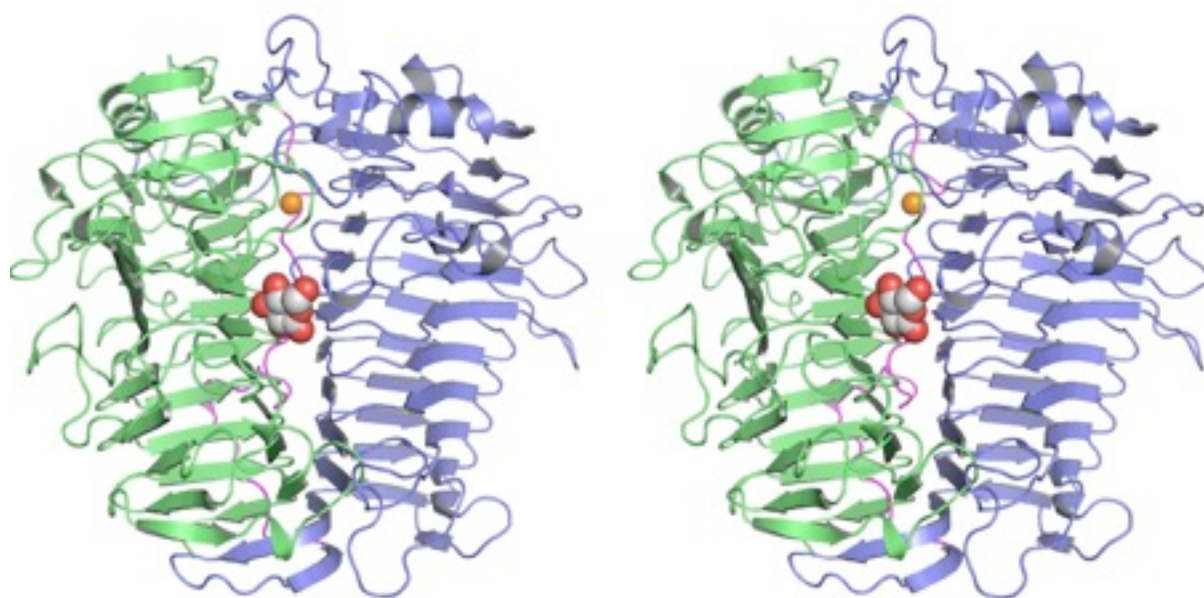
Fig. 3-4

Stereoview of structure of PcLam55A. *A.* Ribbon representation of PcLam55A monomer in the complex with gluconolactone. The N-domain, C-domain and linker region are colored blue, green, and magenta, respectively. The gluconolactone molecule is shown as spheres with carbon and oxygen atoms in white and red, respectively. The zinc atom is shown as an orange sphere.

A

C-domain N-domain

T3-5

T3-6

T1-4

PB2-11 PB2-12

B

Cys5-Cys424 N-linked sugar chain

N-domain

C-domain
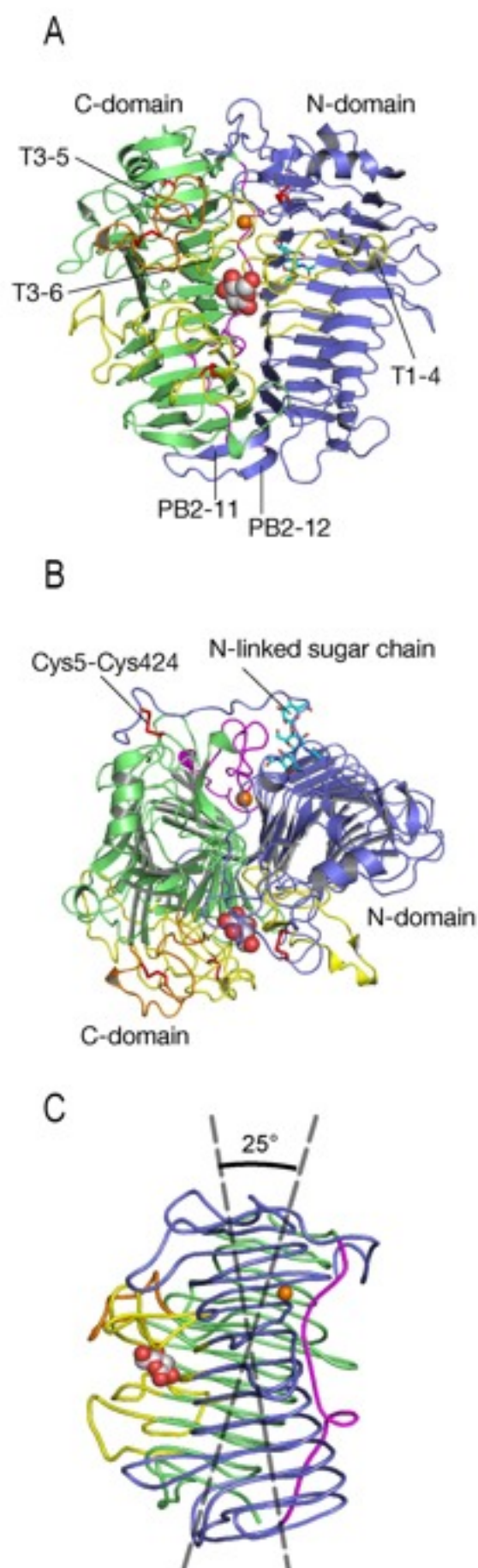
Fig. 3-5

Overall structure of PcLam55A. *A.* Ribbon representation of PcLam55A monomer in the complex with gluconolactone. *B.* The view rotated 90° around the horizontal axis from that in A. The disulfide bonds (Cys5 - Cys424, Cys73 - Cys77, Cys539 - Cys549, and Cys692 - Cys698) are shown in red stick form. The loops forming the substrate-binding pocket (T1-4, T1-5, T1-6, and T1-7 from N-domain; T3-6, T3-7, T3-8, and T3-9 from C-domain) are colored yellow. The T3-5 loop from C-domain is colored orange. N-Linked sugar chain is shown in cyan stick form. *C.* The view rotated 90° around the vertical axis from that in A. The torsion angle between the helical axes of the two β-helix domains is indicated.

C

25°

68

A

```
                                        α0                              PB2-1              PB3-1           α1
                                        0000                            →→ 0000            ⟹  00000000
Ndomain   1 LGSTCSSPLTHGSAAPGDPFWLQNIQHQGIAAFNGNPGGTPVFRNVKNYGAKGDGNTDDTAAIQAAINAGGRCGQGCDST
Cdomain 391 .......................................PS..DFVSVRSQGAKGDGNTDDTQAIKNVFAKY..........
                                                                 →       ⟹  00000000000
                                                                PB2-1   PB3-1
```

```
         PB2-2      PB3-3    PB1-3    PB2-3       PB3-3              PB1-4    B1    B2  T1-4        PB2-4
         →          ⟹        →        →           ⟹                 →      000  000            →
Ndomain  81 TTQPALVIFPPGTIKVSSPLVVLYQTQLIGDAKNLPTLLAAPNFS.....GIALIDADPYLAGGAQYYVNKNNPFRSVRN
Cdomain 422 .AGCKIIFFDAGTIIVTDTIQIPAGTQIVGEV..WSVIMGTGSKFTDYNNPQPVIQVGAP.........GSSGVVEITD
            →         →        →        →           ⟹                →                →
          PB2-2     PB3-3    PB1-3    PB2-3        PB3-3              PB1-4               PB2-4
```

```
        PB3-4         PB1-5         T1-5        PB2-5 PB3-5                            PB1-6    T1-6     PB2-6
        ⟹             →                         →     ⟹                              →                →
Ndomain 156 FVIDLRQVSGSATGIHMQVS.....EATSLINIVFQMS.............TAAG....NQHQGIFMENGQGGFLGD
Cdomain 489 MIFTTRGPAAGAIIVHHNVHDPSGQQAAGANDTHLIIGGTAQSGLQVGQCPTSGAGGNNCFADFLGLHLTSGSSATLEG
            →             →              →                →    ⟹                      →        000    →
          PB3-4         PB1-5                            PB2-5  PB3-5      T3-5              PB1-6    PB2-6
```

```
       PB3-6                        PB1-7  T1-7     PB2-7 PB3-7   PB1-8        PB2-8 PB3-8
       ⟹                           →                →     ⟹     →            →     ⟹
Ndomain 211 LVFNG................GNIGATFGNQQ.FTVRNLTFNNAN.TAINAIWNWGWTFQRITINNC...........
Cdomain 569 MWVWLADHDLDSGGSQQISLWSNGGIMSESQGPVWLIGTASEHHINYQYFLKNAANHYIGLAQTETPYFQPNPNPPAPFI
            →                           →                →     ⟹     →            →     ⟹
          PB3-6      T3-6               PB1-7     T3-7        PB2-7 PB3-7  PB1-8   PB2-8 PB3-8
```

```
                 PB1-9                    PB2-9 PB3-9                       PB1-10              PB2-10
                 →                        →     ⟹                         →                   ⟹
Ndomain 260 ..........QVGFDLTQGGTSNTGAQGVGAEAIIDAVVTN............TQTFVRWSGASSGHLQGSLV
Cdomain 649 TNSNFDPSQLGQGDAWAMTVQ.........NSHGILVFGAGFYSFFSAYNTGCQSPQNCQNQIVNVDS......SSDIA
            →                            →      ⟹                   000    →              →
          T3-8          PB1-9            PB2-9  PB3-9            T3-9           PB1-10        PB2-10
```

```
       PB3-10    PB1-11     PB1-12       PB3-11   PB2-11           PB2-12
       ⟹         →          →            ⟹       →                →
Ndomain 311 LNNIQLTNVPVAVGVKGGPTVLAG......GTTTINSWAQGNVYHGTNGNPTFTQGN
Cdomain 713 FYSLTTVDTTWQFSVNAQ.GVINRSNNPNGFADTITAMTRN................
            →         ⟹         →         000    ⟹
          PB3-10    PB1-11     PB1-12     PB3-11 PB2-11
```

B

C

N318
N290
N258
N236
F234
F213
F185

Fig. 3-6

β-Strands in the two β-helix domains. A. Sequence alignment of N- and C- domains. Arrows for PB1, PB2, and PB3 are colored black, grey, and white, respectively. Identical amino acid residues are boxed in grey. The loops forming the substrate-binding pocket and T3-5 loop from C-domain are indicated by yellow and orange-shaded boxes, respectively. Dashed lines indicate regions involved in antiparallel interaction between β-strands of N- and C-domains. Residues possibly involved in catalysis, Glu633, Gln146, Gln176, and Ser204, are shown in white type boxed in black. B. Superimposition of N-domain (blue) and C-domains (green). PB1, PB2, and PB3 are colored blue, lime green, and red, respectively. Gluconolactone molecules bound to each domain are shown as spheres. The side-chains of residues in N- and C-domains are shown in blue and orange sticks, respectively. Coils are numbered from the N-terminus to the C-terminus of each domain. "AP" indicates a region where β-strands have antiparallel interactions. C. Aromatic stack and asparagine ladder found in the N-domain.
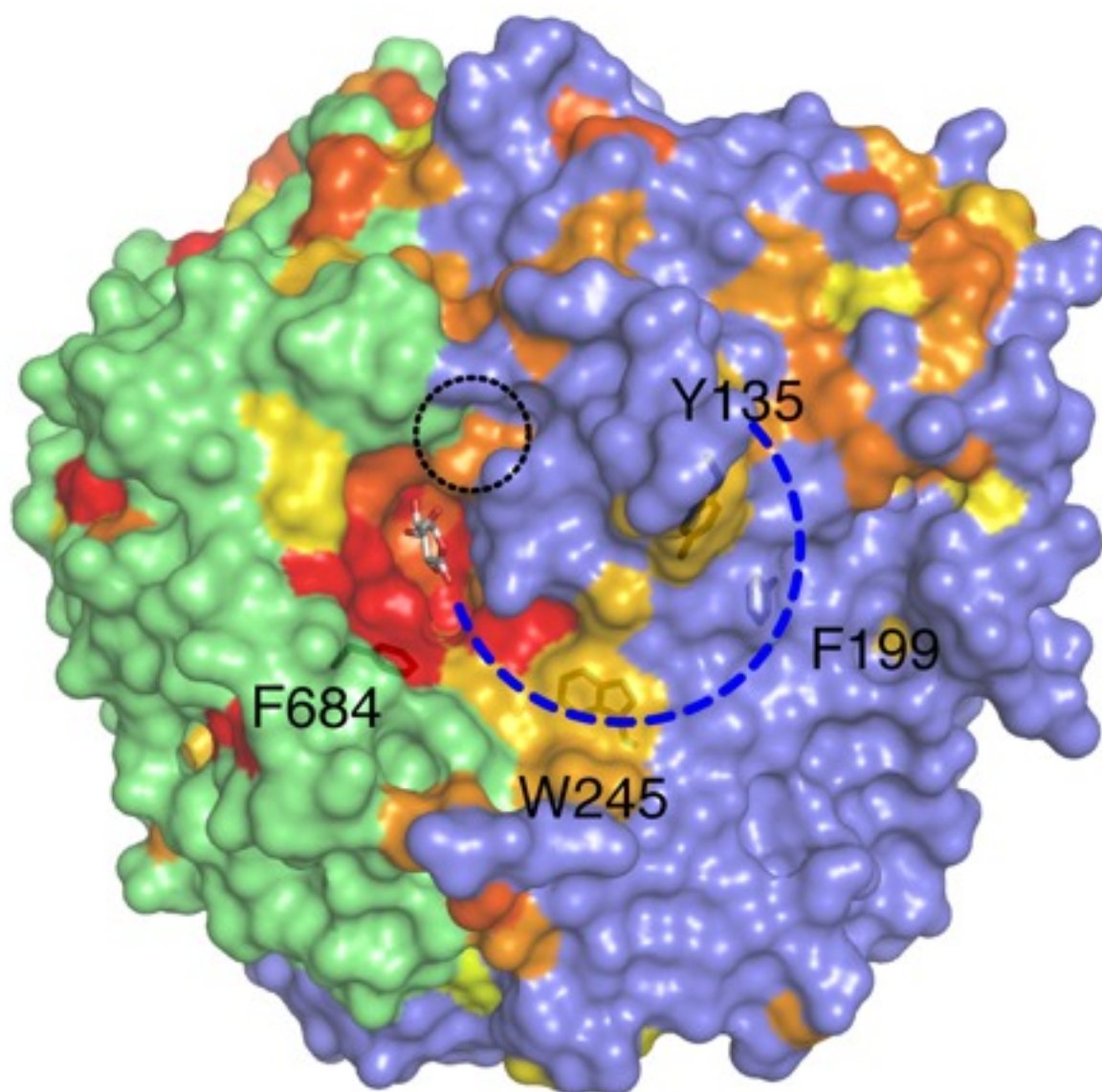
3-3-3 *Gluconolactone complex structure*

Gluconolactone complex structure was determined using a crystal prepared by co-crystallization followed by soaking in the presence of a higher concentration of the ligand (Fig. 3-6A). The gluconolactone molecule exists at the bottom of a deep depression (substrate-binding pocket) between the N- and C-domains (Fig. 3-9). The binding pocket is formed by T1 turns (between PB1 and PB2) in the 4th to 7th coils of the N-domain, and T3 turns (between PB3 and PB1) in the 6th to 9th coils of the C-domain (Fig. 3-6A). A curved groove starting from the gluconolactone-binding pocket runs around the protrusion formed by T1-4 in the N-domain. Several aromatic residues (Phe-684, Trp-245, Phe-199, and Tyr-135) are located along the groove (Fig. 3-9).

The gluconolactone molecule forms direct hydrogen bonds with Asn-147, Trp-572, Asp-575, Glu-610, and Glu-633, and water-mediated hydrogen bonds are formed with Gln-146, Asn-147, Gln-176, Ser-204, Gln-225, and Tyr-636 (Fig. 3-7). Three acidic amino acid residues, Glu-633, Glu-610, and Asp-575, are completely conserved in GH family 55. Among them, Glu-633 is appropriately positioned as the catalytic acid, forming a direct hydrogen bond with the O-1 hydroxyl group of gluconolactone. Glu-610 recognizes the O-2 and O-3 hydroxyl groups, and Asp-575 recognizes the O-4 hydroxyl group. A water molecule appears to be appropriately positioned as the nucleophilic water, and the distance to the C-1 carbon atom is 2.7 Å. However, no carboxylic catalytic base is identified around this water molecule. The water is held by side chains of Ser-204 and Gln-176, and the backbone carbonyl group of Gln-146. Ser-204 and Gln-176 are also highly conserved in GH family 55.

Fig. 3-7

Stereoview of binding of gluconolactone to PcLam55A with the $F_{obs} - F_{calc}$ omit electron density map contoured at 1.5 σ at the active site. Gluconolactone (white), residues from the N-domain (blue) and C-domain (green) are shown as stick models. Water molecules are shown as red spheres. Hydrogen bonds are depicted by black dashed lines. Distances between O1 of gluconolactone and Glu633, and between C1 and proximal water are indicated by red lines. The main chain carbonyl oxygen of Glu146 forms a hydrogen bond with the proximal water.

Fig. 3-8

Multiple alignment of GH family 55 enzymes. Glu633 and other three residues that hold possible nucleophilic water are colored red. Other residues involved in gluconolactone binding are colored blue and green as follows Fig. 3-5.

Fig. 3-9

Molecular surface of the gluconolactone complex structure. Amino acid residues highly conserved in biochemically characterized GH family 55 enzymes, including both exo- and endo-β-1,3-glucanases, are successively colored from yellow (>60%), orange (>80%) to red (100%). Gluconolactone and aromatic residues located along the groove are shown as stick models. A dashed blue line indicates a curved groove on the molecular surface, and a circle with green dotted line indicates the small pocket near the O6 of gluconolactone.

3-4 Discussion

According to the detailed characterization of PcLam55A performed by Kawai *et al.*, the enzyme releases α-glucose or α-gentiobiose from non-reducing end of β-1,3-glucans or β-1,3/1,6-glucans (Kawai, 2006b). This feature is notably similar to that of ExgS from *A. saitoi* (Kasahara *et al.*, 1992, Oda *et al.*, 2002), indicating that GH family 55 enzymes have an inverting mechanism. In the general mechanism of inverting GHs, two acidic residues separated by about 10 Å serve as general acid and base catalysts (McCarter & Withers, 1994, Davies & Henrissat, 1995). The reaction proceeds by proton donation from the catalytic acid to the glycosidic bond oxygen, concurrently with nucleophilic attack by water at the anomeric carbon. A catalytic base is required to activate the nucleophilic water. However, there are several exceptional cases among inverting GHs. For example, the catalytic base of a GH family 6 enzyme, cellobiohydrolase Cel6A, indirectly interacts with nucleophilic water via another water, and the nucleophilic water is held by a serine residue and a main chain carbonyl oxygen (Koivula *et al.*, 2002, Varrot *et al.*, 2003). Further, the identity of the catalytic base of GH family 48 enzymes is still unclear, even though the crystal structures of a number of enzyme complexes with substrates have been determined (Parsiegla *et al.*, 1998, Parsiegla *et al.*, 2000, Guimaraes *et al.*, 2002, Parsiegla *et al.*, 2008). In the reaction mechanism proposed for GH family 95 1,2-α-fucosidase, two asparagine residues are thought to play critical roles in withdrawing a proton from the nucleophilic water, and two neighboring acidic residues (Glu and Asp) are involved in the enhancement of water nucleophilicity (Nagae *et al.*, 2007). In the present study, Glu-633 of PcLam55A is suggested to be the catalytic acid, and There is a candidate for the nucleophilic water, which seems to be positioned appropriately near the C-1 carbon atom of gluconolactone. However, there are no acidic residues that can interact with this water molecule. The nucleophilic water candidate is held by the side chains of Ser-204 and Gln-176, and the main chain carbonyl oxygen of Gln-146. The situation is similar in some respects to the case of the nucleophilic water in Cel6A, but there are no carboxylic acid group around the elements holding the nucleophilic water candidate. Although the catalytic mechanism of PcLam55A can not yet be defined due to the uncertainty in the identity of the catalytic base, GH family 55 enzymes may have a different mechanism from the normal inverting GHs. Alternatively, the orientation of gluconolactone observed here may not mimic the Michaelis complex. There are a number of highly conserved residues around this site, but only three of them (Asp-575, Glu-610, and Glu-633) have the carboxyl side chain. These residues hold the hydroxyl groups of

gluconolactone in the current complex structure, but two of them might act as the general acid and base catalysts in an alternative substarate-binding mode.

Fig. 3-9 shows the molecular surface of PcLam55A colored to show residue conservation within GH family 55 enzymes (the degree of conservation increases in the order of white, yellow, orange, and red), including both exo- and endo-β-1,3-glucanases. The high level of conservation around the gluconolactone-binding pocket strongly indicates that this area is the catalytic cleavage site of GH family 55 enzymes. A long cleft forming an arc from the gluconolactone-binding pocket appears to be available to bind a curved β-1,3-glucan chain. There are some additional aromatic residues lining the cleft, and the cleft exhibits a relatively high level of amino acid residue conservation in the region stretching up to Trp-245. Kinetic parameters shown in Table 3-1 indicate that PcLam55A prefers longer β-1,3-glucan chains with DP up to 5-6 as substrates (Kawai, 2006a). Therefore, this long cleft is suggested to be the location of subsites +1 to +5, and perhaps more. In addition, one side of the substrate-binding pocket of PcLam55A is blocked by a long loop region, which is consistent with the exo mode of hydrolysis of the enzyme demonstrated by HPLC analysis (Kawai, 2006a). This loop region corresponds to T3-6 between PB3-6 and PB1-7 in the C-domain (residues 573–593), and neighboring T3-5 loop region supports the T3-6 loop from the back (Fig. 2A, orange). These loop regions exhibit great sequence variation among GH family 55 exo- and endo-β-1,3-glucanases, suggesting different structure of these loop might have an effect to the mode of action of endo type GH family 55 enzymes. Interestingly, a small pocket, about the size of a single glucose unit, is present beyond the O-6 hydroxyl group of gluconolactone (circled by a green broken line in Fig. 3-9). Although the characterization suggests that the putative binding pocket have low affinity to branched glucose unit, it allows the substrate-binding site of PcLam55A to accept a gentiobiose unit by making space. The pocket for a single β-1,6-branched glucose unit shows a high degree of conservation, in accordance with the fact that many GH family 55 exo-β-1,3-glucanases (often designated as exo-β-1,3/1,6-glucanases) purified from filamentous fungi release gentiobiose units from laminarin containing β-1,6-glucosidic branches (Kasahara *et al*., 1992, Pitson *et al*., 1995, Kawai, 2006b, Martin *et al*., 2006). In a multiple alignment of GH family 55 enzymes, Asn-147 which forms hydrogen bond with O-6 of gluconolactone is substituted with leucine only in two endo type glucanases, Bgn13.1 from *H. lixii* and LamAI from *T. viride*. Since the hydrogen bond may contribute to maintain direction of branched glucose unit in active site of exo type enzymes, two endo type enzymes that lack corresponding interaction are not

accommodated to accept gentiobiose unit in its active site or have different mechanism to interact with branched glucose unit.

A structural similarity search using the DALI server (Holm & Sander, 1995) revealed that both the N- and C-domains of PcLam55A show similarity to those of various carbohydrate-active β-helical enzymes such as GH, polysaccharide lyase (PL), and carbohydrate esterase (CE) family enzymes in the CAZy database. Close structural neighbors (Z scores > 15) include GH family 28, 49, 82, 90, PL1, PL3, PL6, PL9, PL19 (formerly GH family 91), CE8, endorhamnosidase from *Shigella flexneri* Phage Sf6 (Sf6 TSP) (Muller *et al.*, 2008), and A-module of mannuronan C-5-epimerase from *Azotobacter vinelandii* (AlgE4A) (Rozeboom *et al.*, 2008). Sf6 TSP has a glycoside hydrolase activity, but has not yet been assigned to a CAZy family. The N-domain of PcLam55A is most similar to that of AlgE4A (PDB code 2PYH chain B; Z score = 25.2, and RMSD for 249 C-α atoms = 2.3 Å), and GH family 82, Sf6 TSP, and GH family 28 follow in this order (Z scores > 20). On the other hand, the C-domain is most similar to that of Sf6 TSP (PDB code 2VBE chain A; Z score = 22.0, and RMSD for 246 C-α atoms = 2.5 Å), and GH family 28, GH family 82, and PL19 follow (Z scores > 20). A pairwise structural comparison between the N- and C-domains of PcLam55A revealed that they are strikingly similar (Z score = 24.8, and RMSD for 253 C-α atoms = 2.2 Å) as compared with the other enzymes. This result provides strong support for the hypothesis that the two tandem β-helical domains of GH family 55 derive from a gene duplication event (Donzelli *et al.*, 2001).

Although the presence of two β-helix folding motifs was suggested from the amino acid sequences of GH family 55 enzymes (Rigden & Franco, 2002), the orientation of the two β-helix domains and the active site structure were unknown. The structure presented here reveals that the two β-helix domains (N- and C-domains) are located side-by-side and bound tightly via many interactions. Moreover, there is a long linker region between the two domains, having many interactions with both the N- and C-domains; therefore, the linker region may stabilize the association of the two β-helix domains. Such a role of the linker region of PcLam55A is quite different from that of the linker in many other GHs, in which it serves to separate the catalytic domain and carbohydrate-binding module, and to introduce flexibility between the two domains (Henrissat & Davies, 2000).

Most of the known β-helical enzymes, including polysaccharide-degrading enzymes, have their active sites in the groove parallel to the helical axis within a monomer (Jenkins & Pickersgill, 2001). The long concave surface formed by T3 and PB1 has been considered to be

suitable for binding of a long and straight polysaccharide. Recently, two unusual examples, whose active sites are located at the monomer-monomer interface of two identical right-handed parallel β-helical domains, have been reported: PL19 inuline fructotransferase from *Bacillus sp. snu-7* (BsIFTase) (Jung *et al.*, 2007) (Fig. 3-10A) and Sf6 TSP (Muller *et al.*, 2008). Both of them are homotrimeric enzymes, and each monomer consists of a β-helical fold similar to those of the PcLam55A domains(Fig. 3-10D). The structure of PcLam55A provides another example of an active site located at the interface of two β-helical domains, but it is formed by two domains in a single polypeptide (Fig. 3-10C). When the C-α atoms of the N- and C-domains of PcLam55A and two monomers of BsIFTase are superimposed, the active sites of these enzymes almost overlapped (Fig. 3-10A, B). BsIFTase catalyzes inverting intramolecular fructosyl transfer to release the terminal difructosaccharide unit from β-2,1-fructans, such as inulin (Kim *et al.*, 2007). Glu-244 and Asp-233 are suggested to play crucial roles in the catalysis. BsIFTase was once classified into GH family 91 in the CAZy database, but afterwards reclassified to PL19 according to the IUBMB Enzyme Nomenclature because this enzyme actually catalyzes an elimination reaction (EC 4.2.2.18). As illustrated in Fig. 3-7B, the possible catalytic residues of PcLam55A and BsIFTase do not overlap, indicating that the positions of catalytic residues are not conserved between GH family 55 and PL19 enzymes. Sf6 TSP is a retaining enzyme, and the two catalytic residues, Asp-399 and Glu-366, are located in different monomers. Although the identity of the catalytic residues of PcLam55A is still unclear, the putative catalytic acid residue (Glu-633, Fig. 3-7) and the residues holding the nucleophilic water candidate (colored blue in Fig. 3-7) are located in different domains. The possible catalytic residues of PcLam55A and Sf6 TSP do not overlap after structural alignment.

β-Helix is one of the basic scaffolds for binding polysaccharides, since a β-helix domain called CASH (CArbohydrate-binding proteins and Sugar Hydrolases) is widespread among carbohydrate-interacting proteins (Ciccarelli *et al.*, 2002). To date, five GH families (GH28, 49, 55, 82, and 90), six PL families (PL1, 3, 6, 9, 16, 19) and one CE family (CE8) are confirmed to have the right-handed parallel β-helix fold, and two of them (GH28 and 49) are further grouped into the clan GH-N. Rigden and Franco found possible evolutional relationships among GH family 28, 49, 82, and 87 (Rigden & Franco, 2002). However, they suggested that GH family 55 is distinct from other β-helical GH families because of the inconsistency of the positions of catalytic residues. The structure of PcLam55A provide an example of carbohydrate-binding at the interface of two β-helical domains within a single

polypeptide, demonstrating an unexpected variety of carbohydrate-binding modes of β-helical proteins.
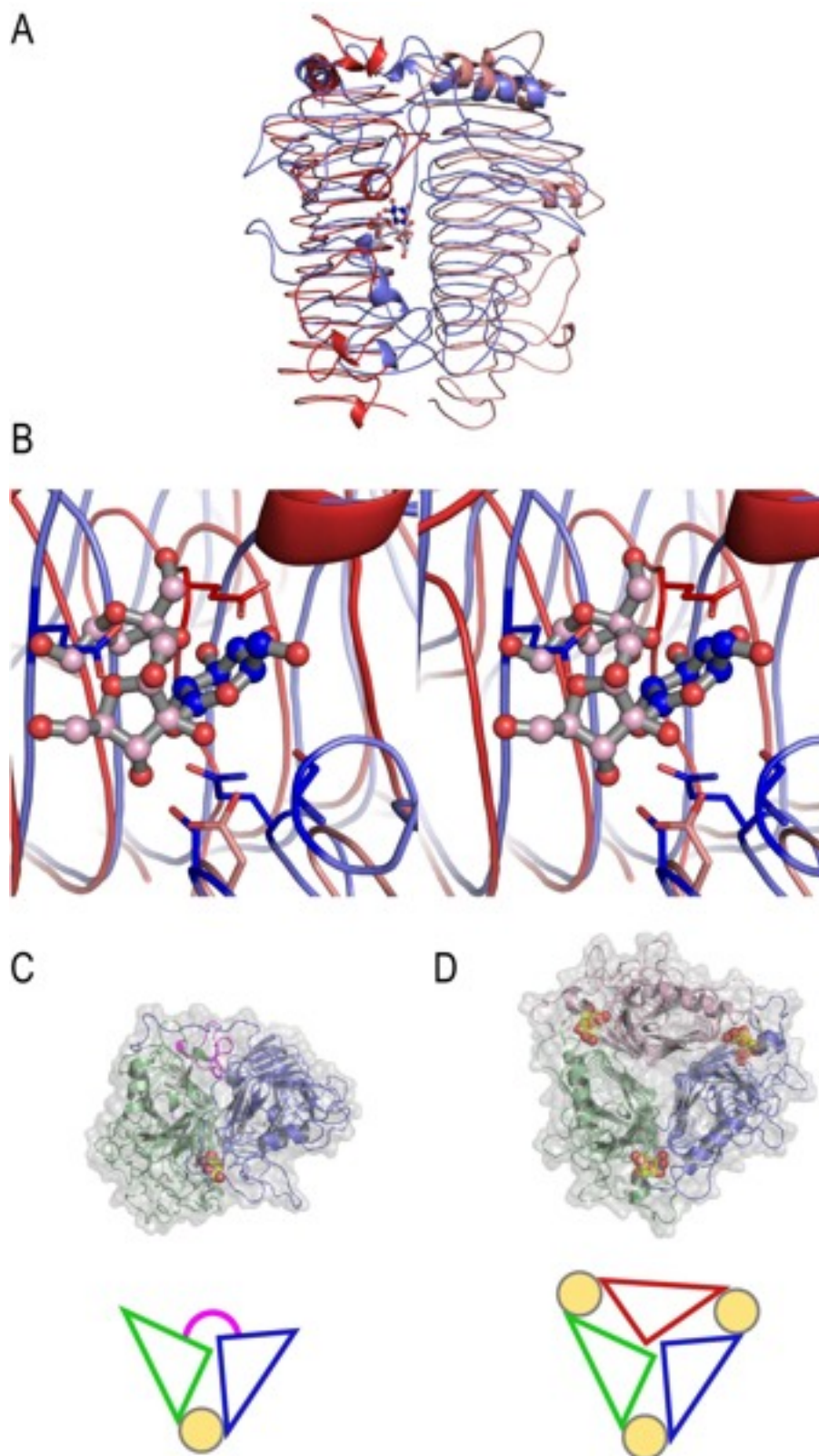
Fig. 3-10
Comparison of active site formation between GH family 55 PcLam55A and PL family 19 (formerly GH family 91) BslFTase. *A.* Superposition of the structures of PcLam55A (blue) and BslFTase (red and pink for two symmetry-related molecules). *B.* Close-up stereoview of the active site. Selected residues in the active site of PcLam55A (Gln146, Gln176, Ser204 and Glu633), and the catalytic residues of BslFTase (Asp233 and Glu244) are shown as stick models. Gluconolactone bound to PcLam55A (carbon atoms in blue) and β-2,1-linked difructosaccharide bound to subsites +1 and +2 of BslFTase (carbon atoms in pink) are shown as ball-and-stick models.

C. and *D.* Top views of monomeric PcLam55A and homotrimeric BslFTase. Schematic diagrams are also shown in these panels. The two domains and the linker region of PcLam55A, and the three symmetry-related chains of BslFTase are colored differently. The ligands are shown as spheres with carbon atoms in yellow. The active site is located at the interface between two domains (GH55) or between two adjacent chains (BslFTase).

3-5 Summary

Similar to the GH family 74 enzymes, GH family 55 exo-β-1,3-glucanases show high specificity to branched substrate. They exhibit unique hydrolysis, producing gentiobiose from laminarin, β-1,3/1,6-glucan. The analysis on sequences of GH family 55 enzymes indicated the repeat of β-helix motif, suggesting that GH family 55 have similar structural property to GH family 74 in addition to the specificity to branched substrate. However, there are no report of structure determination of GH family 55 enzymes. In order to demonstrate molecular basis of GH family 55 enzymes and to compare structural and biochemical property of GH family 55 and 74 enzymes, crystallographic analysis on PcLam55A was conducted.

By means of MAD phasing using selenomethionine labeled PcLam55A expressed by *P. pastoris*, crystal structure of PcLam55A were determined for the first time in GH family 55. PcLam55A has two β-helical domains in a single polypeptide chain. These two domains are connected by a long linker region but are positioned side by side, forming the overall structure resembles a rib cage. In the complex structure, a gluconolactone molecule is bound at the bottom of a pocket between the two β-helix domains. Based on the position of the gluconolactone molecule, Glu-633 appears to be the catalytic acid, whereas the catalytic base residue could not be identified. The substrate binding pocket appears to be able to accept a gentiobiose unit near the cleavage site, and a long cleft runs from the pocket, in accordance with the activity of this enzyme toward linear laminarioligosaccharides with various DPs. Interestingly, both two β-helix domains are involved in construction of both activesite and pocket for β-1,6-branch, suggesting both N- and C-domains are indispensable for the hydrolytic activity and gentiobiose production.

From the view point of domain construction, GH family 55 have similar aspects to GH family 74. The structural similarity between two domains and its deep involvement in the enzymatic activity are elucidated also for GH family 55.

3-6 References

Ciccarelli, F. D., Copley, R. R., Doerks, T., Russell, R. B. & Bork, P. CASH--a beta-helix domain widespread among carbohydrate-binding proteins. *Trends Biochem Sci* **27**, 59-62, (2002).

Cohen-Kupiec, R., Broglie, K. E., Friesem, D., Broglie, R. M. & Chet, I. Molecular characterization of a novel beta-1,3-exoglucanase related to mycoparasitism of Trichoderma harzianum. *Gene* **226**, 147-154, (1999).

Davies, G. & Henrissat, B. Structures and mechanisms of glycosyl hydrolases. *Structure* **3**, 853-859, (1995).

de la Cruz, J., Pintor-Toro, J. A., Benitez, T., Llobell, A. & Romero, L. C. A novel endo-beta-1,3-glucanase, BGN13.1, involved in the mycoparasitism of Trichoderma harzianum. *J Bacteriol* **177**, 6937-6945, (1995).

DeLano, W. L. Unraveling hot spots in binding interfaces: progress and challenges. *Curr Opin Struct Biol* **12**, 14-20, (2002).

Donzelli, B. G., Lorito, M., Scala, F. & Harman, G. E. Cloning, sequence and structure of a gene encoding an antifungal glucan 1,3-beta-glucosidase from Trichoderma atroviride (T. harzianum). *Gene* **277**, 199-208, (2001).

Emsley, P. & Cowtan, K. Coot: model-building tools for molecular graphics. *Acta Crystallogr D Biol Crystallogr* **60**, 2126-2132, (2004).

Giczey, G., Kerenyi, Z., Fulop, L. & Hornok, L. Expression of cmg1, an exo-beta-1,3-glucanase gene from Coniothyrium minitans, increases during sclerotial parasitism. *Appl Environ Microbiol* **67**, 865-871, (2001).

Gouet, P., Courcelle, E., Stuart, D. I. & Metoz, F. ESPript: analysis of multiple sequence alignments in PostScript. *Bioinformatics* **15**, 305-308, (1999).

Guimaraes, B. G., Souchon, H., Lytle, B. L., David Wu, J. H. & Alzari, P. M. The crystal structure and catalytic mechanism of cellobiohydrolase CelS, the major enzymatic component of the Clostridium thermocellum Cellulosome. *J Mol Biol* **320**, 587-596, (2002).

Henrissat, B. & Davies, G. J. Glycoside hydrolases and glycosyltransferases. Families, modules, and implications for genomics. *Plant Physiol* **124**, 1515-1519, (2000).

Holm, L. & Sander, C. Dali: a network tool for protein structure comparison. *Trends Biochem Sci* **20**, 478-480, (1995).

Jenkins, J. & Pickersgill, R. The architecture of parallel beta-helices and related folds. *Prog Biophys Mol Biol* **77**, 111-175, (2001).

Jung, W. S., Hong, C. K., Lee, S., Kim, C. S., Kim, S. J., Kim, S. I. & Rhee, S. Structural and functional insights into intramolecular fructosyl transfer by inulin fructotransferase. *J Biol Chem* **282**, 8414-8423, (2007).

Kasahara, S., Nakajima, T., Miyamoto, C., Wada, K., Furuichi, Y. & Ichishima, E. Characterization and mode of action of exo-1,3-beta-D-glucanase from Aspergillus-saitoi. *J Ferment Bioeng* **74**, 238-240, (1992).

Kawai, R. (2006a). Thesis: The University of Tokyo.

Kawai, R. Functions of extracellular beta-1,3-glucanases from the basidiomycet ePhanerochaete chrysosporium. *Department of Biomaterials sciences* **Ph. D**,(2006b).

Kawai, R., Igarashi, K. & Samejima, M. Gene cloning and heterologous expression of glycoside hydrolase family 55 beta-1,3-glucanase from the basidiomycete Phanerochaete chrysosporium. *Biotechnol Lett* **28**, 365-371,(2006).

Kim, C. S., Hong, C. K., Kim, K. Y., Wang, X. L., Kang, S. I. & Kim, S. I. Cloning, expression, and characterization of Bacillus sp. snu-7 inulin fructotransferase. *J Microbiol Biotechnol* **17**, 37-43,(2007).

Koivula, A., Ruohonen, L., Wohlfahrt, G., Reinikainen, T., Teeri, T. T., Piens, K., Claeyssens, M., Weber, M., Vasella, A., Becker, D., Sinnott, M. L., Zou, J. Y., Kleywegt, G. J., Szardenings, M., Stahlberg, J. & Jones, T. A. The active site of cellobiohydrolase Cel6A from Trichoderma reesei: the roles of aspartic acids D221 and D175. *J Am Chem Soc* **124**, 10015-10024,(2002).

Larsson, A. M., Andersson, R., Stahlberg, J., Kenne, L. & Jones, T. A. Dextranase from Penicillium minioluteum: reaction course, crystal structure, and product complex. *Structure* **11**, 1111-1121,(2003).

Martin, K. L., McDougall, B. M., Unkles, S. E. & Seviour, R. J. The three beta-1,3-glucanases from Acremonium blochii strain C59 appear to be encoded by separate genes. *Mycol Res* **110**, 66-74,(2006).

McCarter, J. D. & Withers, S. G. Mechanisms of enzymatic glycoside hydrolysis. *Curr Opin Struct Biol* **4**, 885-892,(1994).

Muller, J. J., Barbirz, S., Heinle, K., Freiberg, A., Seckler, R. & Heinemann, U. An intersubunit active site between supercoiled parallel beta helices in the trimeric tailspike endorhamnosidase of Shigella flexneri Phage Sf6. *Structure* **16**, 766-775,(2008).

Murshudov, G. N., Vagin, A. A. & Dodson, E. J. Refinement of macromolecular structures by the maximum-likelihood method. *Acta Crystallogr D Biol Crystallogr* **53**, 240-255, (1997).

Nagae, M., Tsuchiya, A., Katayama, T., Yamamoto, K., Wakatsuki, S. & Kato, R. Structural basis of the catalytic reaction mechanism of novel 1,2-alpha-L-fucosidase from *Bifidobacterium bifidum. J Biol Chem* **282**, 18497-18509,(2007).

Nobe, R., Sakakibara, Y., Fukuda, N., Yoshida, N., Ogawa, K. & Suiko, M. Purification and characterization of laminaran hydrolases from Trichoderma viride. *Biosci Biotechnol Biochem* **67**, 1349-1357,(2003).

Nobe, R., Sakakibara, Y., Ogawa, K. & Suiko, M. Cloning and expression of a novel Trichoderma viride Laminarinase AI gene (lamAI). *Biosci Biotechnol Biochem* **68**, 2111-2119,(2004).

Oda, K., Kasahara, S., Yamagata, Y., Abe, K. & Nakajima, T. Cloning and expression of the exo-beta-D-1,3-glucanase gene (exgS) from Aspergillus saitoi. *Biosci Biotechnol Biochem* **66**, 1587-1590,(2002).

Otwinowski, Z., Minor, W. Processing of X-ray diffraction data collected in oscillation mode. *Methods Enzymol* **276**, 307-326,(1997).

Parsiegla, G., Juy, M., Reverbel-Leroy, C., Tardif, C., Belaich, J. P., Driguez, H. & Haser, R. The crystal structure of the processive endocellulase CelF of Clostridium cellulolyticum in complex with a thiooligosaccharide inhibitor at 2.0 A resolution. *Embo J* **17**, 5551-5562,(1998).

Parsiegla, G., Reverbel, C., Tardif, C., Driguez, H. & Haser, R. Structures of mutants of cellulase Cel48F of Clostridium cellulolyticum in complex with long hemithiocellooligosaccharides give rise to a new view of the substrate pathway during processive action. *J Mol Biol* **375**, 499-510,(2008).

Parsiegla, G., Reverbel-Leroy, C., Tardif, C., Belaich, J. P., Driguez, H. & Haser, R. Crystal structures of the cellulase Cel48F in complex with inhibitors and substrates give insights into its processive action. *Biochemistry* **39**, 11238-11246,(2000).

Perrakis, A., Morris, R. & Lamzin, V. S. Automated protein model building combined with iterative structure refinement. *Nat Struct Biol* **6**, 458-463,(1999).

Pitson, S. M., Seviour, R. J., McDougall, B. M., Woodward, J. R. & Stone, B. A. Purification and characterization of three extracellular (1-->3)-beta-D-glucan glucohydrolases from the filamentous fungus Acremonium persicinum. *Biochem J* **308**, 733-741,(1995).

Rigden, D. J. & Franco, O. L. Beta-helical catalytic domains in glycoside hydrolase families 49, 55 and 87: domain architecture, modelling and assignment of catalytic residues. *FEBS Lett* **530**, 225-232,(2002).

Rozeboom, H. J., Bjerkan, T. M., Kalk, K. H., Ertesvag, H., Holtan, S., Aachmann, F. L., Valla, S. & Dijkstra, B. W. Structural and mutational characterization of the catalytic A-module of the mannuronan C-5-epimerase AlgE4 from Azotobacter vinelandii. *J Biol Chem* **283**, 23819-23828,(2008).

Schaeffer, H. J., Leykam, J. & Walton, J. D. Cloning and targeted gene disruption of EXG1, encoding exo-beta 1, 3-glucanase, in the phytopathogenic fungus Cochliobolus carbonum. *Appl Environ Microbiol* **60**, 594-598,(1994).

Terwilliger, T. C. Maximum-likelihood density modification. *Acta Crystallogr D Biol Crystallogr* **56**, 965-972,(2000).

Varrot, A., Macdonald, J., Stick, R. V., Pell, G., Gilbert, H. J. & Davies, G. J. Distortion of a cellobio-derived isofagomine highlights the potential conformational itinerary of inverting beta-glucosidases. *Chem Commun (Camb)* 946-947,(2003).

Vonrhein, C., Blanc, E., Roversi, P. & Bricogne, G. Automated structure solution with autoSHARP. *Methods Mol Biol* **364**, 215-230,(2007).

Xu, B., Muñoz, I. I., Janson, J. C. & Ståhlberg, J. Crystallization and X-ray analysis of native and selenomethionyl beta-mannanase Man5A from blue mussel, Mytilus edulis, expressed in Pichia pastoris. *Acta Cryst*. **D58**, 542-545,(2002).

Yoder, M. D., Lietzke, S. E. & Jurnak, F. Unusual structural features in the parallel beta-helix in pectate lyases. *Structure* **1**, 241-251,(1993).

Yoshida, M., Ohira, T., Igarashi, K., Nagasawa, H., Aida, K., Hallberg, B. M., Divne, C., Nishino, T. & Samejima, M. Production and characterization of recombinant *Phanerochaete chrysosporium* cellobiose dehydrogenase in the methylotrophic yeast *Pichia pastoris*. *Biosci Biotechnol Biochem* **65**, 2050-2057,(2001).

Chapter 4

Conclusion

Polysaccharides are the most abundant biomaterials having huge variety. The numerous diversity of GH family in substrate specificity and mode of action is unsurprisingly needed for degradation and modification of polysaccharides. Since many polysaccharides have branched structure composed of several types of glycosidic linkages, GHs divide the role to achieve efficient degradation. In the xylan degrading system, β-1,4-xylanases and β-1,4-xylosidases, type-B GHs in Fig. 1-6, hydrolyze main-chain linkage at less branched region, whereas the other enzymes such as α-glucuronidases and α-arabinofranosidases, type-A GHs in Fig. 1-6, remove the various side-chains, having affinity to residues attached to main-chain. However, some GHs have ability to hydrolyze main-chain linkages recognizing both main-chain and side-chains, Type-C GHs in Fig. 1-6. Most of family 74 and 55 GHs can be classified into type-C GH, since they are highly specific to branched substrates. Only GH family 74 and 55 include type-C GHs as majority of the family as indicated in Table 1-4. Although abundant structural information about GHs are available now, there are not so many studies on recognition mechanisms of GHs for branched structure in polysaccharides. In this study, X-ray crystallography of family 74 and 55 glycoside hydrolases are performed, and investigation on structure function relationship shared in these families were undertaken.

In chapter 2, detailed characterization of hydrolytic activity and crystallography are performed on a novel GH family 74 xyloglucanase PcXgh74B. The enzyme show high specificity toward glycosidic bonds of unsubstituted glucose residues in TXG. Similar to the previously reported family 74 xyloglucanase *Paenibacilus*XEG74, PcXgh74B exhibit typical property of both endo- and exo- type activity on TXG polymer. However, the accumulation of XGO8 (DP=16-18) were observed as a novel hydrolytic pattern of PcXgh74B. The conservation of amino acid residues involved in substrate binding among GH family 74 enzyme indicated that substitution of small number of amino acid residues in the active site derived the unique hydrolysis by PcXgh74B. Especially, differences of side-chain recognition at Xyl$^{-2'}$ appears to be involved in the accumulation of XGO8.

Many GH family 55 enzymes can be classified into type-C GH in common with GH family 74 enzymes. Moreover, GH family 55 enzymes were predicted to have two β-helical domains based on the analysis of primary sequence, which implies GH family 55 have similar property to GH family 74 not only in substrate specificity but also in protein structure. Therefore, in chapter 3, the crystal structure of PcLam55A were performed for the first time

as a member of GH family 55. The selenomethionine-MAD phasing were successfully conducted using normal strain of *P. pastoris* as an expression host. The structure of PcLam55A demonstrated the contribution of multiple β-helix domain in a single peptide. The two β-helical domains located side by side formed rib-like overall structure, and both domains interact with the ligand bound between them. It was quite similar situation to those found in GH family 74 enzymes, despite that structure of substrate are completely different. In addition, the structure demonstrated mechanism of gentiobiose production which is unique hydrolyzing property of exo-type GH family 55 β-1,3/1,6-glucanases. The small space for gentiobiose unit was found near the active site. The curved cleft running into the active site was found in the molecular surface in accordance with preference toward long substrate suggested by the kinetic parameters.

The overall structure of xyloglucans and β-1,3/1,6-glucans are completely different. Xyloglucan have cellulose-like linear structure thickened by side-chains. On the other hand, β-1,3/1,6-glucans can be considered to take helical structure in solution, since that unbranched β-1,3-glucans form triple helix structure and that laminarioligosaccharides bound to laminarinase in known structure exhibit curved main-chain structure. Largely opened binding cleft of GH family 74 enzymes fit to bind thick-stick structure of xyloglucan molecule, while the curved binding cleft found in PcLam55A structure appears to be appropriate to bind helical structure of β-1,3/1,6-glucans. However, the construction of the whole protein folds of these two enzyme families have some similarity. Both of them consist of two domain having structurally similar folds. GH family 55 and 74 genes are likely to have evolved with gene duplication event. According to *P. chrysosporium* genome database, this fungus have several genes coding GHs having β-propeller fold or β-helix fold, suggesting these genes seems to be a evolutionary origin for GH family 74 or 55 genes. In both case of GH family 74 and 55, the two domains contribute to substrate binding, forming active sites located between them. Moreover, the structure presented in this study suggests that the variety of hydrolytic properties are derived by small changes of amino acid residues at binding site. It can be considered that the domain construction found in GH family 74 and 55 have a benefit in engineering various topology of binding site and subsite structure which derives flexibility of hydrolytic pattern toward branched polysaccharides.

In this study, the homologous domain construction between two distinct GH families

that include type-C GHs as majority were demonstrated for the first time. It suggests that GH family 55 and 74 can form an unique group among type-C GHs and in GH families. Because of the importance of the physiological roles that branched polysaccharides play in nature, more detailed structural information of the polysaccharides are needed. The molecular basis presented here provides useful information for protein engineering of GHs which can be a good tools to investigate structure of branched polysaccharide.

Acknowledgements

森林化学研究室の先輩であり、食品総合研究所 糖質素材ユニット長である徳安健主任研究員をはじめとする森林化学研究室の諸先輩方には、研究室を訪れた際や学会の度毎にご指導ご鞭撻を頂きました。心より御礼申し上げます。

　　東京農工大学農学部の吉田誠特任准教授には、私の大学院進学の際よりお世話になっており、また、折にふれ励ましのお言葉を頂きました。心より感謝申し上げます。川合理恵博士、加治佐平博士は東京大学在学中私を直接指導してくださり、失敗の多かった私に、酵素や遺伝子の実験において根気強く教えてくださいました。心よりお礼申し上げます。他大学から進学してきた私の実験の進め方をいつも近くで見守り、細かなアドバイスをくださいました塚田剛士博士、石黒真希さん、浦川真樹さん、齋藤修啓さんに深く感謝致します。共に励まし合ってきた、同学年の熊倉慧君、鈴木一史君、平石正男君、和田朋子さん、また、卒業した大倉崇君、福田明君、佐久間晶君、博士課程の堀千明さん、石野貴久君、杉本直久君、修士課程の中村彰彦君ほかの森林化学研究室のメンバーのご協力に心より感謝致します。ナガセケムテックス株式会社の原園幸一博士には、酵母を用いたタンパク質の大量発現について御指導頂きました。感謝申し上げます。

　　香川大学情報基盤センターの神鳥成弘教授、吉田裕美准教授をはじめ、神鳥研究室の先輩である東京農工大学工学部生命工学科の大滝証助教、日本原子力研究開発機構 高崎量子応用研究所の山田貢博士研究員、国立病院機構 相模原病院 臨床研究センターの安部暁美研究員を含む元神鳥研究室の皆様には、私が卒業してからも変わらずアドバイスや励ましの言葉を頂き、心より感謝申し上げます。

最後に、これまで私の学生生活を支え、常に暖かく見守り励ましてくれた家族に心より感謝し、謝辞とさせて頂きます。

2010年　3月

Appendix

Substrate recognition by glycoside hydrolase family 74 xyloglucanase from the basidiomycete *Phanerochaete chrysosporium*

Takuya Ishida[1], Katsuro Yaoi[2], Ayako Hiyoshi[2], Kiyohiko Igarashi[1] and Masahiro Samejima[1]

1 Department of Biomaterials Sciences, Graduate School of Agricultural and Life Sciences, University of Tokyo, Japan
2 Institute for Biological Resources and Functions, National Institute of Advanced Industrial Science and Technology (AIST), Tsukuba, Japan

The basidiomycete *Phanerochaete chrysosporium* produces xyloglucanase Xgh74B, which has the glycoside hydrolase (GH) family 74 catalytic domain and family 1 carbohydrate-binding module, in cellulose-grown culture. The recombinant enzyme, which was heterologously expressed in the yeast *Pichia pastoris*, had high hydrolytic activity toward xyloglucan from tamarind seed (TXG), whereas other β-1,4-glucans examined were poor substrates for the enzyme. The existence of the carbohydrate-binding module significantly affects adsorption of the enzyme on crystalline cellulose, but has no effect on the hydrolysis of xyloglucan, indicating that the domain may contribute to the localization of the enzyme. HPLC and MALDI-TOF MS analyses of the hydrolytic products of TXG clearly indicated that Xgh74B hydrolyzes the glycosidic bonds of unbranched glucose residues, like other GH family 74 xyloglucanases. However, viscometric analysis suggested that Xgh74B hydrolyzes TXG in a different manner from other known GH family 74 xyloglucanases. Gel permeation chromatography showed that Xgh74B initially produced oligosaccharides of degree of polymerization (DP) 16–18, and these oligosaccharides were then slowly hydrolyzed to final products of DP 7–9. In addition, the ratio of oligosaccharides of DP 7–9 versus those of DP 16–18 was dependent upon the pH of the reaction mixture, indicating that the affinity of Xgh74B for the oligosaccharides of DP 16–18 is affected by the ionic environment at the active site.

Xyloglucan is a widely distributed hemicellulosic polysaccharide that is found in plant cell walls and seeds. In the cell wall, xyloglucan associates with cellulose microfibrils via hydrogen bonds, forming a cellulose–xyloglucan network [1–3]. During cell expansion and development, partial disassembly of the network is required, and consequently it was proposed that xyloglucan metabolism control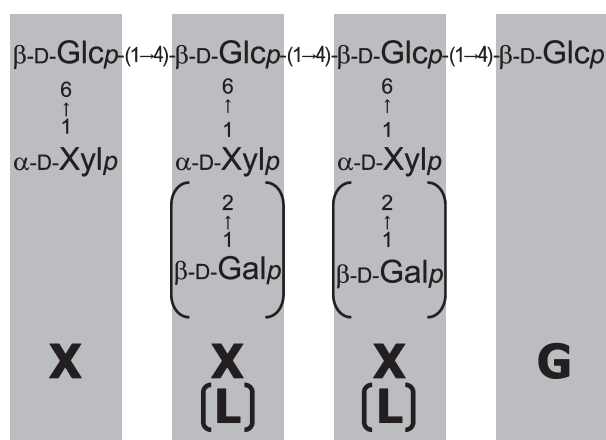s plant cell elongation [4]. In the seeds of some Leguminosae, moreover, xyloglucan acts as a deposited polysaccharide and is available for nutrition when germination occurs. As aqueous solutions of xyloglucan have high viscosity, they are often used as food additives to enhance viscosity and/or as stabilizers. The xyloglucan from tamarind seed (TXG) is one of the best-studied xyloglucans. It consists of a cellulose-like backbone of β-1,4-linked D-glucopyranose

Abbreviations

BMCC, bacterial microcrystalline cellulose; CBM, carbohydrate-binding module; CMC, carboxymethyl cellulose; DP, degree of polymerization; endo-H, endo-β-*N*-acetylglucosaminidase H; GH, glycoside hydrolase; GPC, gel permeation chromatography; PASC, phosphoric acid swollen cellulose; TXG, xyloglucan from tamarind seed; XEG, xyloglucan-specific endo-β-1,4-glucanases; XGH, xyloglucan hydrolase.

residues with side chains of α-D-xylopyranosyl residues attached at the C6 position. Galactose residues are found at the end of the side chain, and single-letter nomenclatures are used to simplify the naming of xyloglucan side chain structures; that is, G, X and L stand for β-D-Glc*p*, α-D-Xyl*p*-(1 → 6)-β-D-Glc*p*, and β-D-Gal*p*-(1 → 2)-α-D-Xyl*p*-(1 → 6)-β-D-Glc*p*, respectively [5]. Compositional analysis of oligosaccharide units in the polymers has shown that TXG has a repeating tetrasaccharide backbone of XXXG, XLXG, XXLG, or XLLG (Fig. 1) [6].

Although many cellulases (EC 3.2.1.4) have been reported to hydrolyze xyloglucan as a substrate analog [7], some endo-β-1,4-glucanases have high activity toward xyloglucan, with little or no activity towards cellulose or cellulose derivatives [8,9]. They have been assigned a new EC number (EC 3.2.1.151) and designated as xyloglucanase, xyloglucan hydrolase (XGH), or xyloglucan-specific endo-β-1,4-glucanases (XEGs) belonging to families 5, 12, 44, and 74, according to a recent classification of glycoside hydrolases (GHs) available at http://afmb.cnrs-mrs.fr/CAZY/[10–12]. Among these enzyme families, xyloglucanases placed in GH family 74 are known to have high specific activity towards xyloglucan, with inversion of the anomeric configuration, and both endo-type and exo-type hydrolases have been found in several microorganisms [13–20]. The exo-type enzymes recognize the reducing end of xyloglucan oligosaccharide (oligoxyloglucan reducing-end-specific cellobiohydrolase, EC 3.2.1.150, from *Geotrichum* sp. M128 [15] and oligoxyloglucan reducing-end-specific xyloglucanobiohydrolase from *Aspergillus nidulans* [20]), whereas the endo-type enzymes
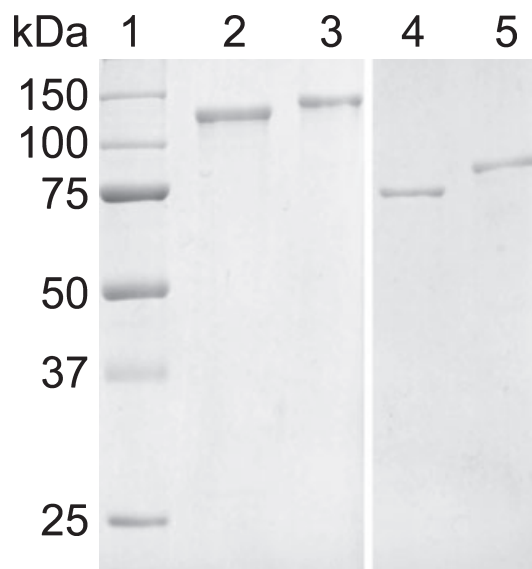
hydrolyze xyloglucan polymer randomly. In addition, XEG74 from *Paenibacillus* sp. KM21 and Cel74A from *Trichoderma reesei* have been reported to have endo-processive or dual-mode endo-like and exo-like activities [13,18].

During the course of wood degradation, the basidiomycete *Phanerochaete chrysosporium* produces two GH family 74 xyloglucanases extracellularly [21]. According to the total genome sequence of the fungus, one of these enzymes, Xgh74B, has the two-domain structure of the N-terminal GH family 74 catalytic domain and the C-terminal domain belonging to the carbohydrate-binding module (CBM) family 1 [21,22]. In the present study, we have heterologously expressed the cDNA encoding Xgh74B in the methylotrophic yeast *Pichia pastoris*, and demonstrated a unique hydrolytic character of the recombinant enzyme.

Results

### Function of CBM1 in recombinant *Ph. chrysosporium* Xgh74B

The cDNA encoding Xgh74B was heterologously expressed in the yeast *Pi. pastoris*, and the recombinant enzymes with and without CBM1 (Xgh74B and Xgh74Bcat, respectively) were purified by column chromatography. As shown in Fig. 2, the molecular masses of purified Xgh74B and Xgh74Bcat were 130

Fig. 1. Tetrameric repeating subunits in TXG [6]. X, L and G represent individual monomeric segments in the single-letter nomenclature. Glc*p*, Xyl*p* and Gal*p* indicate D-glucopyranose, D-xylopyranose and D-galactopyranose, respectively.

Fig. 2. Effect of deglycosylation on purified Xgh74B. Lane 1: molecular weight standards (kDa). Lane 2: Xgh74B incubated with endo-H. Lane 3: Xgh74B. Lane 4: Xgh74Bcat incubated with endo-H. Lane 5: Xgh74Bcat.

and 80 kDa, respectively, being apparently higher than the masses calculated from the amino acid sequences (88.4 and 75.5 kDa, respectively). As there are three N-glycosylation sites in the sequence of the catalytic domain according to the NetNGlyc 1.0 server (http://www.cbs.dtu.dk/services/NetNGlyc/), the N-glycan was eliminated by endo-β-*N*-acetylglucosaminidase H (endo-H) treatment. After the treatment, the molecular mass of Xgh74Bcat became close to the calculated value, whereas that of Xgh74B was still approximately 20 kDa larger than the calculated value. There are numerous O-glycosylation sites between the catalytic domain and the CBM, as predicted by the NetOGlyc 3.1 server (http://www.cbs.dtu.dk/services/NetOGlyc/), so the larger than calculated molecular mass of intact Xgh74B presumably reflects both N-glycosylation and O-glycosylation [23].

The binding properties of Xgh74B and Xgh74Bcat were investigated using solid cellulosic substrates, phosphoric acid-swollen cellulose (PASC), Avicel, and bacterial microcrystalline cellulose (BMCC), as shown in Fig. 3. Xgh74B was adsorbed well on all three cellulose samples, whereas the amount of bound Xgh74Bcat, without CBM1, was lower than that of the intact enzyme. The CBM1 in Xgh74B may contribute to the binding on a crystalline, rather than an amorphous, surface, because increase of crystallinity (PASC < Avicel < BMCC) led to significant differences of adsorption between intact Xgh74B and Xgh74Bcat. The kinetic features of the intact enzyme and catalytic domain were compared as shown in Table 1. The kinetic constants for TXG of the intact enzyme and catalytic domain were all similar, and no significant difference was observed between the two
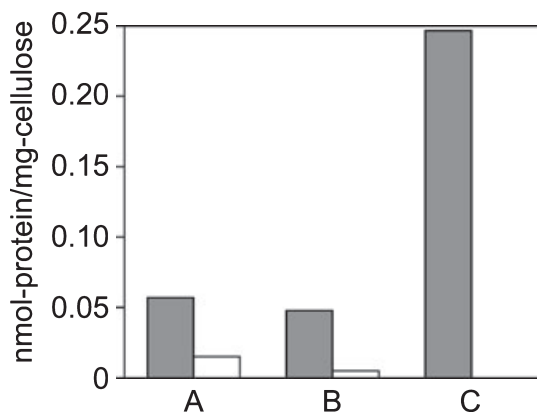
Table 1. Kinetic constants for the hydrolysis of TXG by Xgh74B and Xgh74Bcat.

Enzymes	K_m (mg·mL^{-1})	k_{cat} (s^{-1})	k_{cat}/K_m (mL·mg^{-1}·s^{-1})
Xgh74B	0.25 ± 0.04	28.1 ± 1.4	112
Xgh74Bcat	0.28 ± 0.04	31.9 ± 1.7	114

proteins, suggesting that CBM1 in Xgh74B may contribute to the localization of this enzyme, but not to its function for hydrolysis of the soluble substrate.
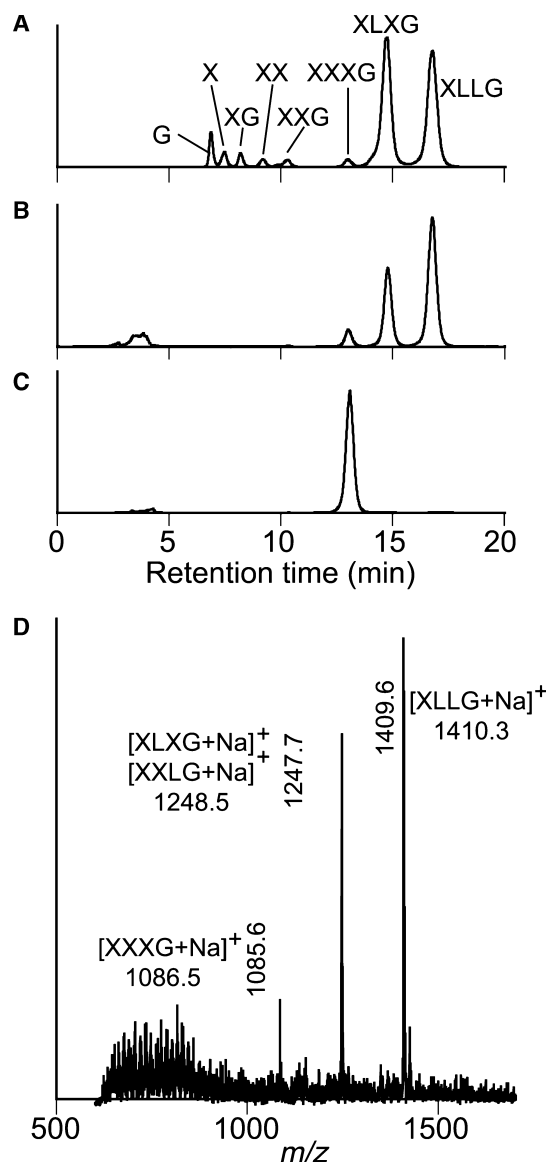
Substrate specificity of Xgh74B

When TXG was used as a substrate, Xgh74B showed optimum hydrolysis at pH 6.0 and 55 °C, and was stable between pH 5.0 and 8.0 at 30 °C (data not shown). The K_m of TXG hydrolysis by Xgh74B was estimated to be 0.25 mg·mL^{-1}, and the k_{cat} was 28.1 s^{-1} when the activity was measured for the reducing sugar. However, Xgh74B showed very low activity (less than 5% relative activity with respect to TXG) towards other β-1,4-glycans, carboxymethyl cellulose (CMC), PASC, Avicel, BMCC, glucomannan, galactomannan, and xylan (data not shown), indicating that Xgh74B has typical characteristics of a GH family 74 xyloglucanase.

The hydrolytic products formed from TXG by Xgh74B were analyzed by normal-phase HPLC and MALDI-TOF MS, as shown in Fig. 4. The results of HPLC suggested that the reaction mixture contained oligosaccharides with three different degrees of polymerization (DP) (Fig. 4B), which showed the same retention times as oligosaccharides with DPs of 7–9, XXXG, XLXG, XXLG, and XLLG. The molecular masses of these fragments estimated by MALDI-TOF MS (Fig. 4D) coincided with those of authentic xyloglucan oligosaccharides. We also analyzed the hydrolytic products of xyloglucan oligosaccharide, XXXGXXXG, and obtained a single peak at the retention time of XXXG (Fig. 4C), suggesting that Xgh74B hydrolyzes the unbranched glucose residues in TXG.
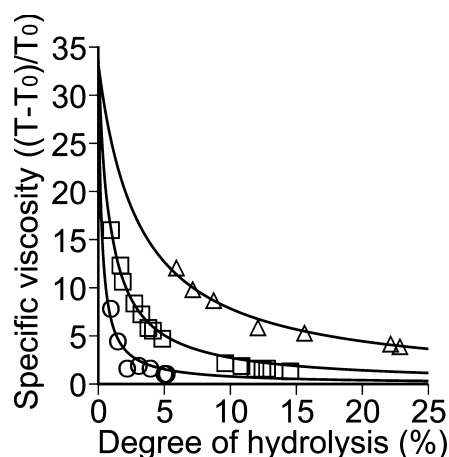
Viscometric assay and gel permeation chromatography (GPC) analysis of TXG hydrolysis

The viscosity of TXG was monitored during the hydrolysis with Xgh74B and XEG from *Geotrichum* sp. M128 (*Geotrichum* XEG), and the viscosity is plotted versus amount of reducing sugar in Fig. 5. A similar plot for XEG74 from *Paenibacillus* sp. strain KM21 (*Paenibacillus* XEG74) is also shown for

Fig. 3. Adsorption of Xgh74B (gray) and Xgh74Bcat (white) on cellulose, quantified by measuring the activity remaining in the supernatant of a mixture of the enzyme and insoluble cellulose (A, PASC; B, Avicel; C, BMCC).

Fig. 4. Analysis of the final products resulting from complete digestion of TXG and xyloglucan oligosaccharide, XXXGXXXG, by Xgh74B. (A) Standards for HPLC analysis (DP values of G, X, XG, XX, XXG, XXXG, XLXG and XLLG are 1, 2, 3, 4, 5, 7, 8 and 9, respectively). (B) HPLC analysis of digestion products of TXG. (C) HPLC analysis of digestion products of XXXGXXXG. (D) MALDI-TOF MS analysis of digestion products of TXG.

Fig. 5. Viscosimetric analysis of TXG incubated with the xyloglucan-ases. After various incubation times, the specific viscosity was calculated and the hydrolysis ratio was determined by measuring the reducing power. The reducing power obtained by complete digestion with excess enzyme was normalized to 100%. Square, Xgh74B. Circle, *Geotrichum* XEG. Triangle, *Paenibacillus* XEG74 (data from [13]).

reference [13]. As described above, Xgh74B effectively hydrolyzed TXG, and a decrease in viscosity was observed, with the production of reducing sugar, indicating that Xgh74B is an endo-type enzyme that cleaves polymeric substrates in the middle of the molecule. However, there were differences among the plots for the three enzymes; the degree of hydrolysis-specific viscosity plot for Xgh74B is intermediate between those of *Geotrichum* XEG and *Paenibacillus* XEG74. Therefore, the change of the molecular mass distribution of TXG during the hydrolysis was analyzed by GPC with a refractive index detector, as shown in Fig. 6. In the case of *Geotrichum* XEG, the molecular mass decreased rapidly even at the initial stage of the reaction, suggesting that the degradation process involved random hydrolysis of β-1,4-linkages in the xyloglucan polymer chain. On the other hand, the degradation pattern of Xgh74B was rather similar to that of *Paenibacillus* XEG74, as the oligosaccharides with DP 7–9 (XXXG, XLXG, XXLG, and XLLG) were observed from the initial stage of the reaction (peak B in Figs 6B and 7D). However, in the case of Xgh74B, there is an additional peak at an earlier retention time (12 min, peak A). Peak A was fractionated and analyzed by MALDI-TOF MS analysis, and was found to consist of oligosaccharides of DP 16–18, as shown in Fig. 7A. In addition, the relative amount of peak A (DP 16–18) was greater when the reaction was carried out at higher pH, suggesting that the charge at the active site influences the affinity for oligosaccharides of DP 16–18.

Discussion

Filamentous fungi produce several extracellular xyloglucanases when they grow on plant cell walls as a carbon source. Before their characterization, fungal GH family 74 xyloglucanases had been thought to be
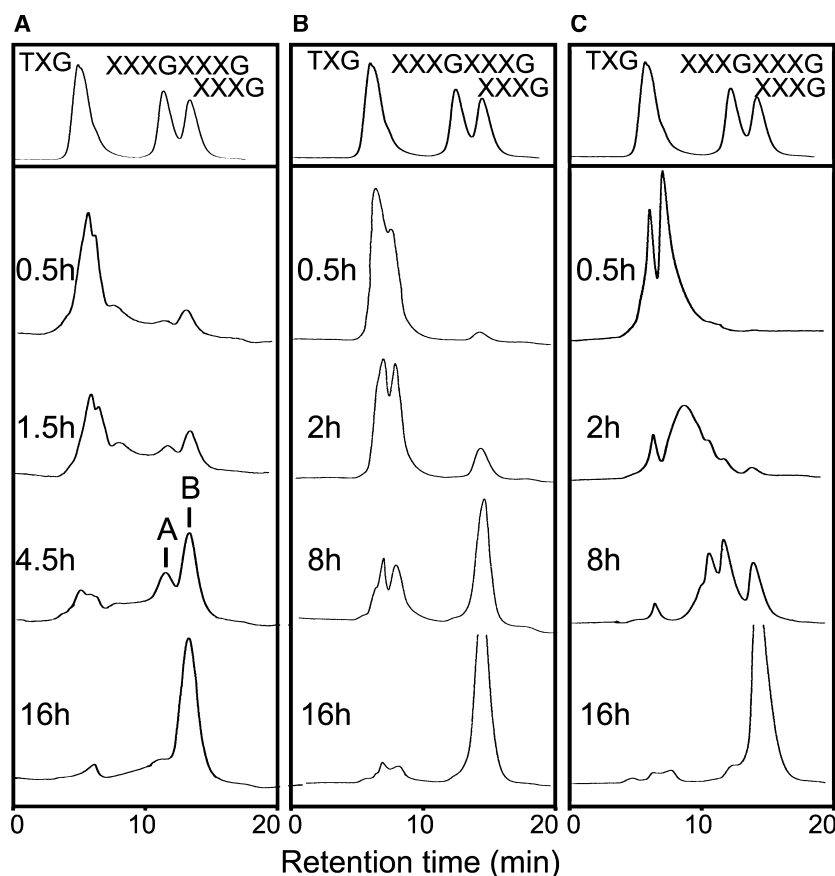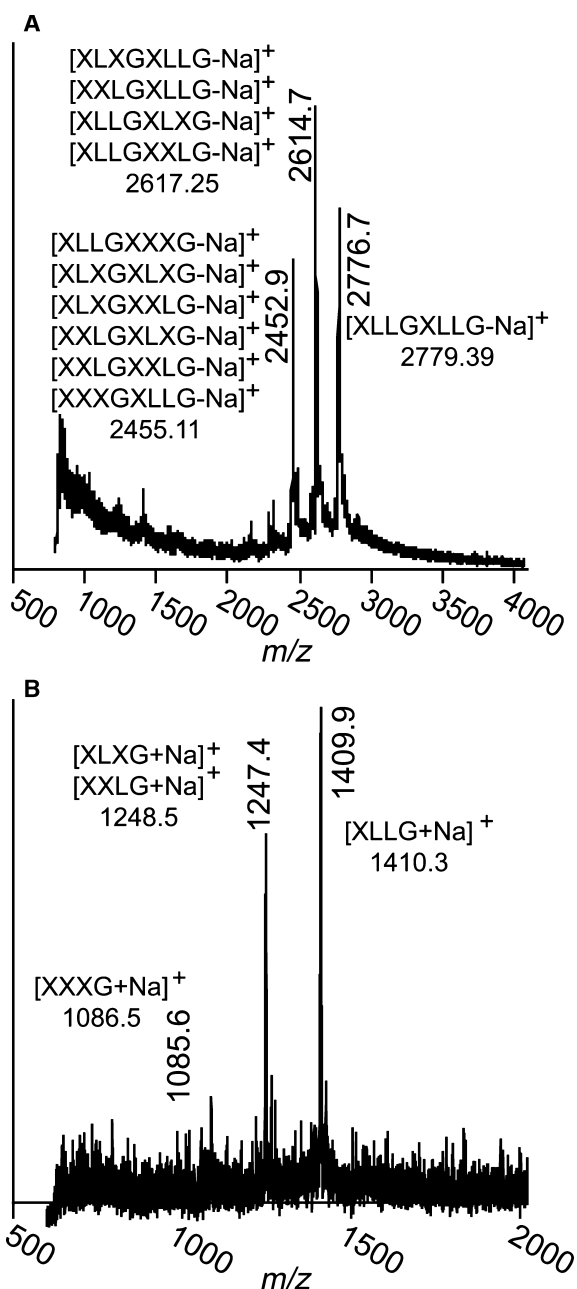
Fig. 6. Analysis of xyloglucan hydrolysis products by means of GPC. TXG was incubated with the xyloglucanases for various times, and the reaction products were applied to a gel permeation column. (A) Xgh74B. (B) *Paenibacillus* XEG74 (data from [13]). (C) *Geotrichum* XEG.

cellulases, as they have apparent activity against amorphous cellulose or soluble cellulose derivatives. Moreover, some fungi produce GH family 74 xyloglucanases with the family 1 CBM, and this also results in enzymes that were characterized as cellulases. According to the total genome sequence of *Ph. chrysosporium*, there are two enzymes belonging to GH family 74 (Xgh74A and Xgh74B), and Xgh74B is known to have the family 1 CBM at the C-terminal region [22]. Therefore, in the present study, we heterologously expressed recombinant Xgh74B in yeast, and the function of CBM1 in Xgh74B was characterized from adsorption and kinetic points of view. Apparent adsorption of intact Xgh74B was observed when solid cellulosic substrates were used, but a comparison of the kinetic parameters of intact Xgh74B and Xgh74Bcat clearly indicates that the CBM in Xgh74B does not contribute to the hydrolytic reaction of soluble xyloglucan substrates. The results suggest that the CBM might determine the localization of this enzyme or help in the hydrolysis of insoluble substrates.

Recently, some diversity of substrate specificity and mode of action has been reported for GH family 74

enzymes; for example, oligoxyloglucan reducing-end specific cellobiohydrolase from *Geotrichum* sp. M128 and OREX from *A. nidulans* have oligoxyloglucan reducing-end-specific exo-activity and cannot hydrolyze xyloglucan polymer [15,20], whereas most enzymes belonging to GH family 74 are β-1,4-glucanases with the highest activity towards xyloglucan [13,14,16–18]. Xgh74B rapidly decreases the viscosity of TXG solutions, consistent with an endohydrolase mechanism. On GPC, however, the final degradation products (XXXG, XLXG, XXLG, and XLLG) were observed to be formed even at the initial stage of the reaction (Fig. 6A). This feature is very similar to that of XEG74 from *Paenibacillus* [13], which initially hydrolyzes TXG in an endo-manner, followed by the production of the final products. However, if we carefully compare the GPC patterns of *Phanerochaete* Xgh74B and *Paenibacillus* XEG74, there is an apparent difference; in the case of *Phanerochaete* Xgh74B, accumulation of oligosaccharides of DP 16–18 was observed at the initial stage of hydrolysis, and these oligosaccharides subsequently disappeared during the course of hydrolysis. Moreover, the oligosaccharides of DP 16–18 apparently remained if the reaction pH was

A

[XLXGXLLG-Na]⁺
[XXLGXLLG-Na]⁺
[XLLGXLXG-Na]⁺
[XLLGXXLG-Na]⁺
2617.25

2614.7

2776.7

[XLLGXXXG-Na]⁺
[XLXGXLXG-Na]⁺
[XLXGXXLG-Na]⁺
[XXLGXLXG-Na]⁺
[XXLGXXLG-Na]⁺
[XXXGXLLG-Na]⁺
2455.11

2452.9

[XLLGXLLG-Na]⁺
2779.39

m/z

B

1409.9

1247.4

[XLXG+Na]⁺
[XXLG+Na]⁺
1248.5

[XLLG+Na]⁺
1410.3

[XXXG+Na]⁺
1086.5

1085.6

m/z

Fig. 7. MALDI-TOF MS analysis of peaks A (A) and B (B) in Fig. 6. The peaks were fractionated and analyzed by MALDI-TOF MS. Peak A included oligosaccharides of DP 16–18, and peak B included oligosaccharides of DP 7–9.

increased (Fig. 8). These results indicate that the hydrolysis of the oligosaccharides of DP 16–18 to oligosaccharides of DP 7–9 does not proceed at higher pH, and suggest that an ionic interaction may play an important role in the interaction of the enzyme and its substrates, or that a pH-dependent conformational change of the enzyme occurs.

The crystal structures of *Geotrichum* oligoxyloglucan reducing-end specific cellobiohydrolase and *Clostridium* Xgh74A have been solved [24–26], and indicate that xyloglucan molecules bind to an open cleft of the enzymes, and that amino acid residues in the cleft recognize the side chain residues as well as the main chain. In addition, our recent study demonstrated that mutants of *Paenibacillus* XEG74 with mutations involving amino acid residues in the substrate-binding cleft showed the accumulation of oligosaccharides of DP 16–18, like *Phanerochaete* Xgh74B (data not shown). These results suggest that the substrate specificities of the enzymes belonging to GH family 74 are dependent not only upon conformational changes of the binding cleft or loop structures, but also upon the nature of a few key amino acids (or their side chains). The specificities of the enzymes are likely to have been precisely honed during the course of evolution. Further investigation is required to elucidate in detail the mechanism involved in the regulation of the enzyme activities.

Experimental procedures

Cloning of cDNA encoding Xgh74B from *Ph. chrysosporium*

Ph. chrysosporium K-3 [27] was cultured at 26.5 °C on Kremer and Wood medium [28] containing 2% cellulose (CF11; Whatman, Clifton, NJ, USA) as a sole carbon source, based on a previous report [29]. After 4 days of cultivation, mycelia were collected by filtration and crushed in liquid nitrogen. Purification of mRNA and first-strand cDNA synthesis were performed as described previously [30]. Based on *Ph. chrysosporium* genome information, the oligonucleotide primers xgh74B-F (5′-GCAAGCCCACAA GCATACACATGGAAG-3′) and xgh74B-R (5′-TCATAG ACACAAATTGCCGGTACTCAC-3′) were designed in order to amplify the cDNA encoding mature Xgh74B. The amplified fragment was ligated into the pCR4Blunt-TOPO vector (Invitrogen, Carlsbad, CA, USA) according to the manufacturer's instructions, and transformed into *Escherichia coli* strain JM109 (Takara Bio, Shiga, Japan). A database search for the deduced amino acid sequence was performed using BLASTP (http://www.ncbi.nlm.nih.gov/BLAST/) [31,32].

Expression and purification of recombinant Xgh74B and Xgh74Bcat

The oligonucleotide primers XGH74B-F (5′-TTTGAATTC GCAAGCCCACAAGCATACACATGGAAG-3′), XGH74B-R1 (5′-TTTGCGGCCGCTCATAGACACAAATTGCCGG
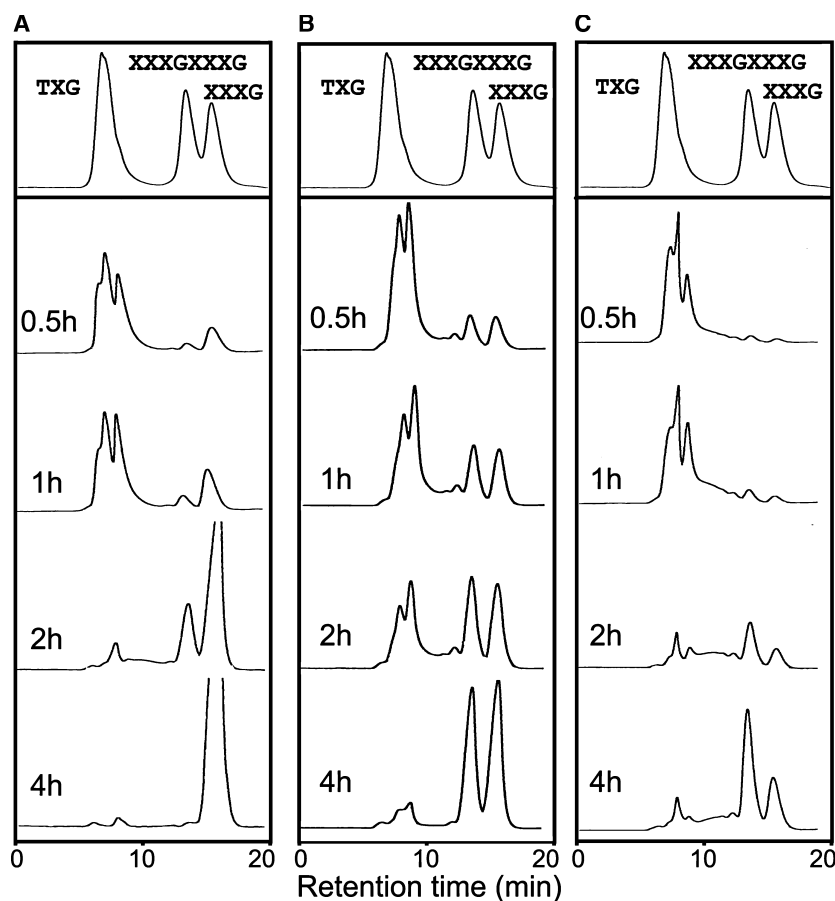
Fig. 8. Gel permeation analysis of xyloglucan hydrolysis products obtained at different pH values. TXG was incubated with Xgh74B in sodium acetate buffer at pH 5.0 (A), sodium phosphate buffer at pH 7.0 (B), or Tris/HCl buffer at pH 8.0 (C) for various incubation times, and the reaction products were applied to a gel permeation column.

TACTCAC-3′) and XGH74B-R2 (5′-TTT**GCGGCCGCT**CAGTCGCCGTAAAAGATGCCGCGA-3′), introducing *Eco*RI (underlined sequence) and *Not*I (bold sequence) cleavage sites, were used to prepare the fragments for expression. The primer pairs XGH74B-F and XGH74B-R1, or XGH74B-F and XGH74B-R2, were used to amplify the sequences encoding mature Xgh74B or Xgh74Bcat, respectively. These fragments were ligated into the pCR4Blunt-TOPO vector and transformed into *E. coli* strain JM109 again. The fragments were digested with restriction enzymes, *Eco*RI and *Not*I, and ligated into the *Pi. pastoris* expression vector, pPICZα-A (Invitrogen), at the same restriction sites. The vectors were transformed into *Pi. pastoris* KM-71H as described previously [33].

The transformants were cultivated in growth medium, and then in induction medium as described previously [33]. After induction for 3 days, the culture was centrifuged (15 min, 1500 ***g***), and the supernatant was then mixed with 5% (w/v) bentonite (Wako Pure Chemical Industries Ltd., Osaka, Japan) and incubated for 30 min at 4 °C. The bentonite was removed by centrifugation (30 min, 1500 ***g***), and the supernatant was concentrated by ammonium sulfate precipitation (70% saturation). The precipitate was dissolved in 20 mM potassium phosphate buffer (pH 7.0) and applied to a Toyopearl HW-40C gel permeation column (22 × 200 mm; Tosoh Co., Tokyo, Japan) for desalting. The protein fractions were concentrated and applied to a DEAE-Toyopearl 650S column (16 × 120 mm; Tosoh) equilibrated with 20 mM potassium phosphate buffer (pH 7.0). The protein was eluted with a linear gradient of 0 mM to 500 mM NaCl at 1 mL·min⁻¹. The fractions were assayed for xyloglucanase activity using tamarind gum (Tokyo Chemical Industry Co., Ltd, Tokyo, Japan) and *p*-hydroxybenzoic acid hydrazide (Pfaltz & Bauer, Waterbury, CT, USA) as described in the following section. Then, the fraction containing xyloglucanase activity was equilibrated against 20 mM sodium acetate buffer (pH 5.0) containing 500 mM ammonium sulfate, and applied to a Phenyl Toyopearl 650S column (16 × 180 mm; Tosoh) equilibrated with the same buffer. The proteins were eluted with a linear gradient of 500 mM to 0 mM ammonium sulfate. The fractions containing the recombinant proteins were collected and equilibrated against 20 mM sodium acetate buffer (pH 5.5).

Deglycosylation was performed using endo-H (New England Biolabs, Beverly, MA, USA) as described previously [34]. Purity and decrease in molecular mass were confirmed by SDS/PAGE.

Determination of reducing sugar concentration

The hydrolyzing activity of the enzymes was measured by determination of reducing power of reaction mixture. For purification, adsorption experiments and examination of hydrolyzing activity towards various β-1,4-glycans, *p*-hydroxybenzoic acid hydrazide was used as described previously [35]. For determination of optimum pH, optimum temperature, pH stability, and thermal stability, the enzyme activity was assayed according to the Nelson and Somogyi method [36–38]. 2,2′-Bicinchoninate (bicinchoninic acid disodium salt; Nacalai Tesque Inc., Kyoto, Japan) was used for determination of kinetic constants, as described previously [13,39,40].

Adsorption of Xgh74B and Xgh74Bcat on insoluble cellulose

Adsorption experiments were performed as described previously [41]. Intact Xgh74B and Xgh74Bcat were incubated with 0.5% PASC, 0.5% Avicel (Funacel SF; Funakoshi Co., Ltd, Tokyo, Japan), or 0.1% BMCC in 20 mM potassium phosphate buffer (pH 6.0). PASC and BMCC were prepared as described previously [42,43]. The mixtures of the protein and carbohydrates were incubated for 1 h at 30 °C and then separated by centrifugation (10 min, 16100 *g*). The supernatants were centrifuged again to remove the precipitates completely, and the remaining activity of the enzyme in each supernatant was determined using tamarind gum and *p*-hydroxybenzoic acid hydrazide as described above. The amount of protein that had been adsorbed on the cellulose and removed by centrifugation was then calculated.

Substrate specificity and kinetic parameters

The hydrolytic activities towards various β-1,4-glycans, CMC (CMC 7LFD; Hercules Inc., Wilmington, DE, USA), PASC, Avicel, BMCC, glucomannan (from Konjac tuber; Wako Pure Chemical Industries), galactomannan (gum, locust bean; Sigma-Aldrich, St Louis, MO, USA), and xylan (from birch wood and from beech wood; Sigma-Aldrich) were examined. Carbohydrates (0.25%, w/v) were incubated with Xgh74B at 30 °C for 6 h in 100 mM sodium acetate buffer (pH 5.0) solutions, and reducing sugar concentration was measured using *p*-hydroxybenzoic acid hydrazide.

The substrate, TXG, was obtained from Dainippon Sumitomo Pharmaceutical Co., Ltd (Osaka, Japan). The temperature and pH effects on recombinant Xgh74B and Xgh74Bcat were analyzed. Xyloglucan-hydrolyzing activity was assayed by measurement of the reducing power using the Nelson–Somogyi method. The optimum temperature for enzyme activity was determined by incubation with TXG (5 mg·mL^{-1}) in 20 mM sodium phosphate buffer (pH 6.0) for 20 min at various temperatures. Thermostability was analyzed by incubating the enzyme without substrate in the same buffer for 20 min at various temperatures, and the remaining activity was then assayed by incubation with TXG (5 mg·mL^{-1}) at 45 °C for 20 min. The optimum pH was determined by incubating the enzyme with TXG (5 mg·mL^{-1}) at 40 °C for 20 min in McIlvaine buffer solutions (0.2 M disodium hydrogen phosphate and 0.1 M citric acid) that varied in pH (from 2.0 to 9.0). The pH stability was assayed by incubating the enzyme in the absence of substrate at 30 °C for 20 min in the same buffer solutions. The buffer solutions were then adjusted to pH 6.0, and the remaining enzyme activity was assayed by incubation with TXG (5 mg·mL^{-1}) at 30 °C for 20 min.

Kinetic constants were determined at TXG concentrations ranging from 0.2 to 5 mg·mL^{-1}, using 2.5 μg enzyme/mL in 20 mM sodium phosphate buffer (pH 6.0). The bicinchoninate assay was used to quantify reducing sugars. The Michaelis constant (K_m), specific activity and catalytic rate (k_{cat}) were calculated from a plot of initial reaction rates versus substrate concentration using KALEIDA-GRAPH 3.6.4 (Synergy, Reading, PA, USA).

HPLC and MALDI-TOF MS analysis

The reaction products of TXG and XXXGXXXG generated by Xgh74B treatment were analyzed by normal-phase HPLC and MALDI-TOF MS. The oligosaccharide, XXXGXXXG, was prepared as described previously [44]. HPLC was carried out with an Amide-80 normal-phase column (4.6 × 250 mm; Tosoh) using 65% acetonitrile (isocratic) at a flow rate of 0.8 mL·min^{-1}. MALDI-TOF MS was performed with a Voyager mass spectrometer (PerSeptive Biosystems, Framingham, MA, USA) at an accelerating energy of 20 kV, in linear mode, and with positive-ion detection. The matrix was 2,5-dihydroxybenzoic acid in 50% acetonitrile at a concentration of 10 mg·mL^{-1}. XXXG (Tokyo Chemical Industry Co., Ltd.) was used as an external calibration standard.

Viscometric assay

Viscosimetric assays were carried out by monitoring the flow time of 0.8% xyloglucan. TXG was incubated with Xgh74B in 20 mM sodium phosphate buffer (pH 6.0) or with *Geotrichum* XEG in 50 mM sodium acetate buffer (pH 5.5) for different times. The flow time of the reaction mixture was determined in an Ostwald viscometer at room temperature, and the reducing sugar content was determined by means of the bicinchoninate assay. The specific viscosity was calculated as $(T - T_0)/T_0$, where T_0 is the flow time measured for the buffer and T is the flow time of the reaction mixture with the enzyme.

Analysis of xyloglucan hydrolysis products by GPC

TXG was incubated with Xgh74B in 20 mM buffer (sodium acetate buffer, pH 5.0, sodium phosphate buffer, pH 6.0 or 7.0, Tris/HCl buffer, pH 8.0), or with *Geotrichum* XEG in 50 mM sodium acetate buffer (pH 5.5). After various incubation times, the reaction solution was applied to a Superdex Peptide 10/300 GL (GE Healthcare Bio-Sciences, Piscataway, NJ, USA) gel permeation column, and the degradation products were analyzed.

Acknowledgements

References

1 Hayashi T & Maclachlan G (1984) Pea xyloglucan and cellulose: I. Macromolecular organization. *Plant Physiol* **75**, 596–604.

2 Fry SC (1989) The structure and functions of xyloglucan. *J Exp Bot* **40**, 1–11.

3 Hayashi T (1989) Xyloglucans in the primary-cell wall. *Annu Rev Plant Phys* **40**, 139–168.

4 Hayashi T, Ogawa K & Mitsuishi Y (1994) Characterization of the adsorption of xyloglucan to cellulose. *Plant Cell Physiol* **35**, 1199–1205.

5 Fry SC, York WS, Albersheim P, Darvill A, Hayashi T, Joseleau JP, Kato Y, Lorences EP, Maclachlan GA, Mcneil M *et al.* (1993) An unambiguous nomenclature for xyloglucan-derived oligosaccharides. *Physiol Plant* **89**, 1–3.

6 York WS, van Halbeek H, Darvill AG & Albersheim P (1990) Structural analysis of xyloglucan oligosaccharides by 1H-n.m.r. spectroscopy and fast-atom-bombardment mass spectrometry. *Carbohydr Res* **200**, 9–31.

7 Vincken JP, Beldman G & Voragen AG (1997) Substrate specificity of endoglucanases: what determines xyloglucanase activity? *Carbohydr Res* **298**, 299–310.

8 Edwards M, Dea IC, Bulpin PV & Reid JS (1986) Purification and properties of a novel xyloglucan-specific endo-(1->4)-β-D-glucanase from germinated nasturtium seeds (*Tropaeolum majus* L.). *J Biol Chem* **261**, 9489–9494.

9 Pauly M, Andersen LN, Kauppinen S, Kofod LV, York WS, Albersheim P & Darvill A (1999) A xyloglucan-specific endo-β-1,4-glucanase from *Aspergillus aculeatus*: expression cloning in yeast, purification and character-ization of the recombinant enzyme. *Glycobiology* **9**, 93–100.

10 Henrissat B (1991) A classification of glycosyl hydrolases based on amino acid sequence similarities. *Biochem J* **280**, 309–316.

11 Henrissat B & Bairoch A (1993) New families in the classification of glycosyl hydrolases based on amino acid sequence similarities. *Biochem J* **293**, 781–788.

12 Henrissat B & Bairoch A (1996) Updating the sequence-based classification of glycosyl hydrolases. *Biochem J* **316**, 695–696.

13 Yaoi K, Nakai T, Kameda Y, Hiyoshi A & Mitsuishi Y (2005) Cloning and characterization of two xyloglucan-ases from *Paenibacillus* sp. strain KM21. *Appl Environ Microbiol* **71**, 7670–7678.

14 Yaoi K & Mitsuishi Y (2004) Purification, characterization, cDNA cloning, and expression of a xyloglucan endoglucanase from *Geotrichum* sp. M128. *FEBS Lett* **560**, 45–50.

15 Yaoi K & Mitsuishi Y (2002) Purification, characterization, cloning, and expression of a novel xyloglucan-specific glycosidase, oligoxyloglucan reducing end-specific cellobiohydrolase. *J Biol Chem* **277**, 48276–48281.

16 Irwin DC, Cheng M, Xiang B, Rose JK & Wilson DB (2003) Cloning, expression and characterization of a family-74 xyloglucanase from *Thermobifida fusca*. *Eur J Biochem* **270**, 3083–3091.

17 Hasper AA, Dekkers E, van Mil M, van de Vondervoort PJ & de Graaff LH (2002) EglC, a new endo-glucanase from *Aspergillus niger* with major activity towards xyloglucan. *Appl Environ Microbiol* **68**, 1556–1560.

18 Grishutin SG, Gusakov AV, Markov AV, Ustinov BB, Semenova MV & Sinitsyn AP (2004) Specific xyloglu-canases as a new class of polysaccharide-degrading enzymes. *Biochim Biophys Acta* **1674**, 268–281.

19 Chhabra SR & Kelly RM (2002) Biochemical characterization of *Thermotoga maritima* endoglucanase Cel74 with and without a carbohydrate binding module (CBM). *FEBS Lett* **531**, 375–380.

20 Bauer S, Vasu P, Mort AJ & Somerville CR (2005) Cloning, expression, and characterization of an oligoxy-loglucan reducing end-specific xyloglucanobiohydrolase from *Aspergillus nidulans*. *Carbohydr Res* **340**, 2590–2597.

21 Wymelenberg AV, Sabat G, Martinez D, Rajangam AS, Teeri TT, Gaskell J, Kersten PJ & Cullen D (2005) The *Phanerochaete chrysosporium* secretome: database predictions and initial mass spectrometry peptide identifications in cellulose-grown medium. *J Biotechnol* **118**, 17–34.

22 Martinez D, Larrondo LF, Putnam N, Gelpke MD, Huang K, Chapman J, Helfenbein KG, Ramaiya P, Detter JC, Larimer F *et al.* (2004) Genome sequence of

the lignocellulose degrading fungus *Phanerochaete chrysosporium* strain RP78. *Nat Biotechnol* **22**, 695–700.

23 Julenius K, Molgaard A, Gupta R & Brunak S (2005) Prediction, conservation analysis, and structural characterization of mammalian mucin-type O-glycosylation sites. *Glycobiology* **15**, 153–164.

24 Yaoi K, Kondo H, Noro N, Suzuki M, Tsuda S & Mitsuishi Y (2004) Tandem repeat of a seven-bladed β-propeller domain in oligoxyloglucan reducing-end-specific cellobiohydrolase. *Structure* **12**, 1209–1217.

25 Yaoi K, Kondo H, Hiyoshi A, Noro N, Sugimoto H, Tsuda S, Mitsuishi Y & Miyazaki K (2007) The structural basis for the exo-mode of action in GH74 oligoxyloglucan reducing end-specific cellobiohydrolase. *J Mol Biol* **370**, 53–62.

26 Martinez-Fleites C, Guerreiro CI, Baumann MJ, Taylor EJ, Prates JA, Ferreira LM, Fontes CM, Brumer H & Davies GJ (2006) Crystal structures of *Clostridium thermocellum* xyloglucanase, XGH74A, reveal the structural basis for xyloglucan recognition and degradation. *J Biol Chem* **281**, 24922–24933.

27 Johnsrud SC & Eriksson KE (1985) Cross-breeding of selected and mutated homokaryotic strains of *Phanerochaete-chrysosporium* K-3 − new cellulase deficient strains with increased ability to degrade lignin. *Appl Environ Microbiol* **21**, 320–327.

28 Kremer SM & Wood PM (1992) Evidence that cellobiose oxidase from *Phanerochaete chrysosporium* is primarily an Fe(III) reductase. Kinetic comparison with neutrophil NADPH oxidase and yeast flavocytochrome b_2. *Eur J Biochem* **205**, 133–138.

29 Habu N, Igarashi K, Samejima M, Pettersson B & Eriksson KE (1997) Enhanced production of cellobiose dehydrogenase in cultures of *Phanerochaete chrysosporium* supplemented with bovine calf serum. *Biotechnol Appl Biochem* **26**, 97–102.

30 Kawai R, Igarashi K, Yoshida M, Kitaoka M & Samejima M (2006) Hydrolysis of β-1,3/1,6-glucan by glycoside hydrolase family 16 endo-1,3(4)-β-glucanase from the basidiomycete *Phanerochaete chrysosporium*. *Appl Microbiol Biotechnol* **71**, 898–906.

31 Altschul SF, Madden TL, Schaffer AA, Zhang J, Zhang Z, Miller W & Lipman DJ (1997) Gapped BLAST and PSI-BLAST: a new generation of protein database search programs. *Nucleic Acids Res* **25**, 3389–3402.

32 Altschul SF, Gish W, Miller W, Myers EW & Lipman DJ (1990) Basic local alignment search tool. *J Mol Biol* **215**, 403–410.

33 Igarashi K, Yoshida M, Matsumura H, Nakamura N, Ohno H, Samejima M & Nishino T (2005) Electron transfer chain reaction of the extracellular flavocytochrome cellobiose dehydrogenase from the basidiomycete *Phanerochaete chrysosporium*. *FEBS J* **272**, 2869–2877.

34 Yoshida M, Ohira T, Igarashi K, Nagasawa H, Aida K, Hallberg BM, Divne C, Nishino T & Samejima M (2001) Production and characterization of recombinant *Phanerochaete chrysosporium* cellobiose dehydrogenase in the methylotrophic yeast *Pichia pastoris*. *Biosci Biotechnol Biochem* **65**, 2050–2057.

35 Lever M (1972) A new reaction for colorimetric determination of carbohydrates. *Anal Biochem* **47**, 273–279.

36 Somogyi M (1952) Notes on sugar determination. *J Biol Chem* **195**, 19–23.

37 Somogyi M (1945) A new reagent for the determination of sugars. *J Biol Chem* **160**, 61–68.

38 Nelson N (1944) A photometric adaptation of the Somogyi method for the determination of glucose. *J Biol Chem* **153**, 375–380.

39 Waffenschmidt S & Jaenicke L (1987) Assay of reducing sugars in the nanomole range with 2,2′-bicinchoninate. *Anal Biochem* **165**, 337–340.

40 Doner LW & Irwin PL (1992) Assay of reducing end-groups in oligosaccharide homologues with 2,2′-bicinchoninate. *Anal Biochem* **202**, 50–53.

41 Yoshida M, Igarashi K, Wada M, Kaneko S, Suzuki N, Matsumura H, Nakamura N, Ohno H & Samejima M (2005) Characterization of carbohydrate-binding cytochrome b_{562} from the white-rot fungus *Phanerochaete chrysosporium*. *Appl Environ Microbiol* **71**, 4548–4555.

42 Wood TM (1988) Preparation of crystalline, amorphous, and dyed cellulase substrates. *Methods Enzymol* **160**, 19–25.

43 Samejima M, Sugiyama J, Igarashi K & Eriksson KEL (1998) Enzymatic hydrolysis of bacterial cellulose. *Carbohydr Res* **305**, 281–288.

44 Hayashi T, Takeda T, Ogawa K & Mitsuishi Y (1994) Effects of the degree of polymerization on the binding of xyloglucans to cellulose. *Plant Cell Physiol* **35**, 893–899.

Crystal Structure of Glycoside Hydrolase Family 55 β-1,3-Glucanase from the Basidiomycete *Phanerochaete chrysosporium*[*][S]

Takuya Ishida[‡1], **Shinya Fushinobu**[§1], **Rie Kawai**[‡], **Motomitsu Kitaoka**[¶], **Kiyohiko Igarashi**[‡], **and Masahiro Samejima**[‡2]

From the Departments of ‡*Biomaterials Sciences and* §*Biotechnology, Graduate School of Agricultural and Life Sciences, The University of Tokyo, 1-1-1 Yayoi, Bunkyo-ku, Tokyo 113-8657 and the* ¶*National Food Research Institute, National Agriculture and Food Research Organization, 2-1-12, Kannondai, Tsukuba, Ibaraki 305-8642, Japan*

Glycoside hydrolase family 55 consists of β-1,3-glucanases mainly from filamentous fungi. A β-1,3-glucanase (Lam55A) from the Basidiomycete *Phanerochaete chrysosporium* hydrolyzes β-1,3-glucans in the exo-mode with inversion of anomeric configuration and produces gentiobiose in addition to glucose from β-1,3/1,6-glucans. Here we report the crystal structure of Lam55A, establishing the three-dimensional structure of a member of glycoside hydrolase 55 for the first time. Lam55A has two β-helical domains in a single polypeptide chain. These two domains are separated by a long linker region but are positioned side by side, and the overall structure resembles a rib cage. In the complex, a gluconolactone molecule is bound at the bottom of a pocket between the two β-helical domains. Based on the position of the gluconolactone molecule, Glu-633 appears to be the catalytic acid, whereas the catalytic base residue could not be identified. The substrate binding pocket appears to be able to accept a gentiobiose unit near the cleavage site, and a long cleft runs from the pocket, in accordance with the activity of this enzyme toward various β-1,3-glucan oligosaccharides. In conclusion, we provide important features of the substrate-binding site at the interface of the two β-helical domains, demonstrating an unexpected variety of carbohydrate binding modes.

Many fungi produce β-1,3-glucans as the main components of the cell wall. The primary role of fungal β-1,3-glucans is structural; that is, to maintain cell wall rigidity and, thus, to protect the cell. The cell wall β-1,3-glucans are also suggested to be degraded for nutritional purposes after exhaustion of external nutrition (1). β-1,3-Glucans on the cell surface are thought to be involved in morphogenetic changes, *i.e.* aggregation and mycelial strand formation (2). Moreover, the hyphal sheath of pathogenic fungi contains extracellular β-1,3-glucans, which play an active role in wood cell wall degradation (3). Fungal β-1,3-glucans often contain some branches with β-1,6 glycosidic linkages, and these molecules are called β-1,3/1,6-glucans. The pattern of branching in β-1,3/1,6-glucans, *e.g.* linkage ratio and branch length, varies depending on fungal species, localization in the cell wall, and the growth phase of the cells.

Fungi are prominent producers of β-1,3-glucanases, possibly due to the wide availability of the substrate in their cell wall (4). β-1,3-Glucanases are often termed laminarinases, as one of the most widely studied natural β-1,3-glucan-containing polymers is laminarin. Degradation of β-1,3-glucans by fungi often involves the cooperative action of multiple β-1,3-glucanases rather than a single enzyme. Although some fungal β-1,3-glucanases are constitutively produced, their expression levels are often controlled by culture conditions (5). Many β-1,3-glucanases have been characterized, and they exhibit a wide variety of substrate specificities and modes of actions (6). These facts suggest the involvement of β-1,3-glucanases in mobilization of cell wall β-glucans, especially in the case of yeast enzymes (7). β-1,3-Glucanases have been classified mainly based on the catalytic properties, *e.g.* endo and exo modes of action (5, 6). In the carbohydrate-active enzymes (CAZy) data base (8–13) enzymes having β-1,3-glucanase activity are found in the glycoside hydrolase (GH)[3] families 5, 16, 17, 55, 64, 72, and 81. All of the biochemically characterized enzymes in GH55 exhibit exo- or endo-β-1,3-glucanase activities, and they are found only in filamentous fungi (14–21). Lam55A is the exo-β-1,3-glucanase (or laminarinase A) from the Basidiomycete *Phanerochaete chrysosporium*, which belongs to GH55. The enzyme has no hydrolytic activity toward β-1,6- or β-1,3/1,4-glucan but shows high activity toward laminarin from *Laminaria digitata* (22), which is a β-1,3/1,6-glucan with an average degree of polymerization (DP) of ~25. Here we report the crystal struc-

[3] The abbreviations used are: GH, glycoside hydrolase; Lam55A, exo-β-1,3-glucanase from *P. chrysosporium*; DP, degree of polymerization; L2, laminaribiose; L3, laminaritriose; L4, laminaritetraose; L5, laminaripentaose; L6, laminarihexaose; L7, laminariheptaose; LG4, 6-*O*-glucosyl-laminaritriose; PL, polysaccharide lyase; Sf6 TSP, endorhamnosidase from *S. flexneri* Phage Sf6; AlgE4A, A-module of mannuronan C-5-epimerase from *A. vinelandii*; BsIFTase, inulin fructotransferase from *Bacillus sp. snu-7*; HPLC, high performance liquid chromatography; MES, 4-morpholineethanesulfonic acid; r.m.s.d., root mean square deviation.

ture of the enzyme, thereby providing the first three-dimensional view of a GH55 family member. We also present a detailed characterization of its hydrolytic activity.

EXPERIMENTAL PROCEDURES

Materials—Laminarioligosaccharides (β-1,3-linked oligomers of D-glucopyranose) with DPs of 2–7 (laminaribiose, L2; laminaritriose, L3; laminaritetraose, L4; laminaripentaose, L5; laminarihexaose, L6; laminariheptaose, L7) were purchased from Seikagaku Corp. (Tokyo, Japan). 6-*O*-Glucosyl-laminaritriose (LG4, β-D-Glc*p*-(1→6)-β-D-Glc*p*-(1→3)-β-D-Glc*p*-(1→3)-D-Glc*p*) was prepared using β-1,3-glucanase Lam16A according to the method reported previously (23).

Protein Preparation—Native Lam55A protein was heterologously expressed in *Pichia pastoris* and purified as described previously (22). Selenomethionine-labeled Lam55A was expressed in buffered minimal methanol media (100 mM potassium phosphate, pH 6.0, 1.34% yeast nitrogen base without amino acids (Wako Pure Chemical Industries Ltd., Osaka, Japan), 4×10^{-5}% biotin, 1% methanol) containing 0.1 mg·ml^{-1} L-selenomethionine, 0.09 mg·ml^{-1} L-isoleucine, 0.09 mg·ml^{-1} L-lysine, and 0.6 mg·ml^{-1} L-threonine using the same transformant of *P. pastoris* as that for native Lam55A. The purification procedures for selenomethionine-labeled Lam55A were the same as those for non-labeled Lam55A. For the crystallization experiments, the enzymes were treated with endoglycosidase H (New England Biolabs, Beverly, MA) as described previously (24) and further purified by gel permeation chromatography.

Kinetic Parameters—Lam55A was incubated with various concentrations of laminarioligosaccharides with DPs of 2–7 in 100 mM sodium acetate buffer, pH 4.5, at 30 °C, and the hydrolytic rate was estimated by monitoring the release of glucose, using Glucose CII-Test Wako (Wako Pure Chemical Industries Ltd.). To determine the Michaelis constant (K_m) and catalytic rate (k_{cat}), experimental data were regressed with the Michaelis-Menten equation using Kaleidagraph™ 3.6.4 (Synergy, Reading, PA).

Analysis of Products from Hydrolysis by Lam55A—High performance anion-exchange chromatography (model D-300 BioLC; Dionex, Sunnyvale, CA) with a CarboPac PA1 column (4×250 mm) was used to estimate the amount of hydrolytic products generated from L7. The column was equilibrated with 100 mM NaOH, and the reaction products were eluted with a linear gradient of 0–500 mM sodium acetate in 100 mM NaOH at a flow rate of 1 ml·min^{-1} over 30 min. A solution of 1 mM L7 was incubated with 12 nM Lam55A for various times, and the reaction mixtures were boiled and applied to the column equilibrated with 100 mM NaOH. The reaction products were eluted with a linear gradient of 0–500 mM sodium acetate in 100 mM NaOH at a flow rate of 1 ml·min^{-1} over 30 min as described previously (25). The anomeric configurations of the products from the first hydrolysis of LG4 and L3 were determined using an isocratic HPLC method (26, 27). Each substrate (20 mM) was incubated with 1.2 μM Lam55A for 1 min, and the reaction mixture was applied to a TSK-GEL Amide-80 column (4.6×250 mm; Tosoh Co., Tokyo, Japan). The hydrolysate from L3 was eluted with 80% acetonitrile at the flow rate of 2 ml·min^{-1}

and from LG4 with 70% acetonitrile at the flow rate of 1.5 ml·min^{-1}. Sugars were detected using a refractive index monitor (RI Model 504, GL Science, Tokyo, Japan). The retention times of α and β anomers of the compounds were determined based on the proportion of the equilibrated anomers (α:β = ~4:6) using equilibrated solutions.

Crystallography—Crystals of native and selenomethionine-labeled Lam55A were obtained by means of the hanging-drop vapor-diffusion method with microseeding. The drops were formed by mixing 2 μl of protein solution (10 mg·ml^{-1}) and 2 μl of the reservoir solution composed of 100 mM zinc acetate, 15% (w/v) polyethylene glycol 3350, 50 mM MES, pH 6.4, 10% (w/v) glycerol, and 2% (v/v) ethanol. The drops were microseeded after equilibration for 48 h at 25 °C. The microseeds were prepared by crushing native Lam55A crystals. The crystals were transferred to reservoir solutions containing 25% glycerol and then flash-cooled in a stream of nitrogen gas at 100 K. To obtain crystals of the complex with gluconolactone, the reservoir solution containing 50 mM gluconolactone was used for co-crystallization, and then 30% gluconolactone instead of glycerol was used as a cryoprotectant for the flash-cooling step. X-ray diffraction data sets were collected using synchrotron radiation at beam lines BL5A and NW12A of the Photon Factory, High Energy Accelerator Research Organization (KEK), Tsukuba, Japan, and data were processed and scaled using the HKL2000 program suite (28). The programs SHARP (29) and RESOLVE (30) were used for initial phase calculation and density modification, respectively. Automated model building was performed using the program ARP/wARP (31). Manual model rebuilding and refinement were achieved using Coot (32) and Refmac5 (33). The gluconolactone complex structure was solved starting from the refined native structure. Data collection and refinement statistics are shown in Tables 1 and 2, respectively. Figs. 1, 2*B*, 2*C*, 3, and 7 were prepared using PyMol (34), and ESPript (35) was used for Fig. 2*A*.

RESULTS

Structure Determination—For the initial phase determination by the multiwavelength anomalous dispersion method, we prepared selenomethionine-substituted crystals from recombinant Lam55A protein produced by *P. pastoris* cells cultured in selenomethionine-containing medium (36). We determined the crystal structures of Lam55A in unliganded and gluconolactone-complexed forms at 1.7 and 2.3 Å resolutions, and they were refined to R-values (R-free) of 14.9% (18.4%) and 14.2% (20.0%), respectively. Both crystal structures contained two molecules (A and B) of mature Lam55A in the asymmetric unit. The structures of the four chains determined here, two molecules from two crystals, are very similar, with the r.m.s.d. for Cα atoms less than 0.22 Å in all combinations of the four. We will describe chain A of each crystal structure unless otherwise noted.

The N-terminal residues from the expression vector (Glu-Ala-Glu-Ala-Glu-Phe) were highly disordered and were removed from the models. Six Zn^{2+} ions, 4 sodium ions, 4 acetate molecules, and 11 glycerol molecules were found in the ligand-free structure, whereas only 2 Zn^{2+} ions were found in the gluconolactone complex structure. At one of the four

TABLE 1
Data collection statistics

Data set	Unliganded	Gluconolactone complex	Selenomethionine		
			Peak	Edge	Remote
Beamline	PF BL-5A	PF BL-5A	PF-AR NW12A	PF-AR NW12A	PF-AR NW12A
Wavelength (Å)	1.000	1.000	0.97898	0.97917	0.96395
Space group	*P*1	*P*1	*P*1		
Cell dimensions					
a (Å)	66.3	66.5	66.1		
b (Å)	67.1	67.1	67.2		
c (Å)	105.2	109.8	105.0		
α (degree)	81.0	93.9	81.1		
β (degree)	76.3	106.8	76.5		
γ (degree)	61.4	97.1	61.4		
Resolution[a] (Å)	50.00-1.70 (1.76-1.70)	50.00-2.25 (2.33-2.25)	50.00-2.18 (2.26-2.18)		
Total reflections	502,749	262,450	604,805	589,541	564,876
Unique reflections	149,947	77,511	78,414	77,974	76,496
Completeness (%)[a]	88.8 (64.5)	91.9 (74.5)	97.8 (91.7)	96.8 (85.0)	94.7 (73.9)
Average $I/\sigma(I)$[a]	19.1 (3.0)	10.9 (2.7)	21.0 (4.92)	20.6 (4.1)	17.9 (3.2)
R_{sym} (%)[a]	6.5 (24.7)	9.7 (25.7)	9.0 (27.0)	9.5 (30.3)	9.7 (33.6)

[a] Values in parentheses are for the highest resolution shell.

TABLE 2
Refinement statistics

Data set	PDB accession code	
	3EQN	3EQO
Resolution (Å)	27.2-1.70	31.5-2.3
R-factor/*R*-free (%)	14.9/18.4	14.2/20.0
No. of reflections	142399	73632
No. of atoms	13,016	12,519
r.m.s.d. from ideal values		
Bond lengths (Å)	0.01	0.02
Bond angles (degree)	1.375	1.797
Average *B*-factor (Å²)		
Protein (chain A/B)	14.5/14.3	18.9/21.1
Sugar chain (chain A/B)	32.9/25.4	44.0/44.8
Glycerol	22.3	
Acetate ion	25.4	
Zinc ion	20.7	39.1
Sodium ion	25.0	
Gluconolactone (chain A/B)		24.6/26.3
Water	29.7	28.8
Ramachandran plot (%)		
Favored (chain A/B)	87.4/87.9	84.5/84.4
Allowed (chain A/B)	12.4/11.9	15.3/15.3
Disallowed (chain A/B)	0.2/0.2	0.2/0.3

potential *N*-glycosylation sites in the Lam55A sequence, Asn-231 exhibited extra electron density arising from its side-chain amide nitrogen atom. The electron density of two *N*-acetyl-β-D-glucosamine (GlcNAc) residues and one β-D-mannose residue was clearly visible, indicating that this glycosylation site was not susceptible to deglycosylation by endoglycosidase H. Further substitution by mannose residues, possibly attached at the O-3 or O-6 position of the terminal mannose residue, was only partially observed, with unclear electron density.

Overall Structure—Lam55A consists of two domains with a right-handed parallel β-helix fold (N domain, residues 1–361; C domain, residues 391–752) connected by a linker region (28 residues, 362–390). The two β-helix domains are positioned side-by-side, forming an overall shape like a rib cage (Fig. 1). As shown in Fig. 1*C*, the torsion angle between the helical axes of the two β-helix domains is ~25°. The two domains are bound tightly via many interactions that include the disulfide bond between Cys-5 and Cys-424. The other disulfide bonds, Cys-73-Cys-77, Cys-539-Cys-549, and Cys-692-Cys-698 exist in long loops between β-strands (Fig. 1, *A* and *B*). A helical repeating

unit of the β-helix fold, which is formed by three β-strands (designated as PB1, PB2, and PB3) linked by three turns (T1, T2, and T3), is termed a "coil" (37). We will hereafter designate the PBm β-strand and Tm turn included in the *n*th coil as PBm-n and Tm-n, respectively. Both the N and C domains of Lam55A consist of 12 coils, but flanking (1st, 2nd, 11th, and 12th) coils are incomplete or irregular (Fig. 2*A*). Both domains lack PB1−1, PB1−2, and PB3−11, and the C domain lacks PB2−12 (Fig. 2, *A* and *B*). Two C-terminal β-strands in the N domain (PB2−11 and PB2−12) protrude to the adjacent C-terminal domain and exhibit antiparallel interactions (Fig. 1*A*). In addition there are several antiparallel interactions in the 11th and 12th coils in both domains (indicated as *AP* in Fig. 2*B*). "Aromatic stack" and "asparagine ladder" are commonly found features in β-helical proteins, in which a number of aromatic (tyrosine and phenylalanine) or asparagine residues are located at equivalent positions in coils (38). Both of these features are found in the N domain of Lam55A but not in the C domain. The aromatic stack and asparagine ladder in the N-terminal domain are formed by three phenylalanine residues (Phe-185, Phe-213, and Phe-234), and four asparagine residues (Asn-236, Asn-258, Asn-290, and Asn-318), respectively (Fig. 2*C*). As shown in Fig. 2, *A* and *B*, the topologies of secondary structures in the two β-helix domains are very similar, whereas the pattern of loop insertion into the turn segments is significantly different.

Gluconolactone Complex Structure—Gluconolactone complex structure was determined using a crystal prepared by co-crystallization followed by soaking in the presence of a higher concentration of the ligand (Fig. 3*A*). The gluconolactone molecule exists at the bottom of a deep depression (substrate binding pocket) between the N and C domains (Fig. 3*B*). The binding pocket is formed by T1 turns (between PB1 and PB2) in the fourth to seventh coils of the N domain, and T3 turns (between PB3 and PB1) in the sixth to ninth coils of the C domain (Fig. 1*A*). A curved groove starting from the gluconolactone binding pocket runs around the protrusion formed by T1−4 in the N domain. Several aromatic residues (Phe-684, Trp-245, Phe-199, and Tyr-135) are located along the groove (Fig. 3*B*).

The gluconolactone molecule forms direct hydrogen bonds with Asn-147, Trp-572, Asp-575, Glu-610, and Glu-633, and
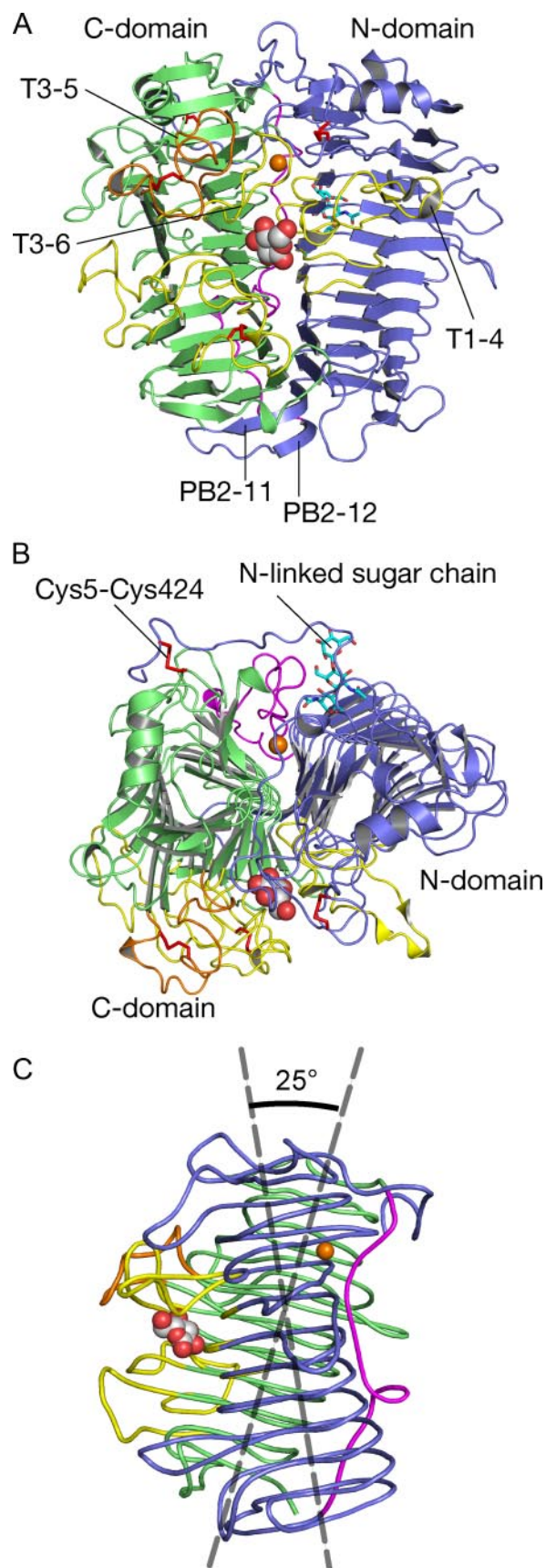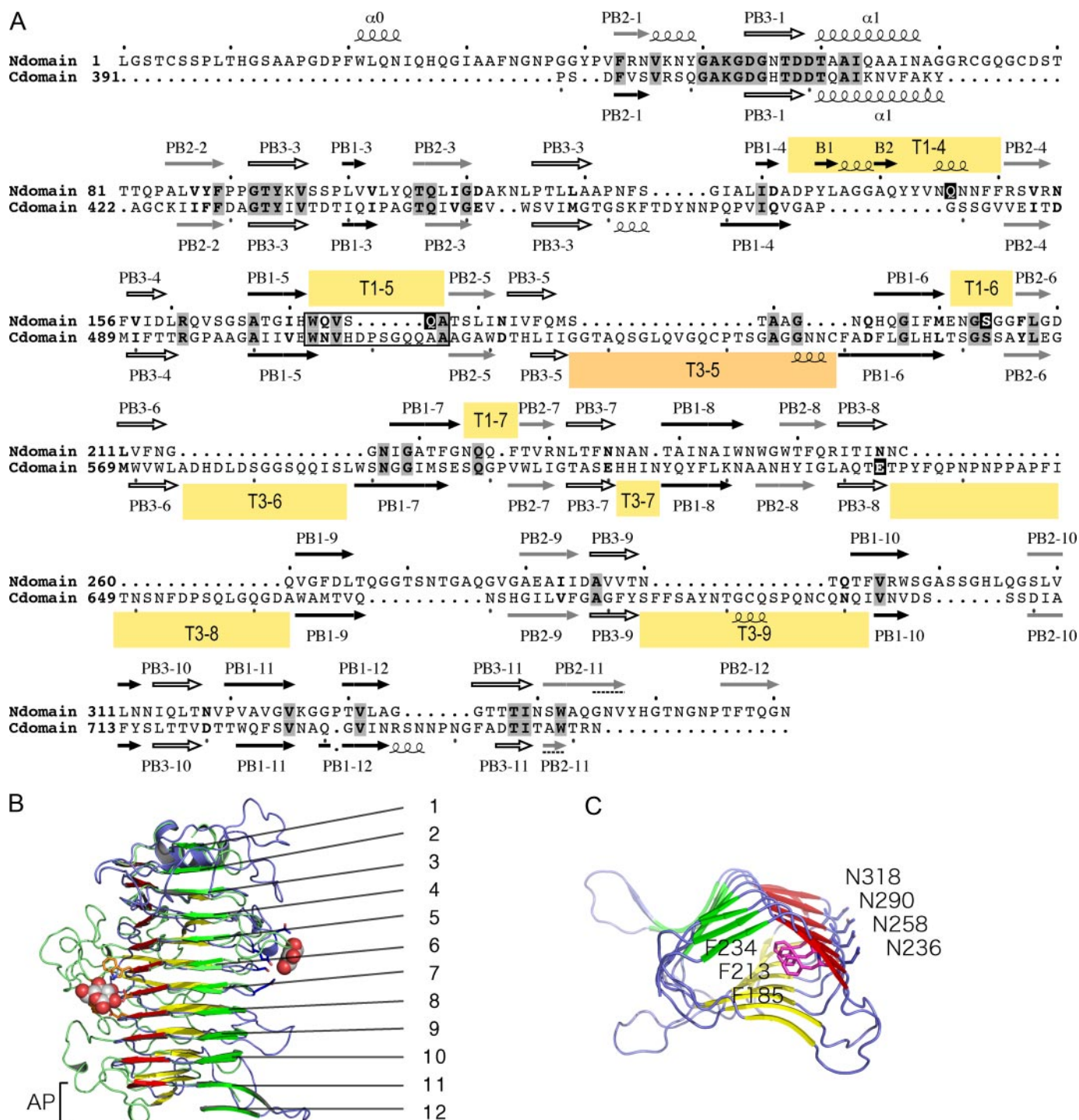
FIGURE 1. **Overall structure of Lam55A.** *A*, ribbon representation of Lam55A monomer in the complex with gluconolactone. *B*, the view rotated 90° around the horizontal axis from that in *A*. The N domain, C domain, and linker region are colored *blue*, *green*, and *magenta*, respectively. The disulfide bonds (Cys-5—Cys-424, Cys-73—Cys-77, Cys-539—Cys-549, and Cys-692—Cys-698) are shown in *red stick* form. The gluconolactone molecule is shown as *spheres* with carbon and oxygen atoms in *white* and *red*, respectively. The loops forming the substrate-binding pocket (T1–4, T1–5, T1–6, and T1–7 from N domain; T3–6, T3–7, T3–8, and T3–9 from C domain) are colored *yellow*. The T3–5 loop from C domain is colored *orange*. The zinc atom is shown as an *orange sphere*. The N-linked sugar chain is shown in *cyan stick* form. *C*, the view rotated 90° around the vertical axis from that in *A*. The torsion angle between the helical axes of the two β-helix domains is indicated.

water-mediated hydrogen bonds are formed with Gln-146, Gln-176, Ser-204, Gln-225, and Tyr-636 (Fig. 3*A*). Three acidic amino acid residues, Glu-633, Glu-610, and Asp-575, are completely conserved in GH55. Among them, Glu-633 is appropriately positioned as the catalytic acid, forming a direct hydrogen bond with the O-1 hydroxyl group of gluconolactone. Glu-610 recognizes the O-2 and O-3 hydroxyl groups, and Asp-575 recognizes the O-4 hydroxyl group. A water molecule appears to be appropriately positioned as the nucleophilic water, and the distance to the C-1 carbon atom is 2.7 Å. However, we could not convincingly identify the carboxylic catalytic base around this water molecule. The water is held by side chains of Ser-204 and Gln-176, and the backbone carbonyl group of Gln-146. Ser-204 and Gln-176 are also highly conserved in GH55.

Catalytic Features of Lam55A—The kinetic parameters of Lam55A for laminarioligosaccharides of various DP (L2–L7) were determined to investigate the correlation between the activity of Lam55A and the DP of substrates. As summarized in Table 3, the K_m values decreased and k_{cat} values increased with increasing DP of the substrates, resulting in a rapid increase of catalytic efficiency (k_{cat}/K_m) for longer substrates. The catalytic efficiency value for L6 and L7 was 1.57×10^4 and 1.11×10^4 times higher than that for L2, suggesting that the enzyme has a long substrate binding cleft with at least five subsites. To investigate the mode of action of Lam55A toward linear β-1,3-glucans, the time course of formation of hydrolysates produced from L7 by the Lam55A was followed with the high performance anion-exchange chromatography system. As shown in Fig. 4, glucose was generated as the major product even at the initial stage of the reaction, indicating that this enzyme is a typical exo-1,3-β-glucosidase (EC 3.2.1.58). L6, L5, and L4 are not accumulated during the reaction, indicating possible multiple attack of the enzyme, *i.e.* hydrolysis might occur several times on a single β-1,3-glucan chain without dissociation of the enzyme-substrate complex. The accumulation of small amounts of L2 and L3 is due to the low affinity of Lam55A for these oligosaccharides (Table 3).

The initial products of Lam55A hydrolysis against L3 and LG4 were analyzed with the HPLC system, which can separates the α- and β-anomers of oligosaccharides. As shown in Fig. 5, *A* and *B*, Lam55A produced glucose and L2 from L3 within 1 min; the generated glucose consisted only of the α-anomer, whereas both the substrate and generated L2 were mixtures of α and β anomers. This result clearly shows that the enzyme hydrolyzes the β-1,3-glucosidic linkage at the non-reducing end of L3 with net inversion of anomeric carbon. When LG4 was used as the substrate (Fig. 5, *C* and *D*), Lam55A produced gentiobiose (β-D-Glc*p*-(1→6)-D-Glc*p*) and L2 within 1 min. The generated gen-

FIGURE 2. **β-Strands in the two β-helix domains.** *A*, sequence alignment of N and C domains. *Arrows* for PB1, PB2, and PB3 are colored *black*, *gray*, and *white*, respectively. Identical amino acid residues are *boxed* in *gray*. The loops forming the substrate binding pocket and T3–5 loop from C domain are indicated by *yellow-* and *orange-shaded* boxes, respectively. *Dashed lines* indicate regions involved in antiparallel interaction between β-strands of N and C domains. Residues possibly involved in catalysis, Glu-633, Gln-146, Gln-176, and Ser-204, are shown in *white type boxed in black*. *B*, superimposition of N domain (*blue*) and C domains (*green*). PB1, PB2, and PB3 are colored *blue*, *lime green*, and *red*, respectively. Gluconolactone molecules bound to each domain are shown as *spheres*. The side chains of residues in N and C domains are shown in *blue* and *orange sticks*, respectively. Coils are numbered from the N terminus to the C terminus of each domain. *AP* indicates a region where β-strands have antiparallel interactions. *C*, aromatic stack and asparagine ladder found in the N domain.

tiobiose, which is released from the non-reducing end of the substrate, was also composed of only the α-anomer, and the amount of L2 produced from L3 and LG4 was almost the same level, suggesting similar activities toward each substrate. These results clearly indicate that Lam55A hydrolyzes β-1,3-glucosidic linkages at the non-reducing end independently of substitution at the O-6 position with a single β-D-glucopyranose residue. Fig. 6 shows a schematic representation of the initial hydrolysis by Lam55A of the oligosaccharides examined in this study.

FIGURE 3. **Binding of gluconolactone to Lam55A.** *A*, stereoview with the $F_{obs} - F_{calc}$ omit electron density map contoured at 1.5 σ at the active site. Gluconolactone (*white*) residues from the N domain (*blue*) and C domain (*green*) are shown as *stick* models. Water molecules are shown as *red spheres*. Hydrogen bonds are depicted by *black dashed lines*. Distances between O-1 of gluconolactone and Glu-633 and between C1 and proximal water are indicated by *red lines*. The main chain carbonyl oxygen of Glu-146 forms a hydrogen bond with the proximal water. *B*, molecular surface of the gluconolactone complex structure. Amino acid residues highly conserved in biochemically characterized GH55 enzymes, including both exo- and endo-β-1,3-glucanases, are successively colored from *yellow* (>60%) to *orange* (>80%) and *red* (100%). Gluconolactone and aromatic residues located along the groove are shown as *stick* models. A *dashed line* indicates a curved groove on the molecular surface, and a *circle* with *green dotted lines* indicates the small pocket near the O-6 of gluconolactone.

TABLE 3

Kinetic parameters for laminarioligosaccharides

Substrate	K_m	k_{cat}	k_{cat}/K_m
	μM	s^{-1}	$\times 10^5 \cdot s^{-1} \cdot M^{-1}$
Laminaribiose	1960 ± 309	3.18 ± 0.20	0.0162
Laminaritriose	284 ± 32	30.4 ± 0.5	1.07
Laminaritetraose	30.4 ± 3.4	53.4 ± 2.2	17.6
Laminaripentaose	8.01 ± 0.23	59.1 ± 0.2	73.8
Laminarihexaose	4.07 ± 0.19	73.4 ± 0.6	180
Laminariheptaose	3.28 ± 0.14	83.3 ± 0.6	254

DISCUSSION

In this study we performed a detailed characterization of the enzymatic action of Lam55A. The mode of action of this enzyme was basically similar to those of several exo-β-1,3-glucanases from filamentous fungi characterized in earlier studies (39–41). Lam55A released α-glucose or α-gentiobiose from the non-reducing end of β-1,3-glucans or β-1,3/1,6-glucans (Fig. 5). This feature is notably similar to that of ExgS from *Aspergillus saitoi* (18). Therefore, our results clearly demonstrate that a GH55 enzyme has an inverting mechanism. In the general mechanism of inverting GHs, two acidic residues separated by about 10 Å serve as general acid and base catalysts (10, 42). The reaction proceeds by proton donation from the catalytic acid to the glycosidic bond oxygen, concurrently with nucleophilic attack by water at the anomeric carbon. A catalytic base is required to activate the nucleophilic water. However, there are several exceptional cases among inverting GHs. For example, the catalytic base of a GH6 enzyme, cellobiohydrolase Cel6A, indirectly interacts with nucleophilic water via another water, and the nucleophilic water is held by a serine residue and a main chain carbonyl oxygen (43, 44). Furthermore, the identity of the catalytic base of GH48 enzymes is still unclear even though the crystal structures of a number of enzyme complexes with substrates have been determined (45–48). In the reaction mechanism proposed for GH95 1,2-α-fucosidase, two asparagine residues are thought to play critical roles in withdrawing a proton from the nucleophilic water, and two neighboring acidic residues (Glu and Asp) are involved in the enhancement of water nucleophilicity (49). In the present study Glu-633 of Lam55A is suggested to be the catalytic acid, and we found a candidate for the nucleophilic water which seems to be positioned appropriately near the C-1 carbon atom of gluconolactone. However, there are no acidic residues that can interact with this water molecule. The nucleophilic water candidate is held by the side chains of Ser-204 and Gln-176 and the main chain carbonyl oxygen of Gln-146. The situation is similar in some respects to
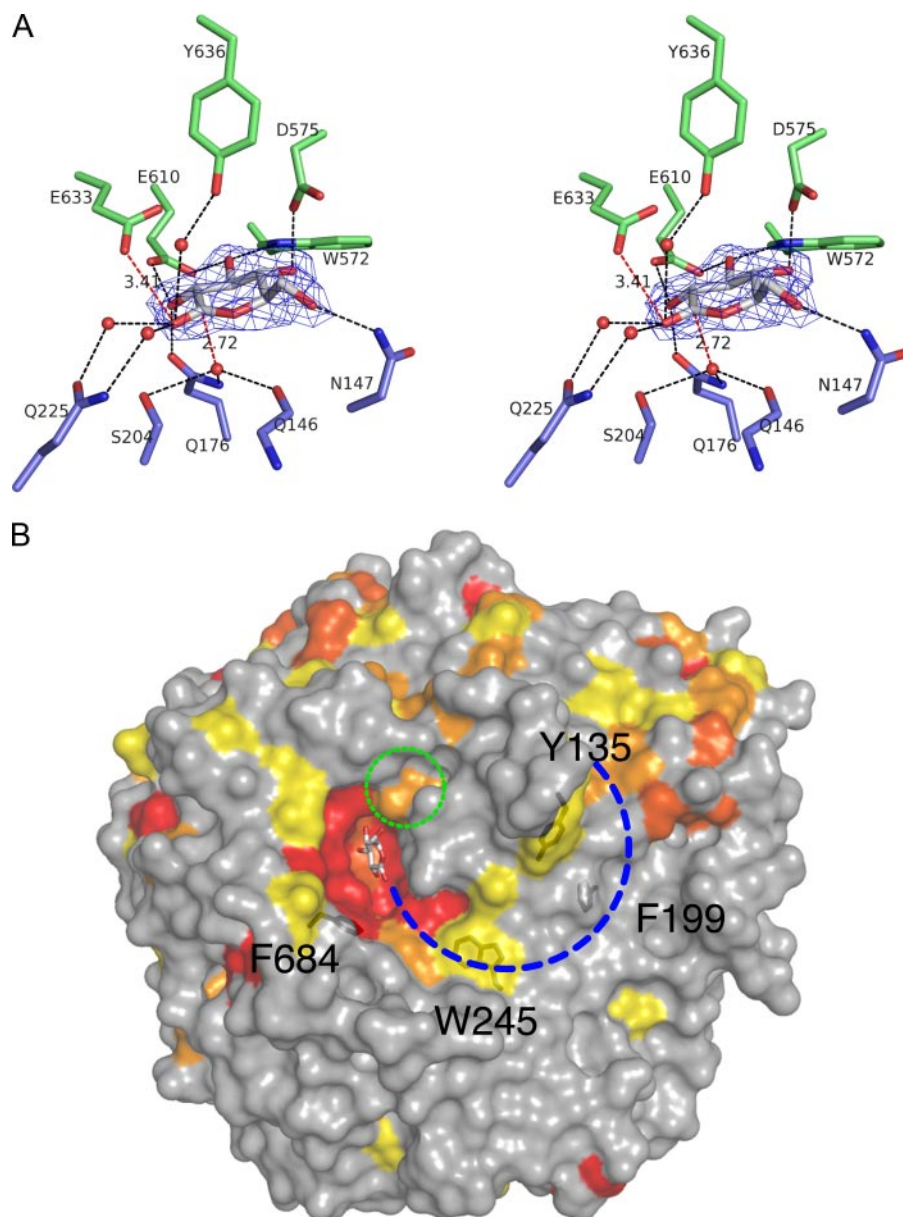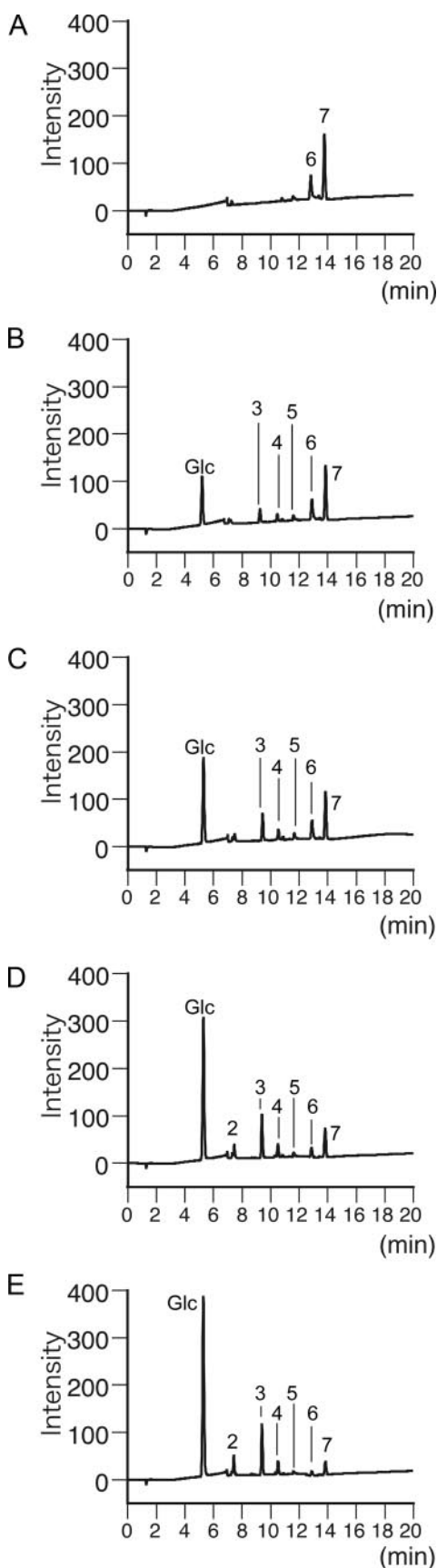
FIGURE 4. **High performance anion-exchange chromatography analysis of hydrolysis products of laminariheptaose (L7).** L7 was incubated with Lam55A for 0 min (*A*), 1 min (*B*), 2 min (*C*), 4 min (*D*), and 8 min (*E*) in 100 mM sodium acetate buffer, pH 4.5, at 30 °C, and the reaction mixture was separated as described under "Experimental Procedures." *2*, laminaribiose; *3*, laminaritriose; *4*, laminaritetraose; *5*, laminaripentaose; *6*, laminarihexaose; *7*, laminariheptaose.

the case of the nucleophilic water in Cel6A, but we could not find a carboxylic acid group around the elements holding the nucleophilic water candidate. Although the catalytic mechanism of Lam55A cannot yet be defined due to the uncertainty in the identity of the catalytic base, GH55 enzymes may have a different mechanism from the normal inverting GHs. Alternatively, the orientation of gluconolactone observed here may not mimic the Michaelis complex. There are a number of highly conserved residues around this site, but only three of them (Asp-575, Glu-610, and Glu-633) have the carboxyl side chain (see supplemental Fig. S1.) These residues hold the hydroxyl groups of gluconolactone in the current complex structure, but two of them might act as the general acid and base catalysts in an alternative substrate binding mode.

Fig. 3*B* shows the molecular surface of Lam55A colored to show residue conservation within GH55 enzymes (the degree of conservation increases in the order of white, yellow, orange, and red), including both exo- and endo-β-1,3-glucanases. The high level of conservation around the gluconolactone binding pocket strongly indicates that this area is the catalytic cleavage site of GH55 enzymes. A long cleft forming an arc from the gluconolactone binding pocket appears to be available to bind a curved β-1,3-glucan chain. There are some additional aromatic residues lining the cleft, and the cleft exhibits a relatively high level of amino acid residue conservation in the region stretching up to Trp-245. Kinetic analysis showed that Lam55A prefers longer β-1,3-glucan chains with DP up to 6~7 as substrates. Therefore, this long cleft is suggested to be the location of subsites +1 to +5 and perhaps more. In addition, one side of the substrate binding pocket of Lam55A is blocked by a long loop region, which is consistent with the exo mode of hydrolysis of the enzyme demonstrated by HPLC analysis (Fig. 4). This loop region corresponds to T3–6 between PB3–6 and PB1–7 in the C domain (residues 573–593), and the neighboring T3–5 loop region supports the T3–6 loop from the back (Fig. 1*A*, *orange*). These loop regions exhibit great sequence variation among GH55 exo- and endo-β-1,3-glucanases. Interestingly, a small pocket, about the size of a single glucose unit, is present beyond the O-6 hydroxyl group of gluconolactone (*circled* by a *green broken line* in Fig. 3*B*). Therefore, the substrate-binding site of Lam55A appears to accept a gentiobiose unit. The putative binding pocket for a single β-1,6-branched glucose unit shows a high degree of conservation, in accordance with the fact that many GH55 exo-β-1,3-glucanases (often designated as exo-β-1,3/1,6-glucanases) purified from filamentous fungi release gentiobiose units from laminarin-containing β-1,6-glucosidic branches (50, 51). To clarify the identity of the catalytic residues and the substrate binding mode of Lam55A, further studies such as construction of mutant enzymes and determination of the structures of the complexes with gentiobiose or longer substrates will be required.

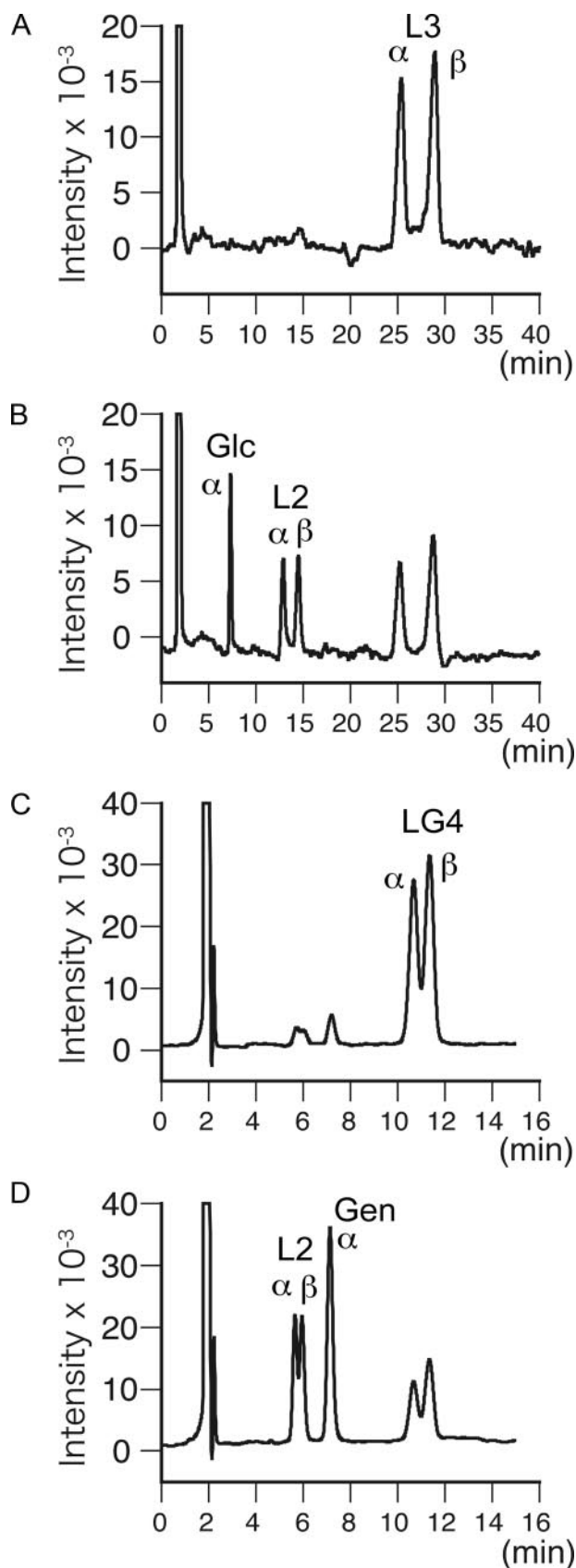A structural similarity search using the DALI server (52) revealed that both the N and C domains of Lam55A show sim-

FIGURE 5. **HPLC analysis of hydrolysis products of laminaritriose (L3) and 6-O-glucosyllaminaritriose (LG4).** Shown are L3 before (*A*) and after (*B*) incubation with Lam55A and LG4 before (*C*) and after (*D*) incubation with Lam55A. Each substrate (20 mM) was incubated with Lam55A for 1 min in 100
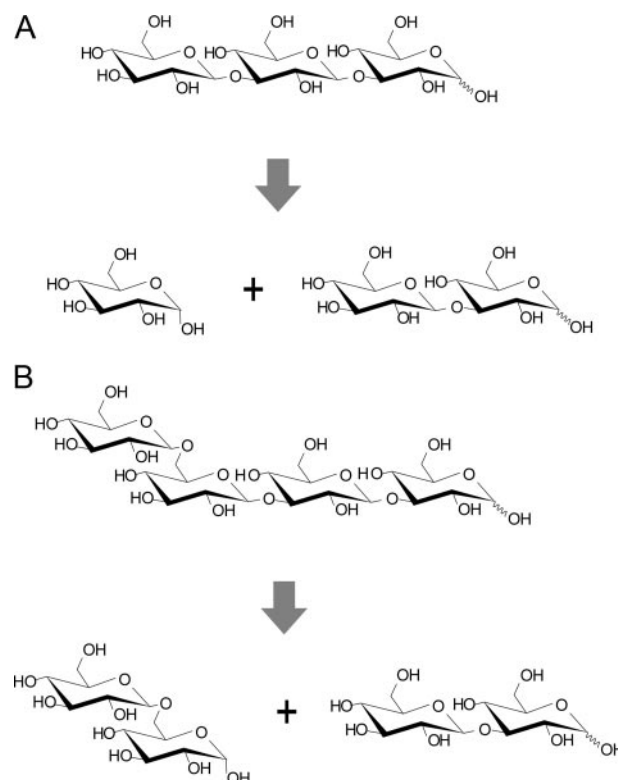

FIGURE 6. **Schematic representation of hydrolysis of laminaritriose (*A*) and 6-O-glucosyl laminaritriose (*B*) by Lam55A.** Lam55A hydrolyzes the glycosidic bond of the glucose residue at the non-reducing end independently of substitution at the O-6 position.

ilarity to those of various carbohydrate-active β-helical enzymes such as GH, polysaccharide lyase (PL), and carbohydrate esterase family enzymes in the CAZy data base. Close structural neighbors (Z scores > 15) include GH28, GH49, GH82, GH90, PL1, PL3, PL6, PL9, PL19 (formerly GH91), carbohydrate esterase 8, endorhamnosidase from *Shigella flexneri* Phage Sf6 (Sf6 TSP) (53), and A-module of mannuronan C-5-epimerase from *Azotobacter vinelandii* (AlgE4A) (54). Sf6 TSP has a glycoside hydrolase activity but has not yet been assigned to a CAZy family. The N domain of Lam55A is most similar to that of AlgE4A (PDB code 2PYH chain B; Z score = 25.2, and r.m.s.d. for 249 C-α atoms = 2.3 Å), and GH82, Sf6 TSP, and GH28 follow in this order (Z scores > 20). On the other hand, the C domain is most similar to that of Sf6 TSP (PDB code 2VBE chain A; Z score = 22.0, and r.m.s.d. for 246 C-α atoms = 2.5 Å), and GH28, GH82, and PL19 follow (Z scores > 20). A pairwise structural comparison between the N and C domains of Lam55A revealed that they are strikingly similar (Z score = 24.8, and r.m.s.d. for 253 C-α atoms = 2.2 Å) as compared with the other enzymes. This result provides strong support for the hypothesis that the two tandem β-helical domains of GH55 derive from a gene duplication event (16).

Although the presence of two β-helix folding motifs was suggested from the amino acid sequences of GH55 enzymes (55), the orientation of the two β-helix domains and the active site

mM sodium acetate buffer, pH 4.5, at 30 °C, and the reaction mixture was separated as described under "Experimental Procedures." L2, laminaribiose; *Gen*, gentiobiose.
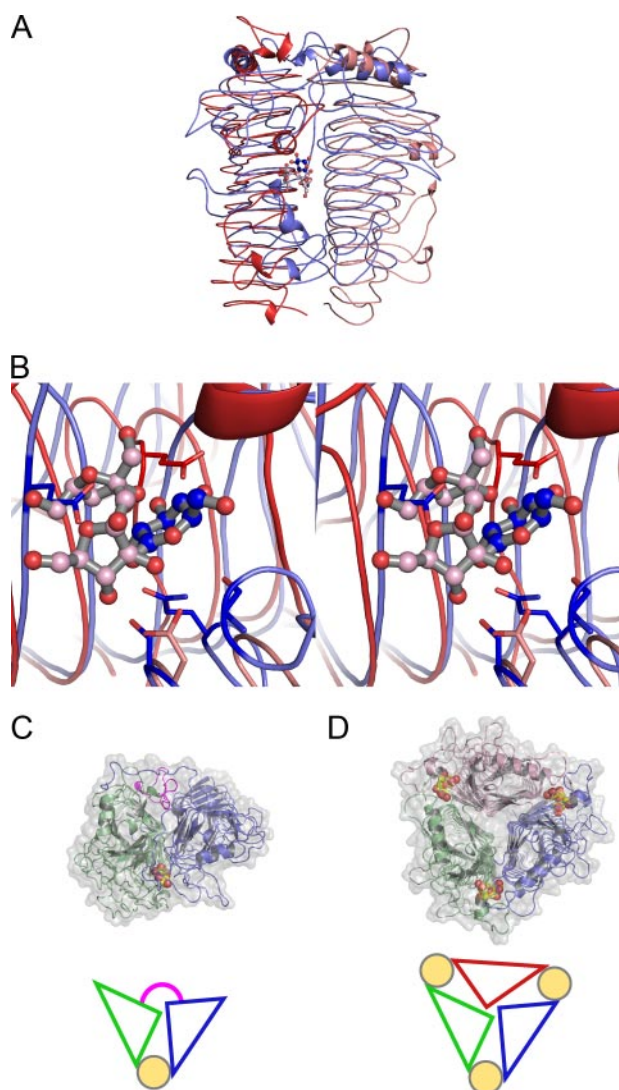
FIGURE 7. **Comparison of active site formation between GH55 Lam55A and PL19 (formerly GH91) BsIFTase.** *A*, superimposition of the structures of Lam55A (*blue*) and BsIFTase (*red* and *pink* for two symmetry-related molecules). *B*, close-up stereoview of the active site. Selected residues in the active site of Lam55A (Gln-146, Gln-176, Ser-204, and Glu-633) and the catalytic residues of BsIFTase (Asp-233 and Glu-244) are shown as *stick* models. Glu-conolactone bound to Lam55A (carbon atoms in *blue*) and β-2,1-linked difructosaccharide bound to subsites +1 and +2 of BsIFTase (carbon atoms in *pink*) are shown as *ball-and-stick* models. Top views of monomeric Lam55A (*C*) and homotrimeric BsIFTase (*D*) are shown. Schematic diagrams are also shown in these panels. The two domains and the linker region of Lam55A and the three symmetry-related chains of BsIFTase are colored differently. The ligands are shown as *spheres* with the carbon atoms in *yellow*. The active site is located at the interface between two domains (GH55) or between two adjacent chains (BsIFTase).

structure were unknown. The structure we present here reveals that the two β-helix domains (N and C domains) are located side by side and bound tightly via many interactions. Moreover, there is a long linker region between the two domains, having many interactions with both the N and C domains; therefore, the linker region may stabilize the association of the two β-helix domains. Such a role of the linker region of Lam55A is quite different from that of the linker in many other GHs, in which it serves to separate the catalytic domain and carbohydrate binding module and to introduce flexibility between the two domains (55).

Most of the known β-helical enzymes, including polysaccharide-degrading enzymes, have their active sites in the groove parallel to the helical axis within a monomer (37). The long concave surface formed by T3 and PB1 has been considered to be suitable for binding of a long and straight polysaccharide. Recently, two unusual examples, whose active sites are located at the monomer-monomer interface of two identical right-handed parallel β-helical domains, have been reported; they are PL19 inuline fructotransferase from *Bacillus* sp. *snu-7* (BsIFTase) (57) (Fig. 7A) and Sf6 TSP (53). Both are homotrimeric enzymes, and each monomer consists of a β-helical fold similar to those of the Lam55A domains. The structure of Lam55A provides another example of an active site located at the interface of two β-helical domains, but it is formed by two domains in a single polypeptide (Fig. 7B). When the C-α atoms of the N and C domains of Lam55A and two monomers of BsIFTase are superimposed, the active sites of these enzymes almost overlapped (Fig. 7, *A* and *B*). BsIFTase catalyzes inverting intramolecular fructosyl transfer to release the terminal difructosaccharide unit from β-2,1-fructans, such as inulin (58). Glu-244 and Asp-233 are suggested to play crucial roles in the catalysis. BsIFTase was once classified into GH91 in the CAZy data base but afterward reclassified to PL19 according to the International Union of Biochemistry and Molecular Biology Enzyme Nomenclature because this enzyme actually catalyzes an elimination reaction (EC 4.2.2.18). As illustrated in Fig. 7B, the possible catalytic residues of Lam55A and BsIFTase do not overlap, indicating that the positions of catalytic residues are not conserved between GH55 and PL19 enzymes. Sf6 TSP is a retaining enzyme, and the two catalytic residues, Asp-399 and Glu-366, are located in different monomers. Although the identity of the catalytic residues of Lam55A is still unclear, the putative catalytic acid residue (Glu-633, colored *green* in Fig. 3A) and the residues holding the nucleophilic water candidate (colored *blue* in Fig. 3A) are located in different domains. The possible catalytic residues of Lam55A and Sf6 TSP do not overlap after structural alignment (data not shown).

β-Helix is one of the basic scaffolds for binding polysaccharides, as a β-helix domain called CASH (carbohydrate-binding proteins and sugar hydrolases) is widespread among carbohydrate-interacting proteins (59). To date, five GH families (GH28, -49, -55, -82, and -90), six PL families (PL1, -3, -6, -9, -16, -19), and one carbohydrate esterase family (CE8) are confirmed to have the right-handed parallel β-helix fold, and two of them (GH28 and -49) are further grouped into the clan GH-N. Rigden and Franco (55) found possible evolutionary relationships among GH28, -49, -82, and -87. However, they suggested that GH55 is distinct from other β-helical GH families because of the inconsistency of the positions of catalytic residues. Here we provide an example of carbohydrate binding at the interface of two β-helical domains within a single polypeptide, demonstrating an unexpected variety of carbohydrate-binding modes of β-helical proteins.

REFERENCES

1. Zevenhuizen, L. P., and Bartnicki-Garcia, S. (1970) *J. Gen. Microbiol.* **61,** 183–188
2. Stone, B. A., and Clarke, A. E. (1992) *Chemistry and Biology of (1,3)-β-glucans*, pp. 283–364, La Trobe University Press, Bundoora, Australia
3. Ruel, K., and Joseleau, J. P. (1991) *Appl. Environ. Microbiol.* **57,** 374–384
4. Bielecki, S., and Galas, E. (1991) *Crit. Rev. Biotechnol.* **10,** 275–304
5. Pitson, S. M., Seviour, R. J., and McDougall, B. M. (1993) *Enzyme Microb. Technol.* **15,** 178–192
6. Martin, K., McDougall, B. M., McIlroy, S., Chen, J., and Seviour, R. J. (2007) *FEMS Microbiol. Rev.* **31,** 168–192
7. Adams, D. J. (2004) *Microbiology* **150,** 2029–2035
8. Bourne, Y., and Henrissat, B. (2001) *Curr. Opin. Struct. Biol.* **11,** 593–600
9. Henrissat, B., and Bairoch, A. (1996) *Biochem. J.* **316,** 695–696
10. Davies, G., and Henrissat, B. (1995) *Structure* **3,** 853–859
11. Henrissat, B., and Bairoch, A. (1993) *Biochem. J.* **293,** 781–788
12. Henrissat, B. (1991) *Biochem. J.* **280,** 309–316
13. Cantarel, B. L., Coutinho, P. M., Rancurel, C., Bernard, T., Lombard, V., and Henrissat, B. (2008) *Nucleic Acids Res.* **37,** 233–238
14. Cohen-Kupiec, R., Broglie, K. E., Friesem, D., Broglie, R. M., and Chet, I. (1999) *Gene (Amst.)* **226,** 147–154
15. de la Cruz, J., Pintor-Toro, J. A., Benitez, T., Llobell, A., and Romero, L. C. (1995) *J. Bacteriol.* **177,** 6937–6945
16. Donzelli, B. G., Lorito, M., Scala, F., and Harman, G. E. (2001) *Gene (Amst.)* **277,** 199–208
17. Giczey, G., Kerenyi, Z., Fulop, L., and Hornok, L. (2001) *Appl. Environ. Microbiol.* **67,** 865–871
18. Kasahara, S., Nakajima, T., Miyamoto, C., Wada, K., Furuichi, Y., and Ichishima, E. (1992) *J. Ferment. Bioeng.* **74,** 238–240
19. Nobe, R., Sakakibara, Y., Fukuda, N., Yoshida, N., Ogawa, K., and Suiko, M. (2003) *Biosci. Biotechnol. Biochem.* **67,** 1349–1357
20. Nobe, R., Sakakibara, Y., Ogawa, K., and Suiko, M. (2004) *Biosci. Biotechnol. Biochem.* **68,** 2111–2119
21. Schaeffer, H. J., Leykam, J., and Walton, J. D. (1994) *Appl. Environ. Microbiol.* **60,** 594–598
22. Kawai, R., Igarashi, K., and Samejima, M. (2006) *Biotechnol. Lett.* **28,** 365–371
23. Kawai, R., Igarashi, K., Yoshida, M., Kitaoka, M., and Samejima, M. (2006) *Appl. Microbiol. Biotechnol.* **71,** 898–906
24. Yoshida, M., Ohira, T., Igarashi, K., Nagasawa, H., Aida, K., Hallberg, B. M., Divne, C., Nishino, T., and Samejima, M. (2001) *Biosci. Biotechnol. Biochem.* **65,** 2050–2057
25. Kawai, R., Igarashi, K., Kitaoka, M., Ishii, T., and Samejima, M. (2004) *Carbohydr. Res.* **339,** 2851–2857
26. Honda, Y., and Kitaoka, M. (2004) *J. Biol. Chem.* **279,** 55097–55103
27. Koga, D., Yoshioka, K., and Arakane, Y. (1998) *Biosci. Biotechnol. Biochem.* **62,** 1643–1646
28. Otwinowski, Z., and Minor, W. (1997) *Methods Enzymol.* **276,** 307–326
29. Vonrhein, C., Blanc, E., Roversi, P., and Bricogne, G. (2007) *Methods Mol. Biol.* **364,** 215–230
30. Terwilliger, T. C. (2000) *Acta Crystallogr. D Biol. Crystallogr.* **56,** 965–972
31. Perrakis, A., Morris, R., and Lamzin, V. S. (1999) *Nat. Struct. Biol.* **6,** 458–463
32. Emsley, P., and Cowtan, K. (2004) *Acta Crystallogr. D Biol. Crystallogr.* **60,** 2126–2132
33. Murshudov, G. N., Vagin, A. A., and Dodson, E. J. (1997) *Acta Crystallogr. D Biol. Crystallogr.* **53,** 240–255
34. DeLano, W. L. (2002) *Curr. Opin. Struct. Biol.* **12,** 14–20
35. Gouet, P., Courcelle, E., Stuart, D. I., and Metoz, F. (1999) *Bioinformatics* **15,** 305–308
36. Larsson, A. M., Andersson, R., Stahlberg, J., Kenne, L., and Jones, T. A. (2003) *Structure* **11,** 1111–1121
37. Jenkins, J., and Pickersgill, R. (2001) *Prog. Biophys. Mol. Biol.* **77,** 111–175
38. Yoder, M. D., Lietzke, S. E., and Jurnak, F. (1993) *Structure* **1,** 241–251
39. Yamamoto, R., and Nevins, D. (1983) *Carbohydr. Res.* **122,** 217–226
40. Tsujihara, Y., Hamada, N., and Kobayashi, R. (1981) *Agric Biol. Chem.* **45,** 1201–1208
41. Pitson, S. M., Seviour, R. J., McDougall, B. M., Woodward, J. R., and Stone, B. A. (1995) *Biochem. J.* **308,** 733–741
42. McCarter, J. D., and Withers, S. G. (1994) *Curr. Opin. Struct. Biol.* **4,** 885–892
43. Koivula, A., Ruohonen, L., Wohlfahrt, G., Reinikainen, T., Teeri, T. T., Piens, K., Claeyssens, M., Weber, M., Vasella, A., Becker, D., Sinnott, M. L., Zou, J. Y., Kleywegt, G. J., Szardenings, M., Stahlberg, J., and Jones, T. A. (2002) *J. Am. Chem. Soc.* **124,** 10015–10024
44. Varrot, A., Macdonald, J., Stick, R. V., Pell, G., Gilbert, H. J., and Davies, G. J. (2003) *Chem. Commun.* 946–947
45. Guimaraes, B. G., Souchon, H., Lytle, B. L., David Wu, J. H., and Alzari, P. M. (2002) *J. Mol. Biol.* **320,** 587–596
46. Parsiegla, G., Juy, M., Reverbel-Leroy, C., Tardif, C., Belaich, J. P., Driguez, H., and Haser, R. (1998) *EMBO J.* **17,** 5551–5562
47. Parsiegla, G., Reverbel, C., Tardif, C., Driguez, H., and Haser, R. (2008) *J. Mol. Biol.* **375,** 499–510
48. Parsiegla, G., Reverbel-Leroy, C., Tardif, C., Belaich, J. P., Driguez, H., and Haser, R. (2000) *Biochemistry* **39,** 11238–11246
49. Nagae, M., Tsuchiya, A., Katayama, T., Yamamoto, K., Wakatsuki, S., and Kato, R. (2007) *J. Biol. Chem.* **282,** 18497–18509
50. Ohno, N., Nono, I., and Yadomae, T. (1989) *Carbohydr. Res.* **194,** 261–271
51. Ohno, N., Hashimoto, Y., and Yadomae, T. (1986) *Carbohydr. Res.* **158,** 217–226
52. Holm, L., and Sander, C. (1995) *Trends Biochem. Sci.* **20,** 478–480
53. Muller, J. J., Barbirz, S., Heinle, K., Freiberg, A., Seckler, R., and Heinemann, U. (2008) *Structure* **16,** 766–775
54. Rozeboom, H. J., Bjerkan, T. M., Kalk, K. H., Ertesvag, H., Holtan, S., Aachmann, F. L., Valla, S., and Dijkstra, B. W. (2008) *J. Biol. Chem.* **283,** 23819–23828
55. Rigden, D. J., and Franco, O. L. (2002) *FEBS Lett.* **530,** 225–232
56. Henrissat, B., and Davies, G. J. (2000) *Plant Physiol.* **124,** 1515–1519
57. Jung, W. S., Hong, C. K., Lee, S., Kim, C. S., Kim, S. J., Kim, S. I., and Rhee, S. (2007) *J. Biol. Chem.* **282,** 8414–8423
58. Kim, C. S., Hong, C. K., Kim, K. Y., Wang, X. L., Kang, S. I., and Kim, S. I. (2007) *J. Microbiol. Biotechnol.* **17,** 37–43
59. Ciccarelli, F. D., Copley, R. R., Doerks, T., Russell, R. B., and Bork, P. (2002) *Trends Biochem. Sci.* **27,** 59–62